Technical Report CHL-97-8
May 1997

US Army Corps of Engineers
Waterways Experiment Station

Hydrodynamic and Sediment Transport, Mill Cove, St. Johns River, Florida

Numerical Modeling Study

by José A. Sánchez, Lisa C. Roig

Prepared for U.S. Army Engineer District, Jacksonville

Technical Report CHL-97-8
May 1997

Hydrodynamic and Sediment Transport, Mill Cove, St. Johns River, Florida

Numerical Modeling

by José A. Sánchez, Lisa C. Roig

U.S. Army Corps of Engineers
Waterways Experiment Station
3909 Halls Ferry Road
Vicksburg, MS 39180-6199

Final report

Approved for public release; distribution is unlimited

Prepared for U.S. Army Engineer District, Jacksonville
Jacksonville, FL 32232-0019

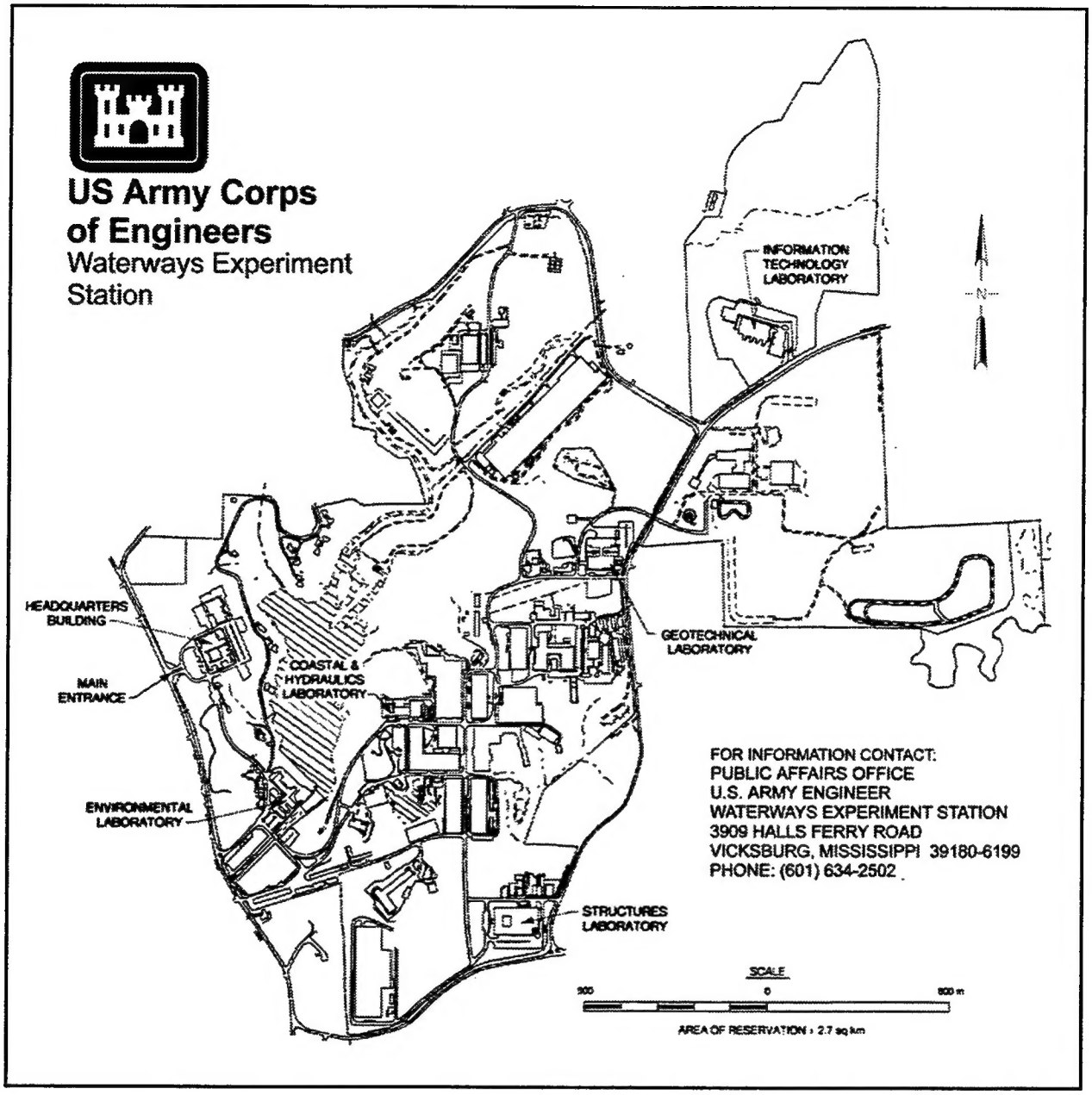

Waterways Experiment Station Cataloging-in-Publication Data

Sanchez, Jose A.

Hydrodynamic and sediment transport, Mill Cove, St. Johns River, Florida : numerical modeling / by Jose A. Sanchez, Lisa C. Roig ; prepared for U.S. Army Engineer District, Jacksonville.

114 p. : ill. ; 28 cm. — (Technical report ; CHL-97-8)

Includes bibliographic references.

1. Sediment transport — Mathematical models. 2. Hydrodynamics — Mathematical models. 3. Saint Johns River (Fla.) I. Roig, Lisa C. II. United States. Army. Corps of Engineers. Jacksonville District. III. U.S. Army Engineer Waterways Experiment Station. IV. Coastal and Hydraulics Laboratory (U.S. Army Engineer Waterways Experiment Station) V. Title. VI. Series: Technical report (U.S. Army Engineer Waterways Experiment Station) ; CHL-97-8.

TA7 W34 no.CHL-97-8

Contents

List of Tables

Preface

This investigation was performed by the Coastal and Hydraulics Laboratory (CHL) of the U.S. Army Engineer Waterways Experiment Station (WES) for the U.S. Army Engineer District, Jacksonville (SAJ). The study was conducted during the period September 1994-March 1996. SAJ and personnel of the Prototype and Field Studies Group, CHL, provided survey data of the prototype area. Current modeling was conducted by the Estuarine Branch, Waterways and Estuaries Division, CHL.

The investigation was conducted by Dr. Lisa C. Roig, Watershed Systems Group, Hydro-Science Division, CHL, and Mr. José A. Sánchez, Estuarine Branch, under the general direction of Messrs. Richard A. Sager, Acting Director, Hydraulics Laboratory; Robert F. Athow, Acting Assistant Director, Hydraulics Laboratory; William H. McAnally, Chief of the Waterways and Estuaries Division; and Dr. Robert T. McAdory, Jr., Chief of the Estuarine Branch. This report was prepared by Mr. Sánchez and Dr. Roig.

This report is being published by the WES Coastal and Hydraulics Laboratory (CHL). The CHL was formed in October 1996 with the merger of the WES Coastal Engineering Research Center and Hydraulics Laboratory. Dr. James R. Houston is the Director of the CHL and Messrs. Richard A. Sager and Charles C. Calhoun, Jr., are Assistant Directors.

At the time of the publication of this report, Director of WES was Dr. Robert W. Whalin. Commander was COL Bruce K. Howard, EN.

1 Introduction

Background

The lower St. Johns River is in the northeast portion of the Florida peninsula (Figure 1). The lower river includes approximately 177 km (110 miles) of tidally influenced river channel with a nominal width that varies from 183 m (600 ft) to 2.4 km (1.5 miles). Jacksonville Harbor is located approximately 34 km (21 miles) from the river mouth, which discharges into the Atlantic Ocean. A 42-km (26-mile) dredged navigation channel is maintained from the river mouth to Jacksonville to afford a minimum depth of 38 ft mllw[1]. Two parallel jetties, spaced 488 m (1,600 ft) apart, stabilize the entrance. At km 16 (mile 10) a large embayment known as Mill Cove opens onto the main stem of the St. Johns River. Between km 24.1 (mile 15) and km 25.7 (mile 16) there exists a second, larger opening between Mill Cove and the main stem of the River.

According to Brogdon (1979), "Tides occurring in the St. Johns River are semidiurnal in nature and have a mean range of about 5.2 ft at the entrance, which diminishes to about 2.0 ft at Jacksonville. The estuary is partially mixed, with differences between surface and bottom salinity concentration at the entrance of about 4.0 to 6.0 ppt. Under the influence of normal tides and freshwater discharge, salinity intrusion extends upstream about 32 miles.... Average freshwater discharge is about 4,475 cfs and ranges from negative freshwater inflow (evaporation exceeds inflows) in the summer months to 9,300 cfs in the winter months."

The U.S. Army Engineer District, Jacksonville, is seeking to improve tidal flushing in Mill Cove to maintain water quality and to prevent excessive sedimentation. The District also wants to increase water current velocities mainly in the southern part of the cove. Four plans have been proposed to reshape the shoreline within Mill Cove. One additional proposed plan will also modify the bathymetry of the cove. In this study a two-dimensional, vertically averaged hydrodynamic model was used to compare the circulation patterns that occur in the present-day Mill Cove against the circulation patterns that would result from the five plan configurations. Sediment transport was simulated using a

[1] All elevations (el) and depths in this report are in feet referred to mean lower low water (mllw). To convert to meters, multiply by 0.3048.

two-dimensional, vertically averaged model of sediment advection and dispersion in the water column, with the channel bed acting as a source and/or sink for sediment as it deposits and erodes. Two grain sizes were considered in separate simulations: fine sand and medium grained sand. Only noncohesive sediments were modeled.

The St. Johns River model was developed to study concurrently the Mill Cove hydrodynamic circulation and sediment transport, the hydrodynamic and sediment transport impacts of two navigation channel deepening plans, and the hydrodynamic impact of a third channel deepening plan derived from the previous two. The modeled effects of the channel deepening plans are to be reported in a separate navigation channel hydrodynamic and sediment modeling report. The model also produced the water current velocity vectors used in a ship simulator study, the results of which are reported separately (McCollum, in preparation). In the present report, the modeled currents and sediment transport for the Mill Cove plans are compared against the existing configuration. The study will address changes within the cove as well as any influence these changes may have in the navigation channel.

Objectives

The objectives of this study were as follows:

a. To investigate the flushing characteristics of Mill Cove by developing a two-dimensional, vertically averaged numerical model of the existing tidal hydrodynamics for the lower St. Johns River, with particular emphasis on the Mill Cove area.

b. To investigate the sediment transport characteristics by developing a two-dimensional, vertically averaged numerical model of the existing non-cohesive sediment transport in the lower St. Johns River.

c. To compare modeled circulation patterns for the existing Mill Cove shoreline against four engineering plans that involve modification of the Mill Cove shoreline and a fifth plan that also involves a change in bathymetry.

d. To compare the modeled tidal exchange through the Mill Cove inlets under base and proposed Mill Cove plans.

e. To compare modeled patterns of noncohesive sediment erosion and deposition under base and proposed Mill Cove plans.

2 Technical Approach

The Jacksonville District is interested in providing sufficient tidal exchange through the Mill Cove area to maintain water quality and to prevent excessive sedimentation within the cove. Five plans have been proposed to improve tidal exchange and increase water flow velocities in the southern part of Mill Cove. These plans involve modifications to the Mill Cove shoreline by means of diking and filling. Plan 5 also involves the modification of the bathymetry of the cove.

In this study, the changes in water flow and noncohesive sediment transport that would result if the proposed plans were built were tested using a two-dimensional, vertically averaged, numerical hydrodynamic model. The hydrodynamic model used in this study employs the Galerkin finite element formulation to solve the vertically averaged Reynolds form of the Navier-Stokes equations with hydrostatic assumption applied. These equations are commonly known as the vertically integrated shallow-water equations. The hydrodynamic model, known as RMA2-WES, was originally written by Dr. Ian King and Mr. William Norton of Resource Management Associates (RMA) in Lafayette, CA, under contract to the U.S. Army Corps of Engineers (USACE). The model is maintained and has been enhanced by personnel of the USACE Waterways Experiment Station (WES) in Vicksburg, MS. The version used in this study was RMA2-WES Version 4.295. The sediment transport model, known as SED2D-WES Version 1.05 (formerly STUDH), uses the Galerkin finite element formulation to solve the advection-dispersion equation for suspended sediment transport in the water column. The channel bed is considered to be either a source or sink of sediment, dependent upon the bed shear stress that results from the velocity field calculated by RMA2-WES. This sediment transport model was originally developed by Dr. Ranjan Ariathurai of RMA and has been subsequently maintained and enhanced by personnel of WES.

The numerical models RMA2-WES and SED2D-WES were chosen for this study for the following reasons. First, the finite element method permits the modeler to develop an unstructured mesh to define the channel geometry. The lower St. Johns River has many tributaries and secondary channels that are difficult to discretize in the sense of a structured, index-based grid. The finite element method uses freely connected three-sided and four-sided elements that are knitted together by means of an element connection table, thus permitting the modeler more flexibility to resolve important geometric features that may be required to accurately compute the flow field. Second, a vertically averaged

description of the hydrodynamics was sufficient to answer the questions that were posed concerning the relative impacts of the engineering plans on tidal flushing in Mill Cove. Third, RMA2-WES has been successfully applied in over 100 estuarine and riverine modeling studies conducted by the USACE. SED2D-WES and its predecessor, STUDH, have also been applied and tested in a variety of studies conducted by WES.

Hydrodynamic Model Data

The five Mill Cove plan simulations were compared against a base simulation that includes the existing 1995 ship channel and the present-day Mill Cove shoreline. The St. Johns River mesh was built using data from a variety of sources. The bathymetric data used to generate most of the numerical mesh were digitized from the National Oceanic and Atmospheric Administration (NOAA) Nautical Charts, National Ocean Survey (NOS) Nautical Chart No. 11491, November 20 , 1993 (27th ed.), and NOS Chart No. 11492, July 18, 1992 (17th ed.). The bathymetry of the navigation channel was provided by the Jacksonville District.

The grid for the existing (base) condition (Figure 2) has 9,806 elements, 28,835 nodes, and a maximum element front width of 324. The depths, in reference to the mean lower low water (mllw), range from 0.03 m (0.09 ft) along some lateral boundaries of the grid to 24.4 m (80 ft) at the jetties. Depths at the offshore boundary are between 15.2 and 18.3 m (50 and 60 ft). Most of the navigation channel is 12.2 m (40 ft) deep, except by the Blount Island Channel, 9.1 m (30 ft), and the Terminal Channel, which averages 10.7 m (35 ft) (Figure 3). The average depths in the Mill Cove area are between 0.3 m (1 ft) at the eastern end and 1.2 m (4 ft) at the western end. Depths in the rest of the mesh from Jacksonville to Buffalo Bluff range between 3.0 and 6.1 m (10 and 20 ft).

The numerical model mesh was carefully designed to address questions of navigation and circulation in the vicinity of the proposed projects. More resolution was added to the navigation channel and adjacent areas than to the rest of the grid. This resolution was needed to decrease errors within the study area and to provide a high-resolution flow field as input for the ship simulator. The average size of elements in the navigation channel were 152.4 m (500 ft) long and 51.8 m (170 ft) wide. The computational domain was extended far from the area of interest to ensure that the solution was not unduly influenced by errors in the boundary condition data. Lateral shoreline boundaries were smoothed to improve the accuracy of the mass conservation computations (McCollum and Donnell 1994).

The model hydrodynamic boundary conditions were the same for the base and the proposed plans. The water discharge into the system was constant. The tributary stream values (Table 1) were historical means collected from the U.S. Geological Survey (1992).

Table 1
Tributary Stream Values

Tributary	Discharge	
	cu m/sec	cfs
Black Creek	9.9109	350.00
Dunns Creek	4.5760	161.60
Deep Creek	0.2398	8.47
Rice Creek	5.4368	192.00
Julington Creek	0.3030	10.70
Oretga River	1.0194	36.00
St. Johns River at Buffalo Bluff	125.95	4,448.00

The offshore boundary was defined to be 7.02 km (4.36 miles) away from the coastline. A boundary condition was applied consisting of a dynamically varying water surface elevation representing the tidal fluctuations at sea (Figure 4). The tide selected for the runs was the spring tide of October 6, 1994. A period of large tidal range was chosen to provide the strongest currents for the ship simulator tests. The period of the initial simulation was 72 hours, which permitted the model to stabilize before the occurrence of the spring tide. This practice is commonly referred to as model spin-up. The 72 hours of simulation were divided into half-hour time-steps. Tide data were obtained from the TIDE 1 database package developed by NOAA. The most convenient tide gauge available was the Mayport station. To apply these tide data to the offshore boundary, it was necessary to amplify the tide range slightly, thus keeping the original tide as it reached the Mayport station.

Hydrodynamic Model Verification

The parameters available to calibrate the model are channel bed roughness and eddy viscosity. The roughness is controlled by means of the correct spatial assignment of the Manning's n coefficient values. The coefficient values are assigned by associating a material type with each of the elements in the mesh. Several different material types can be defined to describe the different physiographic regions of the estuary. For this model the material types represent either regions of a specific range of depth, an area of interest like the navigation channel, or an obstruction to the natural flow of the water. The assignment of material types by depth is equivalent to assigning materials that differ by vegetation cover and bed composition. The eddy viscosity coefficients describe the degree to which small-scale turbulent flow features dissipate energy in the flow field. A high eddy viscosity coefficient indicates high levels of turbulent energy dissipation. This parameter accounts for small-scale flow features that are not specifically resolved by the numerical mesh. Therefore the value of eddy viscosity is a function of both the local flow field and the local grid size. As a rule of thumb, eddy viscosity is often assigned according to a grid Peclet number

criterion. The grid Peclet number is defined (Brigham Young University 1994) as:

$$P = (\rho\ V\ \Delta x)/E_{ij} \quad (1)$$

where

ρ = density, kg/cu m (slugs/ft^3)

V = velocity along a particular streamline, m/sec (ft/sec)

Δx = mesh spacing, m (ft)

E_{ij} = turbulent eddy viscosity, Pa-sec (lbf-sec/ft^2)

A Peclet number less than 50 is desirable for numerical stability. This is the criterion that was applied for the assignment of eddy viscosity values in this study. Table 2 shows the resultant roughness and viscosity coefficients assigned for each material type in the St. Johns River numerical mesh. In one case, near the docking facility (material 5), an extremely high eddy viscosity value was applied to account for the energy dissipation caused by small-scale loading and docking facilities that are not explicitly resolved by the numerical mesh.

The platform used to run the model was a DEC 3000 Model 500 AXP workstation using the Digital Equipment Corporation 21064 RISC processor. On average the simulation required 12 central processing unit (cpu) hours to run the 72-hour simulation.

To verify the hydrodynamic model, the results were compared to prototype data collected by WES personnel. The prototype data available included flow discharge and velocity profiles at several river cross sections, or ranges, during an average time of 6 hours. Data were available for five to six ranges for each day during the period of October 2, 1994, to October 10, 1994. Also, the water surface elevation was measured at Mayport and South Jacksonville, FL, during the whole period. The spin-up time of the model was approximately 2 days; therefore, real-time comparison between the model and the prototype was done for the third day of simulation, which corresponded to October 6,1994 (spring tide).

Tide fluctuations from the model and prototype water surface elevations are compared in Figures 5 and 6. A nearly perfect fit of the model and prototype tidal waves at Mayport is observed. This result is to be expected since the tidal boundary condition was derived from the tidal record at Mayport. At Jacksonville, the tidal signal of the model has a phase lag of about half an hour when compared to the prototype; the tidal range is practically the same. In general, the tidal wave shape of the model is a satisfactory match to the prototype for the purposes of this study. The differences between model and prototype can be attributed to one of several causes. First, the river geometry is necessarily

Table 2
Material Type Properties

Material No.	E_{xx}		E_{xy}		E_{yx}		E_{yy}(lbf·s/ft²)		Mannings n	Description
	Pa-sec	lbf-sec/ft²	Pa-sec	lbf-sec/ft²	Pa-sec	lbf-sec/ft²	Pa-sec	lbf-sec/ft²		
1	2,872.8	60	2,872.8	60	2,872.8	60	2,872.8	60	0.024	6-24 m (20-80 ft) deep
2	2,872.8	60	2,872.8	60	2,872.8	60	2,872.8	60	0.024	Navigation channel
3	2,872.8	60	2,872.8	60	2,872.8	60	2,872.8	60	0.024	Navigation channel
4	3,351.6	70	3,351.6	70	3,351.6	70	3,351.6	70	0.031	Dock piers
5	4.788×10^6	1×10^5	4.788×10^6	1×10^5	4.788×10^6	1×10^5	4.788×10^6	1×10^5	0.027	Docking facility
6	38,304	800	38,304	800	38,304	800	38,304	800	0.024	Sea
7	33,516	700	33,516	700	33,516	700	33,516	700	0.024	Sea
8	19,152	400	19,152	400	19,152	400	19,152	400	0.024	Sea-channel transition
9	3,351.6	70	3,351.6	70	3,351.6	70	3,351.6	70	0.031	0-1.2 m (0-4 ft) deep
10	3,351.6	70	3,351.6	70	3,351.6	70	3,351.6	70	0.029	1.2-3 m (4-10 ft) deep
11	3,351.6	70	3,351.6	70	3,351.6	70	3,351.6	70	0.027	3-6 m (10-20 ft) deep
12	11,970	250	11,970	250	11,970	250	11,970	250	0.027	Docking facility
13	3,351.6	70	3,351.6	70	3,351.6	70	3,351.6	70	0.04	Sea marsh transition at Little Talbot Island

simplified for numerical simulation. In particular, the expansive tidal marshes on the north side of the river near its mouth were schematized for the purposes of this simulation. These marshes have a marked if unknown effect on the timing of the tide as it propagates through the system. Second, the tributary flows supplied to the model were historic mean flows, and not synoptic time-varying flows for the period of simulation. Because several of these tributaries no longer support active gauging stations, synoptic data were not available for the period of simulation. Last, the effects of winds were not explicitly accounted for in the simulation model. Wind effects were omitted because the objective of this study was to compare the impacts of the proposed plans on tidal circulation in the Mill Cove area. Winds induce varying effects that depend upon the speed, duration, and direction of the wind field. Choosing one wind field for simulation could possibly obscure the effects of the Mill Cove plans on the tidal circulation because of wind effects that are actually transient in nature.

During spring tide, prototype data were collected at ranges 24, 25, 26, 27, 28, and 29 (Figure 3). Flow discharges from the model and prototype are compared in Figures 7-12. The shapes of the flow discharge curves at all ranges for prototype and model are close, but in general the prototype has a half-hour delay in phase. For ranges 25-29 there is a shift of the prototype curves to the flood side. This situation is explained by the action of the 24- to 40-km/hr (15- to 25-mph) northeast winds that were present during the day of the survey and increased the flood discharge. "Winds have considerable effects on the water level and velocity currents. Strong northerly winds raise the water level about 2.0 ft at Jacksonville; strong winds from the opposite direction lower the water level about 1 ft and may increase or decrease flood and ebb current velocities" (Brogdon 1979). At range 24 the prototype discharge curve shifted to the ebb side, showing higher ebb discharge than the model. The cause for this difference in flow could be that the ebb currents at Drummond Creek Range have the resistance of the northeast winds and find it easier to deviate through Mill Cove. To confirm the statement about the effects of the winds over the currents, peak discharges in other parts of the channel (Figure 3) were compared (Table 3).

At range 5 the maximum ebb discharge from the prototype was very close to the model value, even when the prototype tidal range was smaller than the model tidal range. Winds during that day were in favor of the ebb currents. The prototype ebb discharge at range 16 was very low compared with the model discharge. At the time of the survey, the tidal range was smaller in the prototype than in the model. On this day the winds were in the opposite direction to the ebb current. The day when data for range 41 were collected had negligible winds and as a result the discharges were as expected; flood discharge in the prototype was slightly smaller than in the model due to the smaller tidal range of the prototype.

From the previous description it can be concluded that the wind is an important variable in the complex St. Johns River estuary system. Although the wind forces are not simulated by this model, the water flow discharges through the system were acceptable considering that the tests the model is required to make are fairly insensitive to model adjustment. As expected, the velocities in

Table 3
Model Verification of Maximum Discharges

Range	Date and Prototype Time hr	Maximum Prototype Discharge cu m/sec (cfs)	Model Time hr	Maximum Model Discharge cu m/sec (cfs)	Percent Error	Winds km/hr (mph)
5	10/2/94 10:20	6,512 (229,990) (ebb)	67.7	6,529 (230,600) (ebb)	0.26	SW 16-32 (10-20)
16	10/4/94 14:06	4,535 (160,160) (ebb)	68.0	5,808 (205,100) (ebb)	28.06	NE 32-48 (20-30) AM 24-32 (15-20) PM
41	10/9/94 13:45	4,032 (142,406) (flood)	63.0	4,276 (151,000) (flood)	6.03	Calm morning Light SE afternoon

the model were consistent with a depth-averaged value of the velocities measured in the prototype.

Sediment Transport Model Data

The data available for the development of the unverified sediment model were a maintenance dredging map dated November 12, 1993, and historical core boring logs of the navigation channel from 1960 to 1993. Both sources of information were provided by the Jacksonville District. Erosion and shoaling problems were identified by District personnel. Based on the information provided, the predominant bed material in the navigation channel was determined to be fine- to medium-grained sand.

Sediment Transport Model Verification

The state of the art in cohesive sediment transport modeling is such that extensive field data are required to calibrate such a model and to define the sediment properties. The data collection effort required to perform a cohesive sediment modeling study was beyond the scope of this project. Noncohesive sediment modeling was used to determine whether the proposed Mill Cove plans would induce significantly different sediment transport behaviors than are observed under the existing conditions.

Two runs were made for the existing condition and each of the first four plans. One run considered sand grains sized 0.08 mm (2.625×10^{-4} ft) in diameter (fine-grained sand) while the other run considered sand grains sized 0.20 mm (6.562×10^{-4}) ft in diameter (medium-grained sand).

The initial bed condition for the sediment study was a sand bed of uniform thickness over the mesh. This is not a realistic condition because, in reality, the sand bed varies in thickness over the estuary. However, this initial condition permitted the modeler to observe the potential rates of erosion that would occur given an infinite supply of sand from the bed. This is useful when comparing the potential for erosion between base and plan conditions. The result is that erosion will be overestimated when compared with the prototype, which has a limited supply of sediment from the bed; but the comparisons between base and plan will be consistent.

The model was calibrated by adjusting the roughness and fall velocity of the sand particles on a regional basis. The modeled sediment erosion and deposition patterns were found to be qualitatively similar to those observed in the prototype. The roughness of the sand grains is described by the effective Manning coefficient. The roughness values used were between 0.001 in the navigation channel and 0.027 on the banks of the river. The fall velocity for the fine-grained sand was 0.0025 m/sec (0.0082 ft/sec) and 0.020 m/sec (0.066 ft/sec) for the medium-grained sand.

The sediment simulation period was 15 days and 15 hours. The flow field used to drive the sediment transport model was generated by RMA2-WES. A limitation of the SED2D-WES model is that the sediment computations are effectively decoupled from the hydrodynamic computations. This limitation can be overcome by periodically updating the hydrodynamic flow field. In other words, any changes in the flow field that would occur due to erosion or deposition of the channel during the SED2D-WES run require the RMA2-WES model to be run again with the new channel bathymetry applied. It was determined through model testing that the rates of erosion and deposition in the St. Johns River would permit the sediment transport model to be run for approximately 3 days before updating the RMA2-WES flow field. The sequence of simulation for running the sediment transport model was as follows:

a. *Step 1.* The hydrodynamic model, RMA2-WES, was run for 72 hours to develop a realistic flow field. The boundary conditions applied were the same as those described for the verification of the hydrodynamic model. The bathymetry for this model run was the original bathymetry developed from the navigation charts.

b. *Step 2.* The flow field resulting from Step 1 was used as an initial condition for an RMA2-WES simulation with the 19-year mean tidal elevation signal applied at the ocean boundary. This tidal signal was obtained from the Tide Tables for 1982 (U.S. Coast and Geodetic Survey 1982). The tidal signal was repeated for the duration of the simulation period, which was 3 tidal days or 75 hours. The bathymetry for this model run was the original bathymetry.

c. *Step 3.* The sediment transport model, SED2D-WES, was run using the flow field developed in the preceding RMA2-WES run. The simulation period for this SED2D-WES run was 3 tidal days or 75 hours. The bed of the estuary was allowed to erode and deposit sediment as dictated by the

model equations. At the end of the run, a new bathymetry file was saved reflecting the bed changes that occurred during 3 days of sediment simulation.

d. *Step 4*. The flow field generated by the previous RMA2-WES run was used as an initial condition for a new RMA2-WES simulation using the 19-year mean tidal elevation signal at the ocean boundary and the bathymetry derived from the previous SED2D-WES run. The duration of the new RMA2-WES simulation was 3 tidal days.

e. *Step 5*. Steps 3 and 4 were repeated until a total of 15 tidal days of sediment transport simulation were accomplished. The final product of this simulation is a map of net bed change over the 15-day simulation period.

3 Model Results

Base Versus Plan Hydrodynamic Model Results

The numerical meshes used for the base and proposed plans in the Mill Cove area are illustrated in Figures 13-18. The plans to be tested were provided by the Jacksonville District. The purpose of these plans is improving tidal flushing in Mill Cove to maintain water quality and to prevent excessive sedimentation mainly in the southern part of the cove. In Plan 1 the west opening between Quarantine Island and an island used as spoil area was closed. Plan 2 is the same as 1 with the addition of another closure between Quarantine Island and William Island. Plan 3 is the same as Plan 2 with the addition of a third closure between the east end of Quarantine Island and Marion Island. Plan 4 is a modification of Plan 3 with a change in the shape of the second closure. The bathymetry of the open water areas remained unchanged under each of the first four plans.

Plan 5 is another modification to Plan 3 that includes the addition of a circulation channel, the shallowing of some areas, and the extension of the second closure by reaching Newcastle Island. The circulation channel is located mainly at the south of the bay and extends from the northeast opening to the west opening of the bay. At the western opening, the channel is 3.6 m (12 ft) deep, 198 m (650 ft) wide, and 1,158 m (3,800 ft) long. At the northeast opening, the channel is 3.6 m (12 ft) deep, 396 m (1,300 ft) wide, and 1,036 m (3,400 ft) long. The rest of the circulation channel is 1.8 m (6 ft) deep and 24 m (80 ft) wide. Shallowing of the north part of the bay was done by gradually decreasing depth between the circulation channel and the northern coastline (Figure 19). In general, the depths at the north are less than 0.9 m (3 ft).

RMA-WES permits the user to specify a list of nodes where summaries of the output will be printed. The output summary is a time-history of the Cartesian velocity components and the water surface elevation over the period of simulation. In addition, continuity check lines can be specified at various cross sections to calculate the discharge across the check line at each time-step of simulation. Eleven time-history nodes were located in the Mill Cove area (Figure 20) to measure differences in the computed velocities and the computed water surface elevations caused by the testing of the five plans. For convenience, station numbers will be discussed instead of node numbers (Table 4). Continuity check

Table 4
Assignment of Station Number to the Corresponding Numerical Mesh Node

Station No.	Node Number of Base and Plans 1,2,3, and 4	Node Number for Plan 5
1	16964	18012
2	16993	18162
3	15984	17743
4	16000	17012 16699 (circulation channel)
5	15315	17245
6	15327	16681
7	14205	16969
8	13799	12419
9	12390	12013
10	12148	11851 11843 (circulation channel)
11	11430	11249
12[1]	20969	20931
13[1]	16045	15309
14[1]	10663	10231

[1] Stations 12-14 are in the navigation channel and will be discussed in the section, "Effects of the Mill Cove Plans on the Navigation Channel."

lines were placed at two openings of Mill Cove into the main river to detect changes in the volume of water flowing through the cross-section.

The depth at each station during existing conditions and the magnitude of total velocity for every model run are plotted in Figures 21-45. Water surface elevation at stations 2,7, and 9 is also included to detect any considerable change in the cove caused by the proposed plans. Plots of the flow discharge at ranges 24 and 35+36, which are located in the two Mill Cove openings, are presented in Figures 46 and 47. These discharges will be used to calculate the tidal flushing in the cove. Velocity vector plots of the maximum ebb and flood discharges show water flow patterns during existing conditions and proposed plans. These vector plots are displayed in Figures 48-59.

Plan 1

The maximum magnitude of velocities at the eastern and central parts of the Mill Cove area increased between 6 percent and 18 percent. Velocities increased at the north of the central islands (station 7) by 8 percent, but were unchanged at

the south (station 8). The northwest part of the area (station 9) kept the same velocity magnitude during flood, but it decreased by 40 percent during ebb flow. At the southwest part of the area (station 10) the velocity magnitude increased 10 percent during flood and decreased 8 percent during the ebb. The maximum velocity magnitude decreased by 7 percent during flood at the western opening (station 11), but increased 19 percent during ebb tide. Also, the maximum magnitude of flood velocity was delayed by 1 hour and the maximum for ebb was delayed by 2.5 hr. There was an average reduction in the tidal range of 0.036 m (0.12 ft) (3.3 percent) from 1.10 m (3.62 ft) at the center of the Mill Cove area.

A 12 percent increase of the maximum flood discharge and a 9 percent increase of the maximum ebb discharge was observed at range 24. Ranges 35+36 had a 13 percent decrease in the maximum flood discharge and a 32 percent decrease in the maximum ebb discharge. These reductions are caused by the closure of the opening where Range 35 was located. Range 35 is not active in any of the plans.

Plan 2

The maximum velocities in the eastern part of the cove were increased, but were slightly smaller than for Plan 1. At station 4 the maximum ebb velocity was increased by 4 percent compared to 16 percent from Plan 1. From stations 5 and 6 a slight increase in the maximum ebb velocity of 3 percent and approximately a 13 percent decrease during flood were observed. At the south of the second closure (station 8) a 92 percent increase in the maximum flood velocity and a 61 percent increase for ebb occurred. Near the last closure (station 7), maximum velocity magnitudes dropped by 54 percent on average. The maximum velocity magnitudes at station 9 were greatly affected. A 37 percent reduction in velocity magnitude was observed during flood and 54 percent during ebb. At the southwestern part of the area (station 10) the maximum velocity during flood was reduced by 5 percent and during ebb by 18 percent. Station 11 had a 23 percent reduction in maximum flood velocity and 10 percent increase in maximum ebb velocity. The tide range on the eastern side of the second closure (station 7) was increased by 0.061 m (0.2 ft) (5.4 percent) and decreased 0.076 m (0.25 ft) (7.0 percent) to the west (station 9).

At range 24 the maximum flood discharge increased 11 percent and the maximum ebb increased 8 percent; here the values were 1 percent lower than in Plan 1. A 29 percent decrease in the maximum flood discharge was observed at ranges 36+35; this change was bigger than the change observed under Plan 1. A decrease of 34 percent of the maximum ebb discharge occurred at the same location.

Plan 3

The maximum magnitude of velocities at the eastern opening of the Mill Cove area was increased by one-half of the increase observed under Plan 1. At the east the maximum magnitude of velocities increased approximately 23 percent. The

velocities to the west of the third closure (station 3) dropped almost to zero; at the south of the same closure the velocities were increased by 44 percent on average. A reduction of 10 to 20 percent of the maximum velocities was experienced in the central area (stations 5 and 6). Velocities to the south of the second closure were significantly increased, but not as much as for Plan 2. At the east of the same closure the reduction in velocities was slightly larger than the one created by Plan 2. The western area of Mill Cove did not suffer any considerable change in the magnitude of velocities. The tidal range increased 2 percent at station 7. A bigger effect occurred at station 9 where the tidal range was decreased by 0.082 m (0.27 ft) (7.7 percent).

At range 24 the maximum flood discharge was increased by 5 percent and the ebb by 4 percent. A decrease in the discharge of 31 percent was observed during maximum flood and of 26 percent during maximum ebb at ranges 36+35.

Plan 4

The maximum velocities follow closely the values obtained from Plan 3. The exception to this occurs at station 7, where the velocities are higher than Plans 2 and 3, but are far below the existing conditions and Plan 1. At station 9 velocities were lower than any other plan. In general the maximum velocities at the southwestern part of Mill Cove were slightly lower than Plan 3 during ebb tide. No considerable change in water head occurred between Plan 3 and Plan 4.

The water discharge at range 24 was less than 2 percent smaller than Plan 3. At range 36 there was a 2 percent decrease in the maximum flood discharge and an 11 percent decrease in the ebb when compared to Plan 3.

Plan 5

The numerical mesh for Plan 5 was renumbered due to considerable modifications. Nodes of the numerical mesh at the same location of the nodes selected for other plans were examined to compare the results of Plan 5 to the previously tested plans. Two extra nodes in the circulation channel were selected because the original nodes were near but outside the circulation channel. The new node number corresponding to each station is presented in Table 4.

At station 1 the maximum flood velocity was decreased to 0.378 m/sec (1.24 ft/sec), a 24.4 percent decrease. The decrease in maximum ebb velocity was 12.6 percent for a new value of 0.381 m/sec (1.25 ft/sec). This reduction in velocities was due to the widening and deepening of the northeast opening. The rest of the plans showed increased velocities.

The increase in maximum velocities at station 2 for Plan 5 was approximately two times greater than for any other plan. The maximum flood velocity was increased by 71.2 percent from the original velocity of 0.049 m/sec (0.16 ft/sec) to the new velocity of 0.082 m/sec (0.27 ft/sec). During ebb, the maximum velocity was increased to 0.085 m/sec (0.28 ft/sec), a 43.9 percent change.

At station 3 the velocities were less than 0.03 m/sec (0.1 ft/sec), considered negligible as in Plans 3 and 4. This result satisfies the objective of having lower velocities at the north of the Mill Cove area.

Out of all of the plans, Plan 5 resulted in the highest velocity at station 4. The new maximum flood velocity was 0.408 m/sec (1.34 ft/sec), a 55.8 percent increase. The maximum ebb velocity was increased by 42.6 percent from 0.308 m/sec (1.01 ft/sec) to 0.436 m/sec (1.43 ft/sec). Maximum velocities in the circulation channel near station 4 were even higher, 0.439 m/sec (1.44 ft/sec) and 0.482 m/sec (1.58 ft/sec) for flood and ebb, respectively.

In Plan 5 the maximum ebb velocity was increased at station 6 more than the other plans, followed closely by Plan 1; Plan 5 increased the maximum velocity to 0.232 m/sec (0.76 ft/sec), a 20.5 percent change. During flood, the maximum velocity was decreased by 2.3 percent from 0.241 m/sec (0.79 ft/sec), falling short of the performance obtained from Plan 1, an increase in velocity of 8.5 percent.

At stations 5,7, and 9, a reduction in velocities is desirable to increase sediment deposition and therefore shift most of the water flow to the southern part of the cove. The maximum velocities at station 5 were reduced by amounts similar to the ones obtained by Plan 3 and 4. During flood the maximum velocity was decreased by 18.2 percent from 0.256 m/sec (0.84 ft/sec), and the maximum ebb velocity was decreased to 0.195 m/sec (0.64 ft/sec), a 10.6 percent change. The velocities at station 7 were reduced more than in any other plan. The maximum velocities during existing conditions were 0.213 m/sec (0.70 ft/sec) and 0.186 m/sec (0.61 ft/sec) for flood and ebb, respectively. The reduction in maximum flood velocity using Plan 5 was 71.5 percent, and the reduction in maximum ebb velocity was 75.8 percent. At station 9 the maximum velocities were considerably reduced by Plan 5, although Plans 2, 3, and 4 had a greater reduction. The reductions were 34.4 percent from 0.155 m/sec (0.51 ft/sec) to 0.100 m/sec (0.33 ft/sec) and 46.6 percent from 0.210 m/sec (0.69 ft/sec) to 0.113 m/sec (0.37 ft/sec) for flood and ebb, respectively.

Station 8 had by far the highest maximum velocities when using Plan 5. The maximum flood velocity was increased by 148.1 percent, and the maximum ebb velocity was increased by 122.3 percent. Original maximum velocities for flood and ebb were 0.198 m/sec (0.65 ft/sec) and 0.174 m/sec (0.57 ft/sec), respectively.

During flood the maximum velocity at station 10 was increased by 6.9 percent for a value of 0.137 m/sec (0.45 ft/sec). The maximum ebb velocity was increased to 0.146 m/sec (0.48 ft/sec), a 13.6 percent change. This increase was slightly higher during flood in Plan 1, which had the same velocity encountered in the circulation channel of Plan 5, 0.140 m/sec (0.46 ft/sec). With Plan 5, the maximum ebb velocity was the same at station 10 and in the circulation channel.

At the western opening, where station 11 is located, the maximum flood velocity was greatly decreased by 39.6 percent to a value of 0.268 m/sec (0.88 ft/sec); this maximum velocity was the smallest of all the proposed plans. During ebb the maximum velocity was kept almost at the same magnitude, with only a slight increase of 3.1 percent to reach a velocity of 0.399 m/sec

(1.31 ft/sec). Plan 5 also suffered the change in phase experienced by the rest of the proposed plans; the maximum flood velocity had a delay of 1.5 hours and the maximum ebb, 2.5 hours when compared to the existing conditions.

The maximum water surface elevation at station 2 was increased from 1.652 m (5.42 ft) to 1.676 m (5.50 ft), and the minimum water surface elevation was decreased from 0.366 m (1.20 ft) to 0.338 m (1.11 ft) for a tidal range increase of 4.2 percent.

At station 7 the maximum water surface elevation was increased by 2.6 percent for a value of 1.640 m (5.38 ft), and the minimum water surface elevation was decreased by 4.3 percent for a value of 0.454 m (1.49 ft). Therefore, the tidal range was increased by 5.5 percent.

Contrary to the previous stations, the tidal range at station 9 was decreased by 8.9 percent. The maximum water surface elevation was reduced from 1.579 m (5.18 ft) to 1.545 m (5.07 ft), and the minimum water surface elevation was raised from 0.500 m (1.64 ft) to 0.561 m (1.84 ft).

With Plan 5, the changes in the tidal range within the cove were slightly greater than with the rest of the proposed plans. The magnitude of the changes is still small and does not represent an adverse effect to Mill Cove.

At range 24 the maximum flood discharge was increased 3 percent and the ebb by 27 percent. A decrease in the discharge of 29 percent was observed during maximum flood and a decrease of 35 percent was observed during ebb at ranges 36+35.

Net Water Discharge and Tidal Flushing in Mill Cove

The net water discharge at two additional sections, sections 1 and 2 (Figure 20), for the existing conditions and the proposed plans was calculated (Table 5). Figures 60 and 61 show graphic representations of the results.

The net water discharge at each section was calculated by means of the integration of the water discharge values at each time-step through the last tidal cycle of the simulation, hours 59.5 to 72.0. The net flow through Mill Cove during this specific period was in the flood direction. All the plans but Plan 1 reduced the net flow of water through the cove in a similar way. Plan 1 showed a slight increase at Section 1, and about half the decrease achieved by the other plans at Section 2.

The volume of water used for the tidal flushing calculations was computed as the tidally averaged water volume in the cove between the northeast and west openings to the main river. The procedure was to calculate the average water surface elevation at Mill Cove during the last tidal cycle. This value was applied as the boundary condition during a steady state run of the model. A new material type was assigned to the area of interest, allowing the model to calculate the water volume for each material type.

Table 5
Net Water Discharge Rate at Sections 1 and 2

Plan	Section 1			Section 2		
	Net Water Discharge Rate, Flood		Change %	Net Water Discharge Rate, Flood		Change %
	cu m/sec	cfs		cu m/sec	cfs	
Base	54.1945	1,915		39.903	1,410	
1	55.5812	1,964	2.6	33.5072	1,184	-16.0
2	43.1009	1,523	-20.5	26.036	920	-34.8
3	43.2424	1,528	-20.2	26.6303	941	-33.3
4	41.601	1,470	-23.2	27.4793	971	-31.1
5	44.2046	1,562	-18.4	26.0643	921	-34.7

The flushing time was calculated as the number of tidal cycles required to completely replace the water volume in Mill Cove (Table 6). This was done by the simple integration of all the water flowing into the cove through ranges 24, 35, and 36 during a tidal cycle. Any flow out was set to zero. Figures 62, 63, and 64 show graphic representations of the water volume, water flow into Mill Cove during one tidal cycle, and flushing time, respectively.

Table 6
Water Volume, Water Inflow During One Tidal Cycle, and Flushing Time at Mill Cove

Plan	Volume		Water Flow into Mill Cove During One Tidal Cycle		Flushing Time No. of cycles
	10^6 cu m	10^6 cu ft	10^6 cu m	10^6 cu ft	
BASE	26.4404	944.3	30.254	1,080.5	0.92
1	26.4572	944.9	21.5012	767.9	1.23
2	25.746	919.5	19.866	709.5	1.30
3	25.6368	915.6	19.1856	685.2	1.34
4	24.2368	865.6	18.5584	662.8	1.31
5	25.4492	908.9	18.2084	650.3	1.40

All the plans experienced an increase in flushing time. Plan 5 experienced the largest change, with an increase of 52 percent. The calculated flushing time values do not guarantee that the volume of water contained within the area of interest is going to be completely replaced. The water movement through the cove depends on local flow patterns and can be affected by the existence of stagnation zones.

Note that the tidal signal applied to the model was nonrepeating (a real spring tide was used) and that the duration of one tidal cycle is 12.42 hours. Therefore, the

calculated net discharges through Mill Cove and the flushing time do not represent the long-term mean values and are only a representation of the specific model conditions.

Effects of the Mill Cove Plans on the Navigation Channel

Plan 5 will improve navigation conditions in the main navigation channel by reducing the magnitude of crosscurrent velocities at each of the openings of the Mill Cove area (Figures 22 and 45).

Three stations located in the main river were selected to explore any adverse effect of the proposed Mill Cove plans on navigation (Figure 65). Plots of the velocity magnitude and water surface elevation at each station (Figures 66-71) do not show a considerable change.

Base Versus Plan Sediment Model Results

In this section the results of the runs using fine-grained sand are summarized. Runs made using medium-grained sand were representative of the same erosion patterns but on a smaller scale because of the reduced mobility of the larger grained sediment. Contours of the bed change as a result of the sediment runs are shown in Figures 72-81. The scope of this study did not include a sediment transport model for Plan 5.

Plan 1

At the eastern opening, erosion was increased from 0.128 to 0.265 m (0.42 ft to 0.87 ft) at the west bank and from 0 to 0.372 m (0 ft to 1.22 ft) at the east bank. Erosion was a problem in the western opening where erosion increased from 0.036 to 0.546 m (0.12 ft to 1.79 ft).

Plan 2

The erosion at the western opening was lower than Plan 1, totaling 0.418 m (1.37 ft). The opening located at the east of the Mill Cove area had erosion of 0.280 m (0.92 ft) in the west bank and 0.213 m (0.7 ft) in the east bank. Up to 0.917 m (3.01 ft) of new erosion took place between William Island and Newcastle Island.

Plan 3

The erosion was 0.652 m (2.14 ft) in the western opening, higher than the rest of the plans. Erosion was lower than for Plan 2 between the islands located at the

center of the area, 0.555 m (1.82 ft). The eastern opening also had lower erosion than Plan 2, 0.164 m (0.54 ft) at the west bank and 0.107 m (0.35 ft) at the east bank.

Plan 4

Erosion created with Plan 4 was lower than with the rest of the plans, but not lower than existing conditions. At the western opening, the erosion was 0.357 m (1.17 ft). Erosion was 0.143 and 0.067 m (0.47 ft and 0.22 ft) at the west and east banks of the eastern opening, respectively. Between the central islands the erosion was 0.347 m (1.14 ft), less than Plans 2 and 3.

Table 7
Reduction in Deposition Rate at the East Section of Fulton-Dame Point Cutoff Range

Plan	Reduction in Deposition Rate, %
1	4.7
2	7.6
3	10.2
4	11.6

Fulton-Dame Point Cutoff Range

There is great concern about the excessive sediment deposition occurring under existing conditions in the eastern section of the Fulton-Dame Point Cutoff Range. The deposition rate was reduced when each of the proposed plans, 1 through 4, was applied (Table 7). Plan 4 caused the most significant change with an 11.6 percent reduction in the deposition rate.

Table 8
Increase in Deposition Rate at the Eastern Half of Drummond Creek Range

Plan	Reduction in Deposition Rate, %
1	33.5
2	44.8
3	44.8
4	44.0

Drummond Creek Range

The partial closure of Mill Cove's western opening to the main river resulted in a change in sediment transport patterns at Drummond Creek Range. Sediment material, eroded from the river banks, increased. Most of this material deposited in the navigation channel section located in front of the closure. All of the proposed plans show this same behavior. The magnitudes of the deposition rate increases estimated from the model are given in Table 8.

Note that this is an unverified sediment model; therefore, the results have to be interpreted as a potential for deposition or erosion, not as the exact values.

4 Conclusions

In general, the maximum velocities obtained from Plan 5 at the south of the Mill Cove area were higher than any of the other proposed plans. The maximum velocities at the north were greatly decreased, similar to the results obtained from Plans 3 and 4.

Plan 5 reduced water current velocities at the openings of the Mill Cove area more than any other plan. This situation improved navigation conditions in the main river.

All the plans increased flushing time. Plan 5 experienced the largest change, with an increase of 52 percent.

When the proposed plans were modeled, the water surface elevation did not suffer considerable changes within the cove.

The first four plans do not produce a dramatic general improvement in the water velocities through Mill Cove. However, the plans do offer some localized improvements and may warrant special consideration to address other needs. There were local increases in velocity. An increase in the flow velocity was observed at the south of each of the closures, but the currents were in general weaker between them. All the plans offer new areas for dredged material disposal, with Plan 4 the one offering the greatest potential.

Plans 1 through 4 experienced increased sediment erosion at the eastern and western openings of Mill Cove. Plan 4 had the lowest increase in erosion. All the plans included the partial closure of Mill Cove's western opening to the main river. This closure resulted in sediment erosion of the river banks at Drummond Creek Range and deposition of this material in the navigation channel. The sediment deposition rate in the eastern section of the Fulton-Dame Point Cutoff Range was reduced when each of the proposed plans was applied. Plan 4 caused the most significant reduction with 11.6 percent.

Three objectives of the Mill Cove study were to increase the water velocities at the south of the area, decrease the velocities at the north, and reduce the flushing time in the cove. Although Plan 5, as well as the others, did not reduce the flushing time in the cove, it is the proposed design that meets the first two objectives most

consistently. Plan 5 also reduced the strength of the water crosscurrent velocities in the river navigation channel coming from Mill Cove.

References

Brigham Young University. (1994). "TABS primer," Brigham Young University Computer Graphics Laboratory, Provo, UT.

Brogdon, N. J., Jr. (1979). "Mayport-Mill Cove model study; Report 1, Hydraulic, salinity, and shoaling verification; Hydraulic model investigation," Technical Report HL-79-12, U.S. Army Engineer Waterways Experiment Station, Vicksburg, MS.

McCollum, R. A. "Jacksonville Harbor, St. Johns River, Florida, navigation study" (in preparation), U.S. Army Engineer Waterways Experiment Station, Vicksburg, MS.

McCollum, R. A., and Donnell, B. A. (1994). "Claremont Terminal Channel, New York Harbor," Technical Report HL-94-14, U.S. Army Engineer Waterways Experiment Station, Vicksburg, MS.

U.S. Coast and Geodetic Survey. (1982). "Tide tables, high and low water predictions, East coast of North and South America, including Greenland," Washington, DC.

U.S. Geological Survey. (1992). "Water Resources Data for Florida, Water Year 1992, Vol 1A: Northeast Florida—Surface Water," Report FL-92-1A, National Technical Information Service, Springfield, VA.

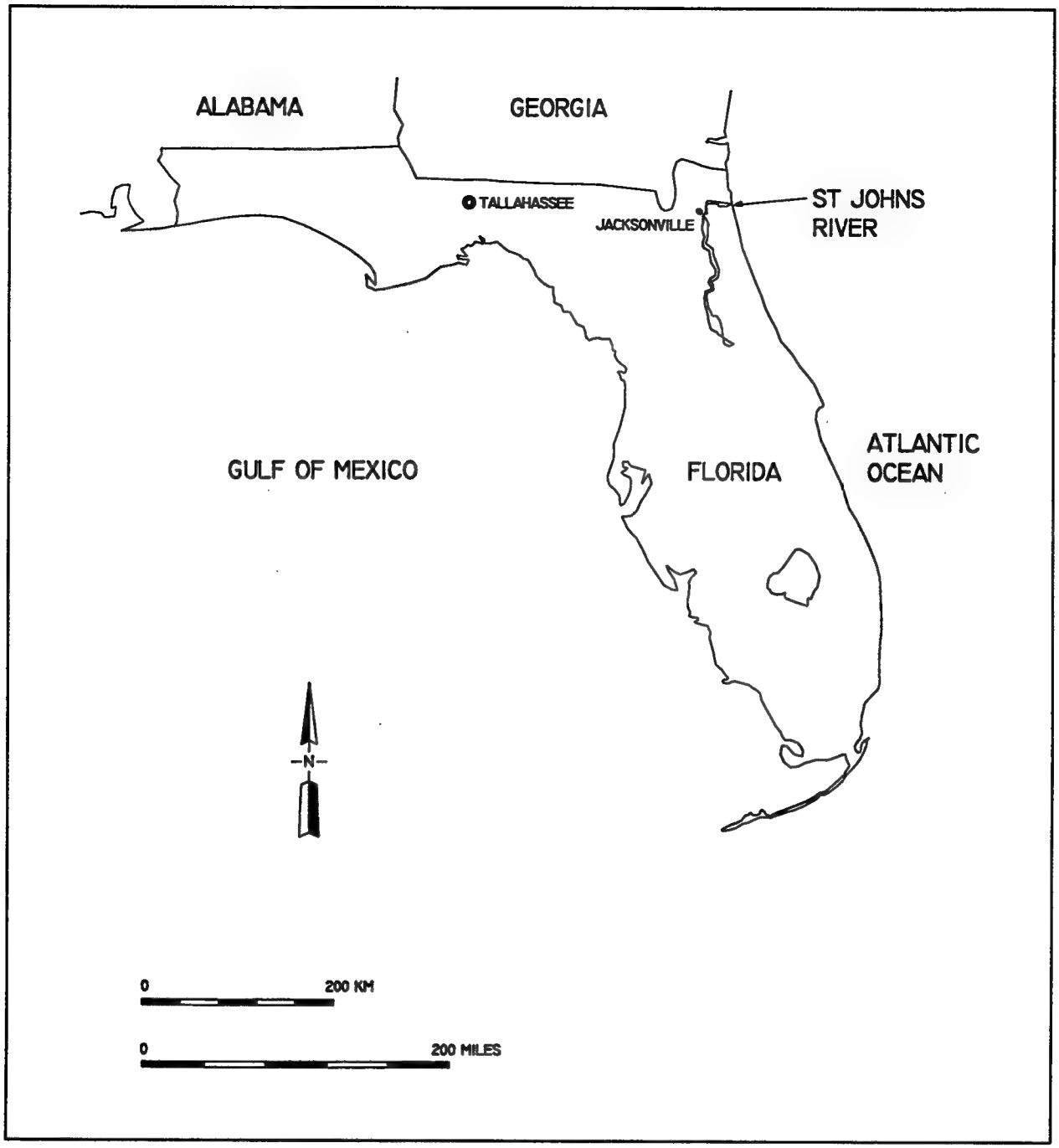

Figure 1. Location map

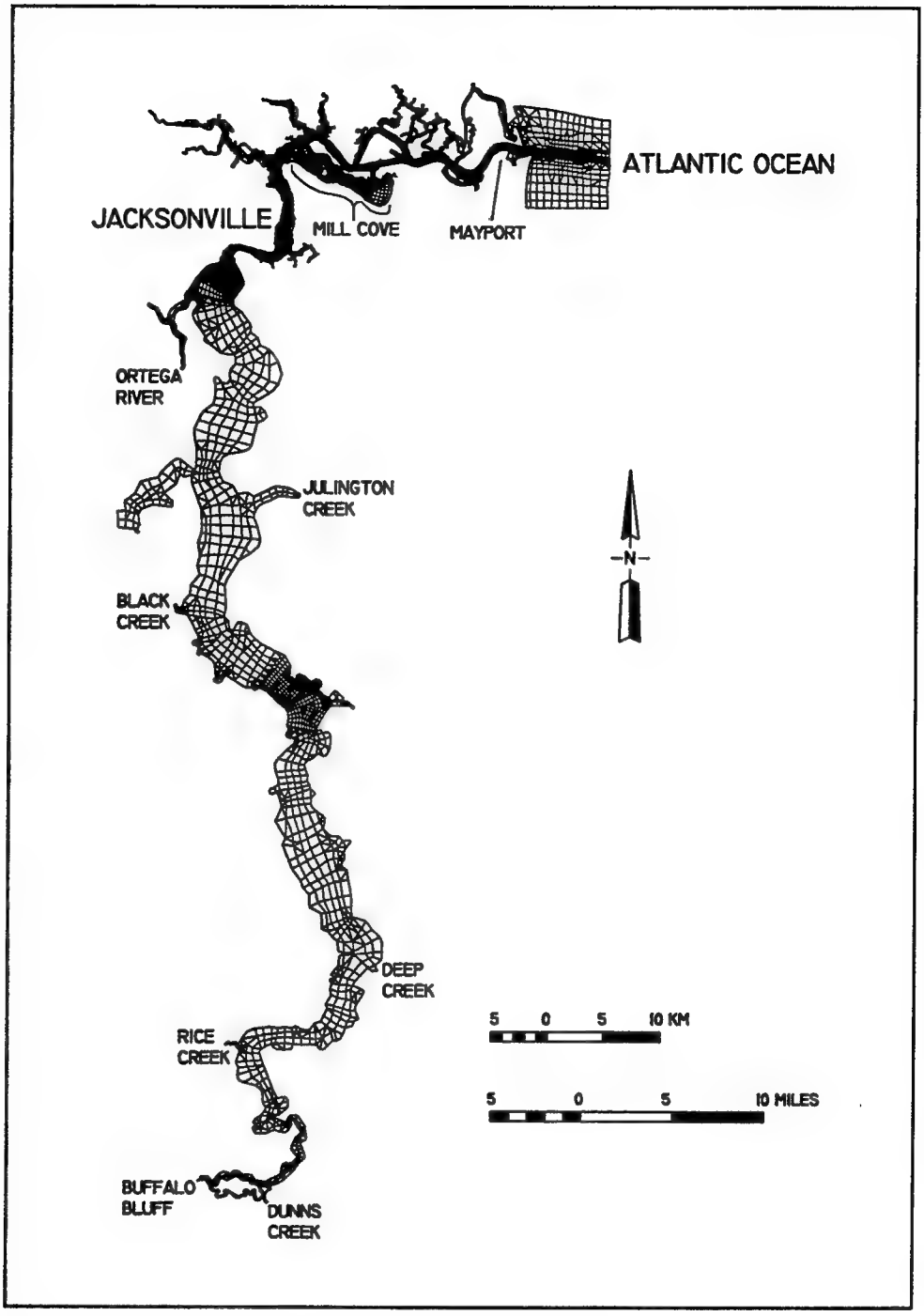

Figure 2. Numerical mesh for the lower St. Johns River

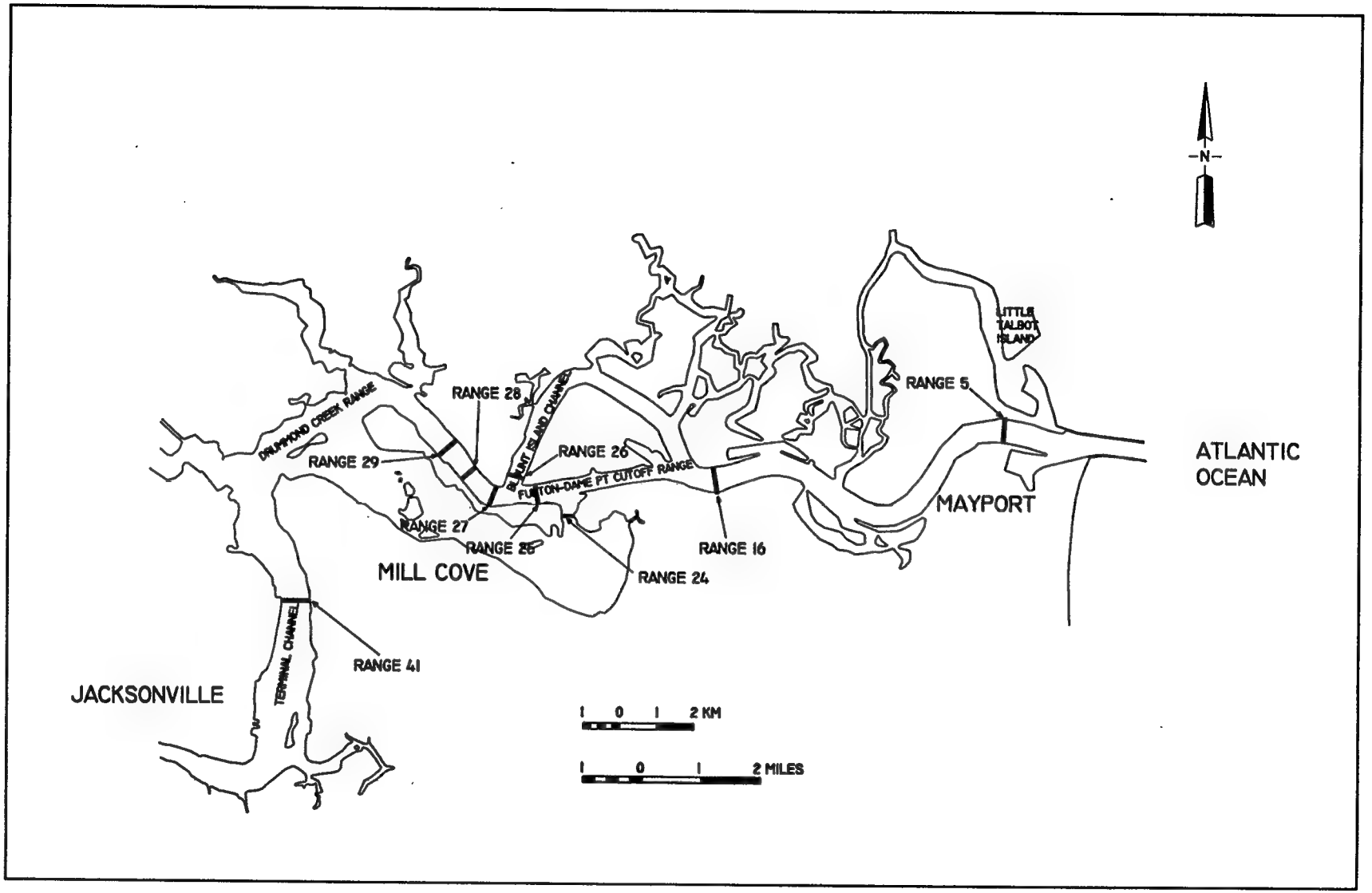

Figure 3. Location of ranges used for model verification

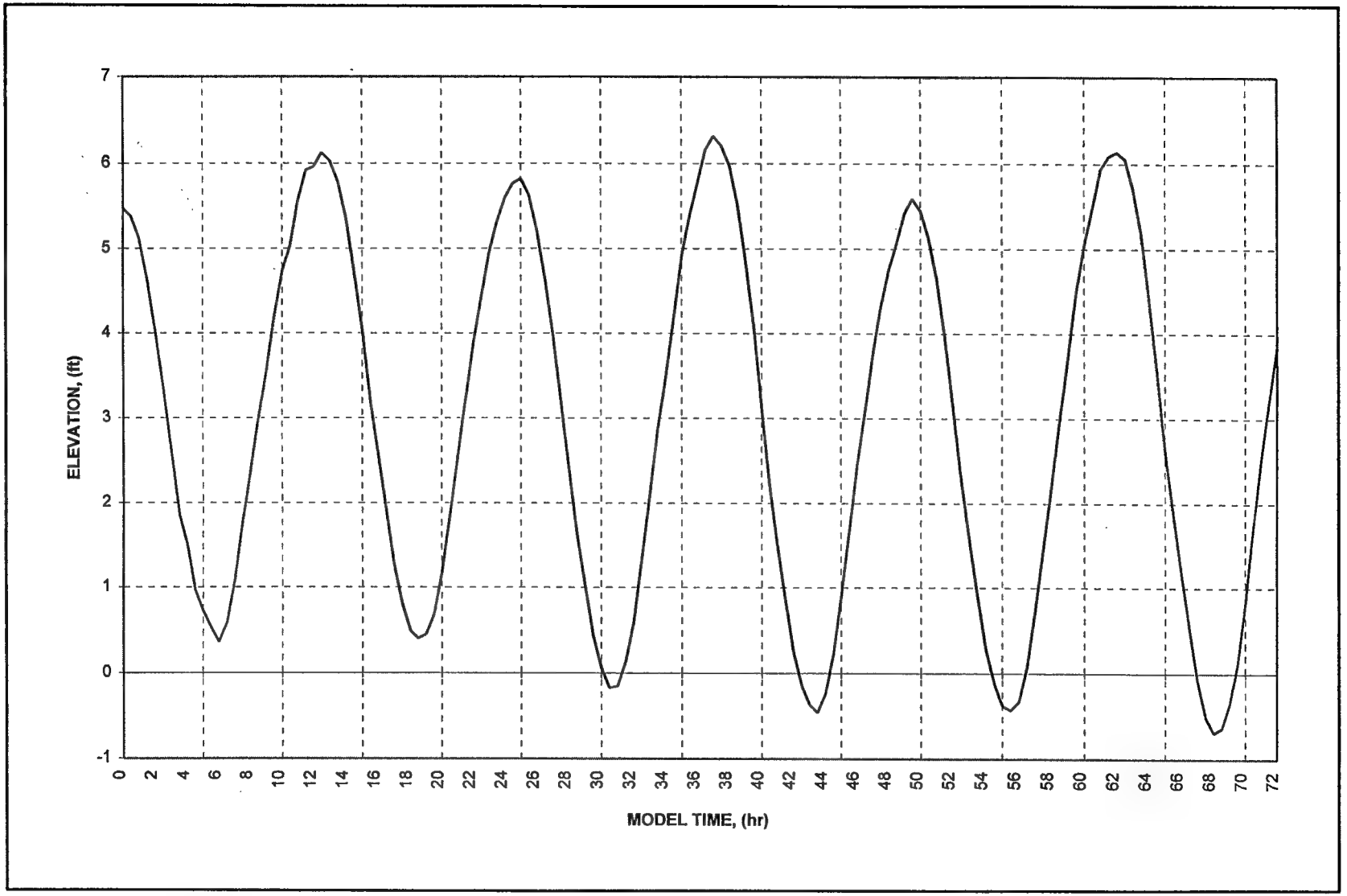

Figure 4. Water surface elevation at boundary (offshore)

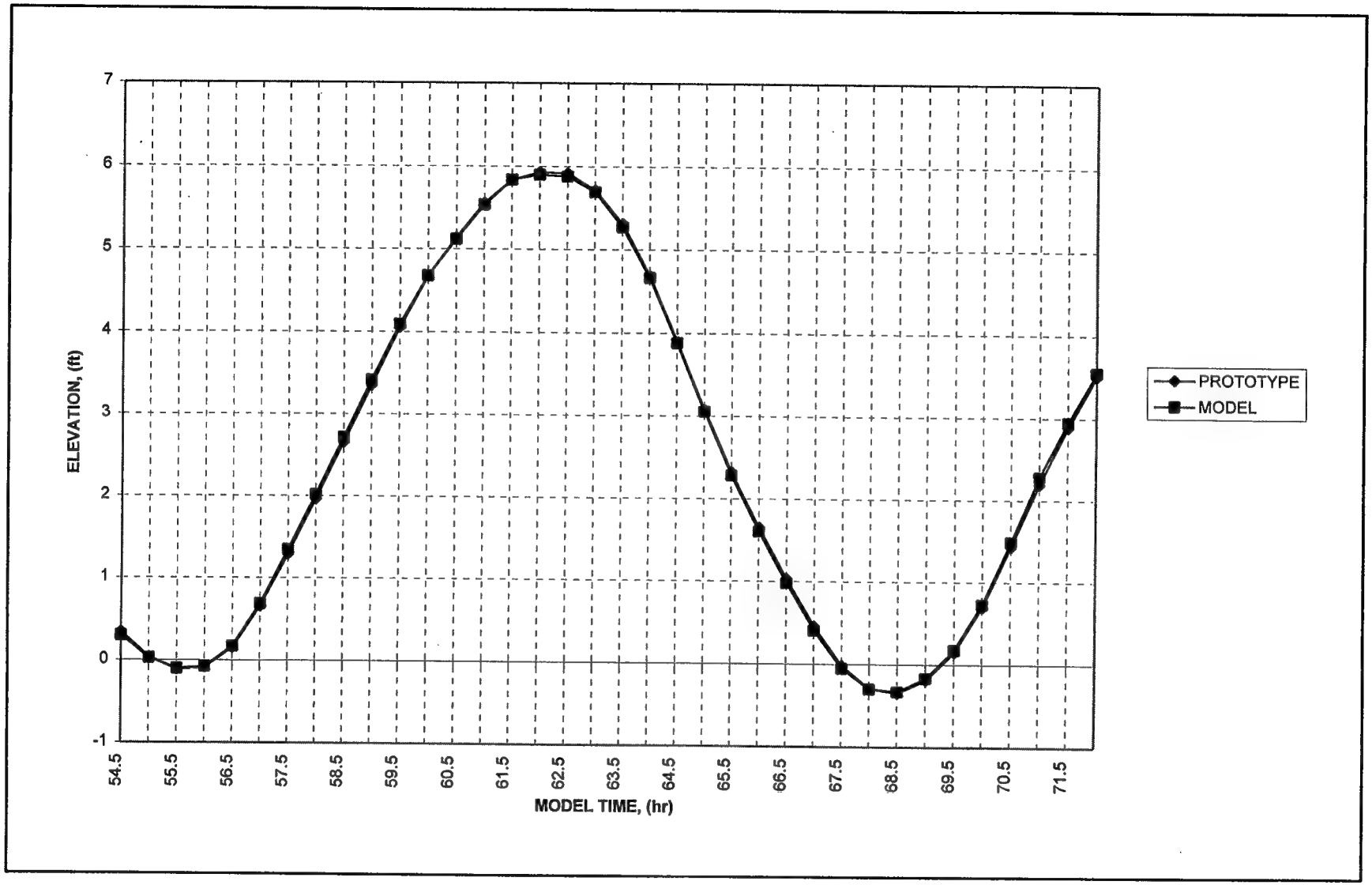

Figure 5. Water surface elevation at Mayport

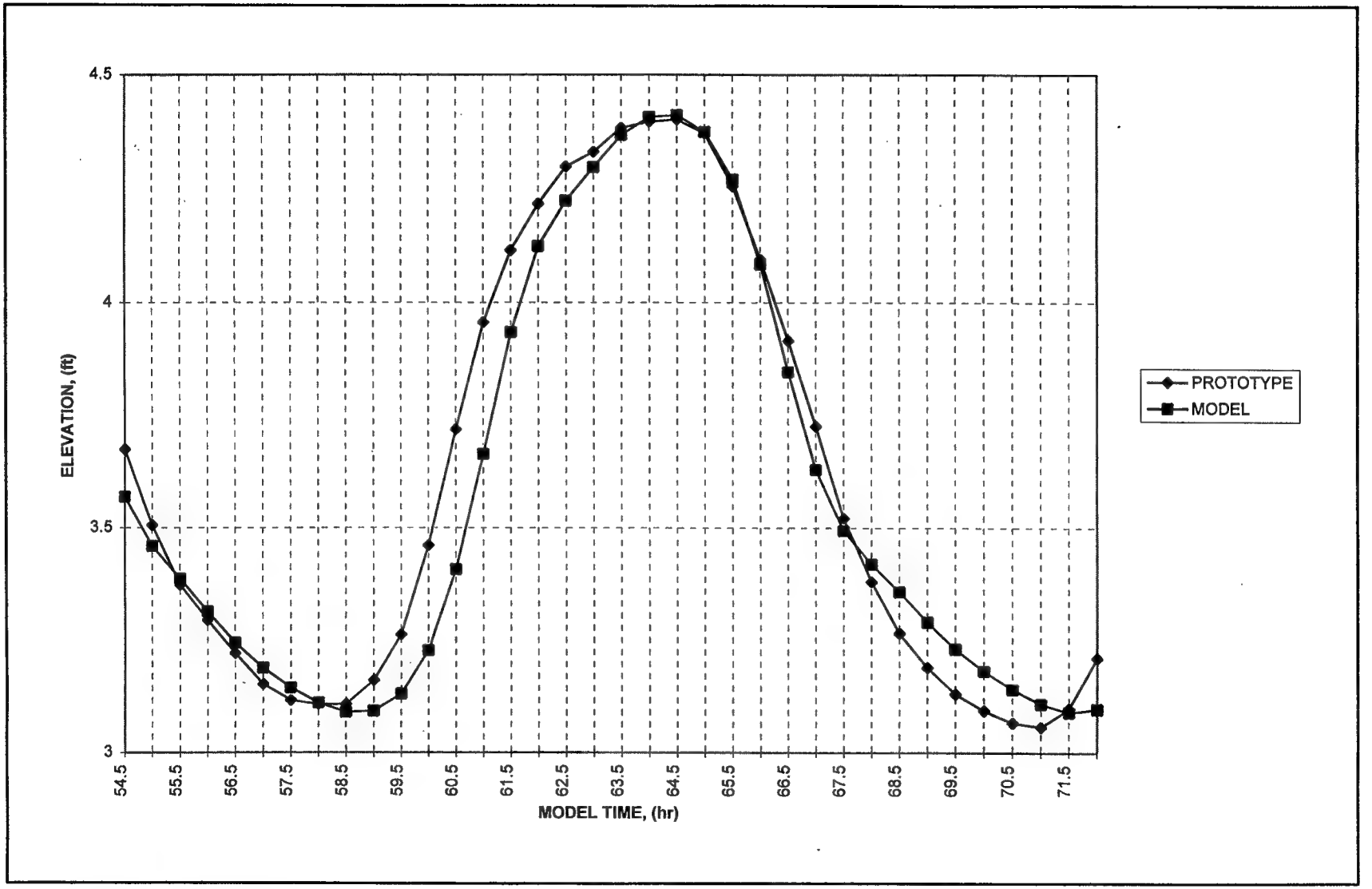

Figure 6. Water surface elevation at South Jacksonville

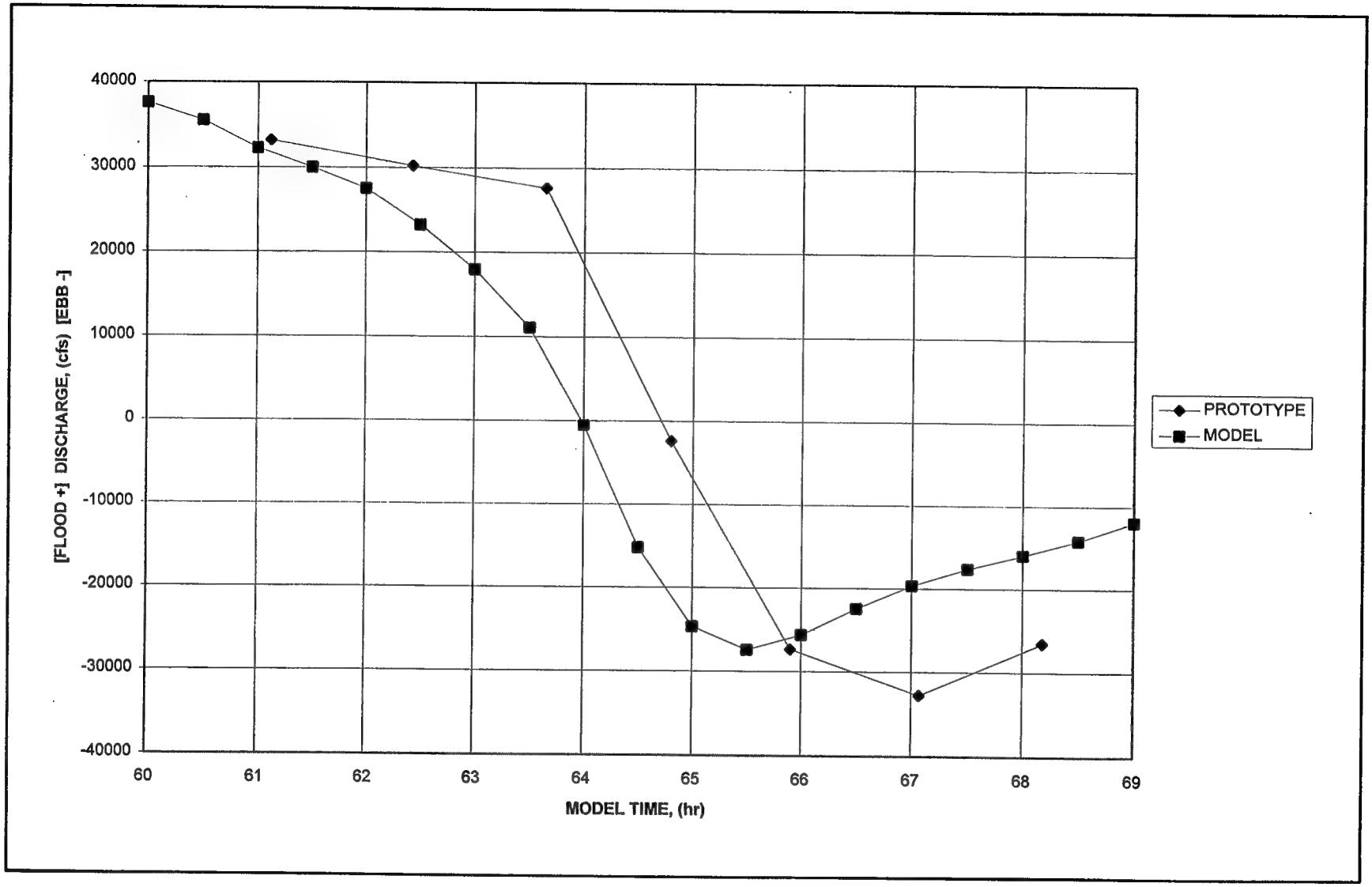

Figure 7. Water discharge at range 24 (to convert discharges to cu m/sec, multiply by 0.0283)

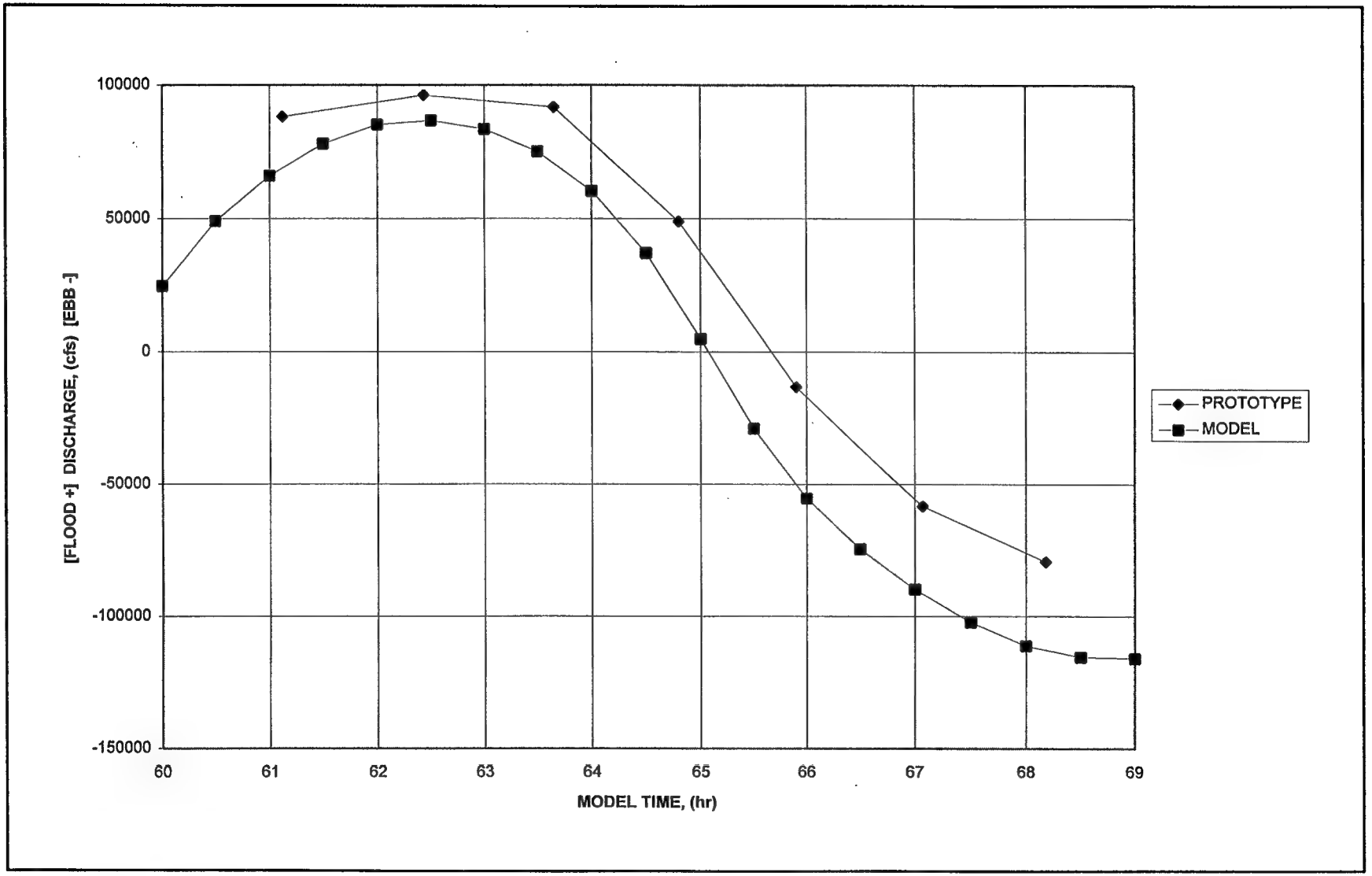

Figure 8. Water discharge at range 25 (to convert discharges to cu m/sec, multiply by 0.0283)

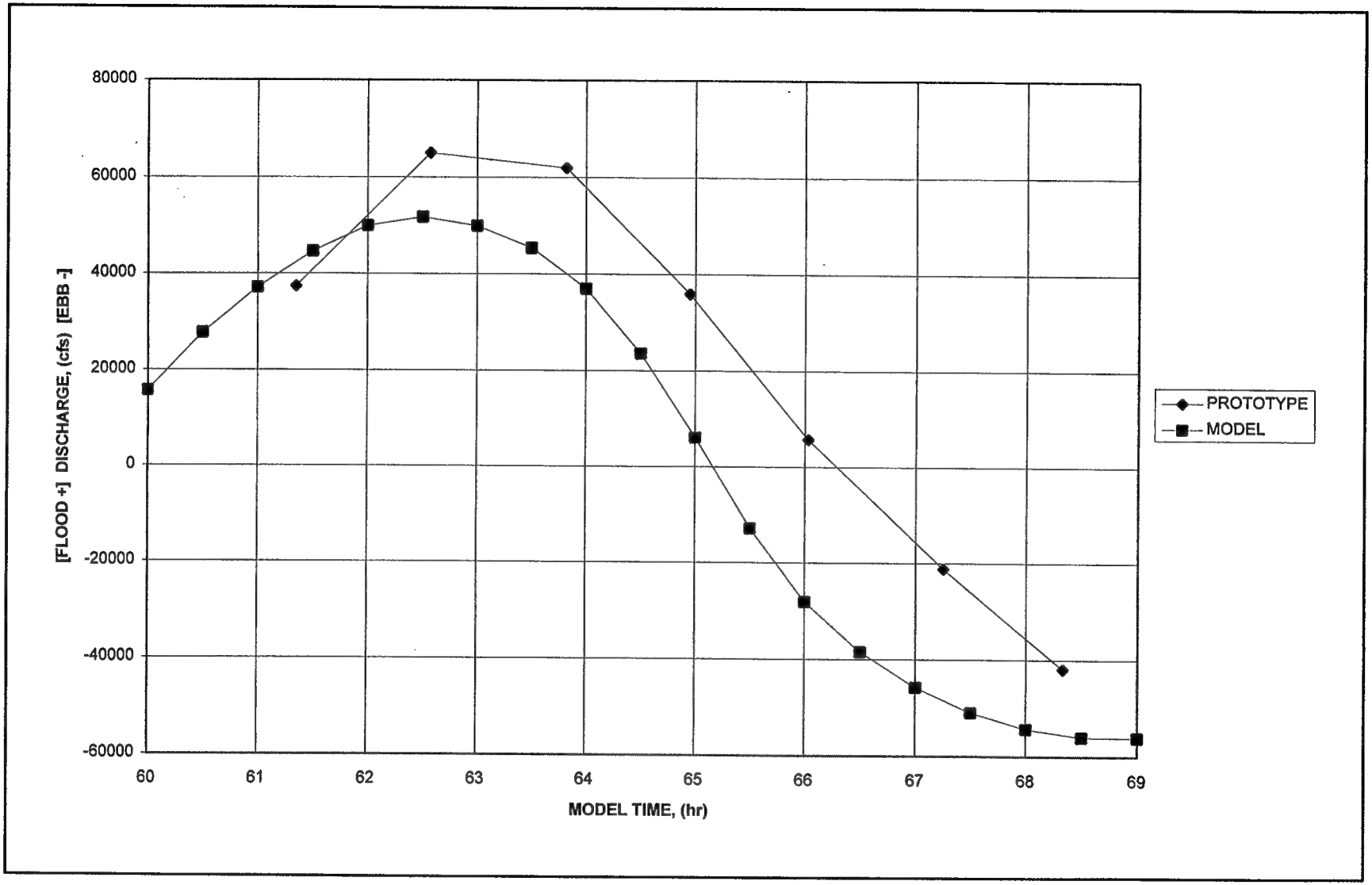

Figure 9. Water discharge at range 26 (to convert discharges to cu m/sec, multiply by 0.0283)

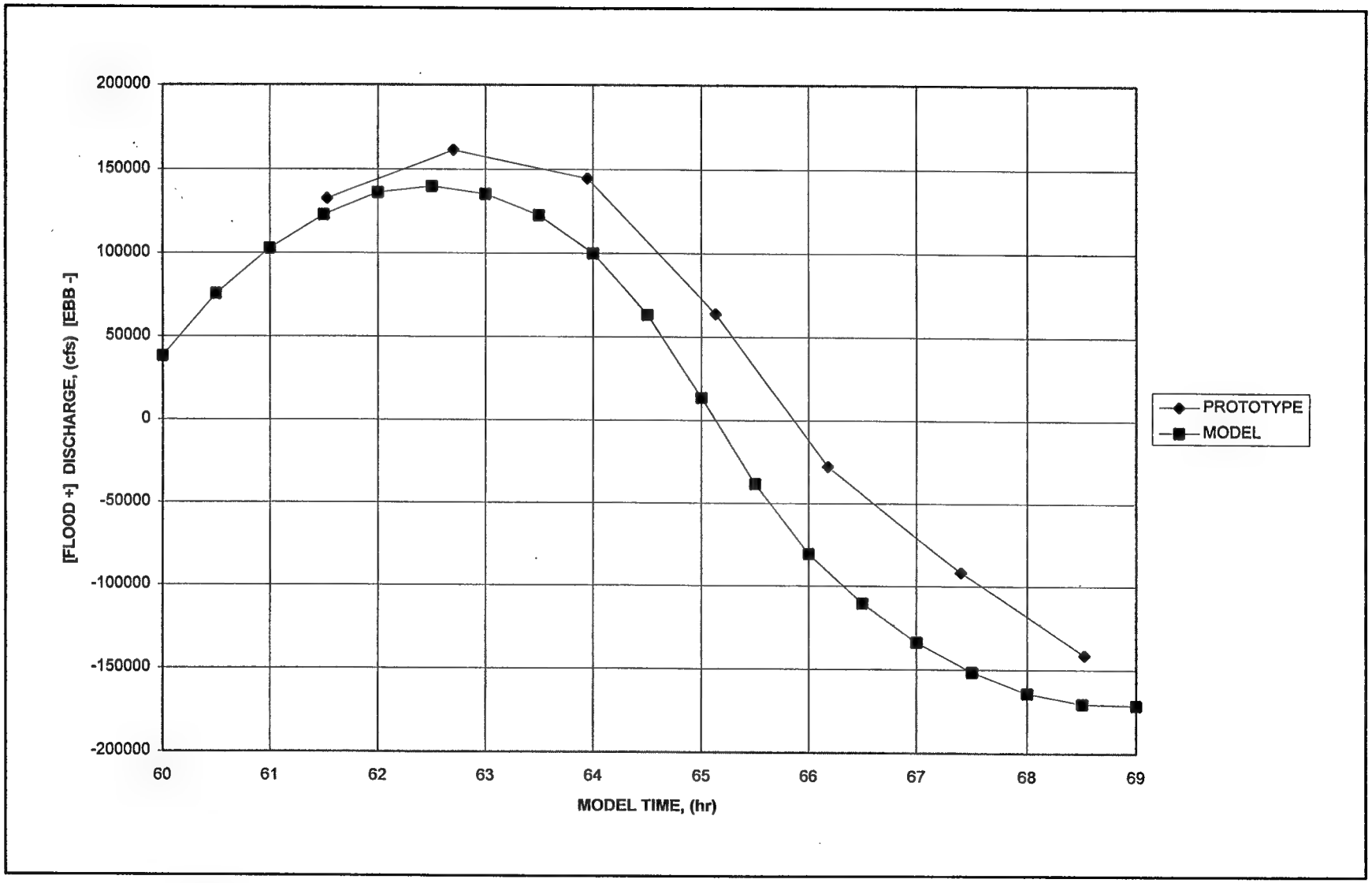

Figure 10. Water discharge at range 27 (to convert discharges to cu m/sec, multiply by 0.0283)

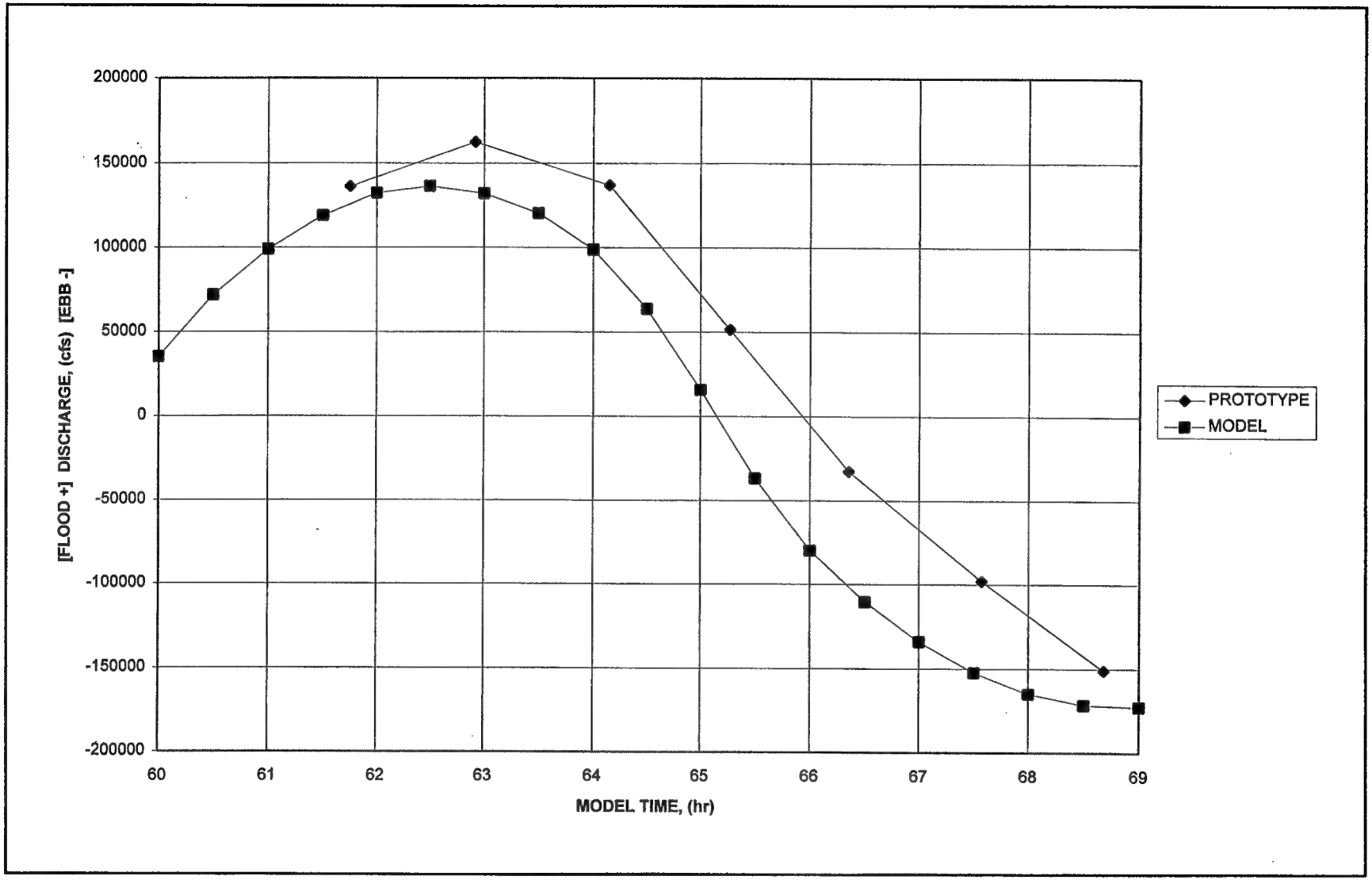

Figure 11. Water discharge at range 28 (to convert discharges to cu m/sec, multiply by 0.0283)

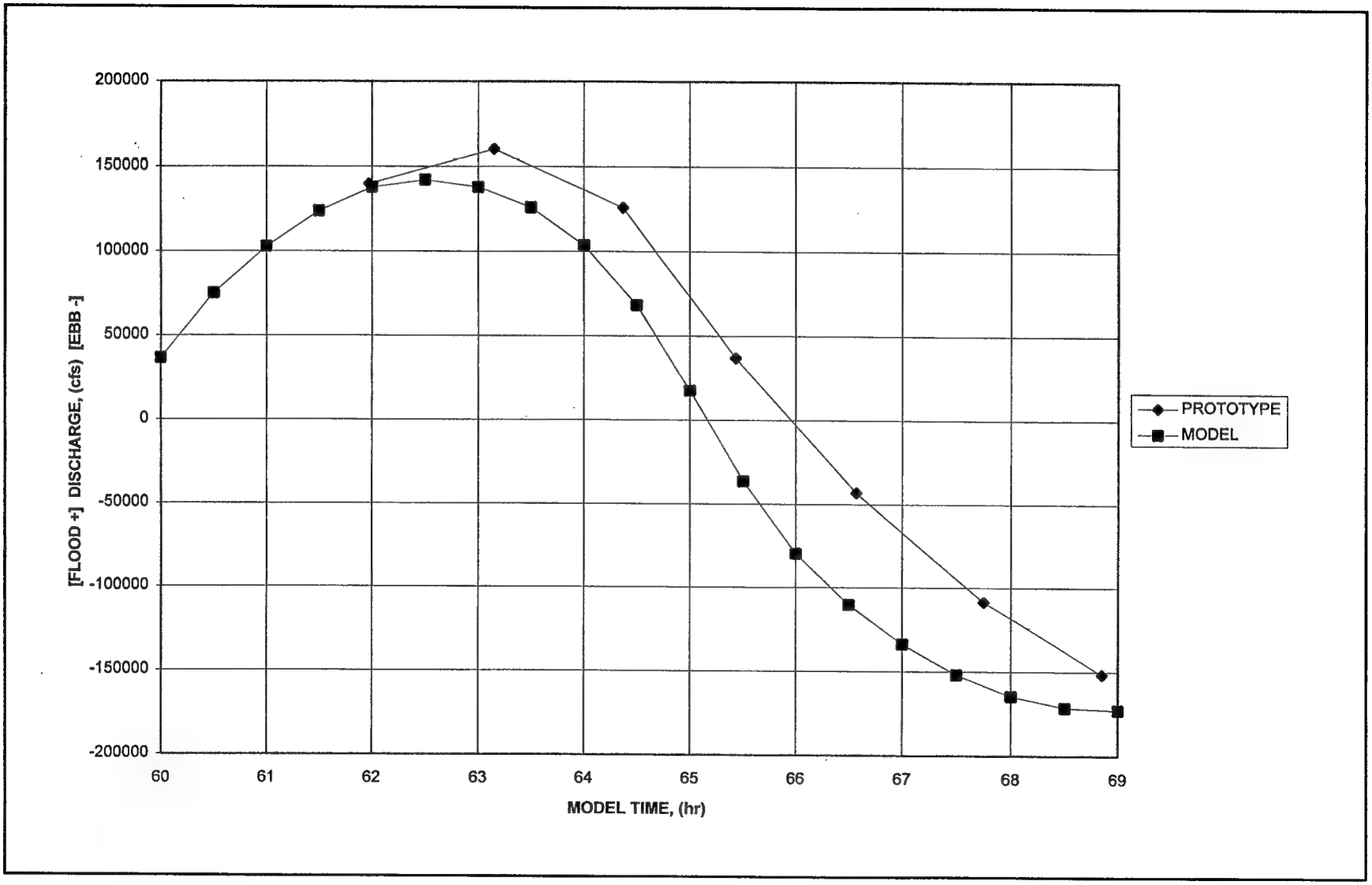

Figure 12. Water discharge at range 29 (to convert discharges to cu m/sec, multiply by 0.0283)

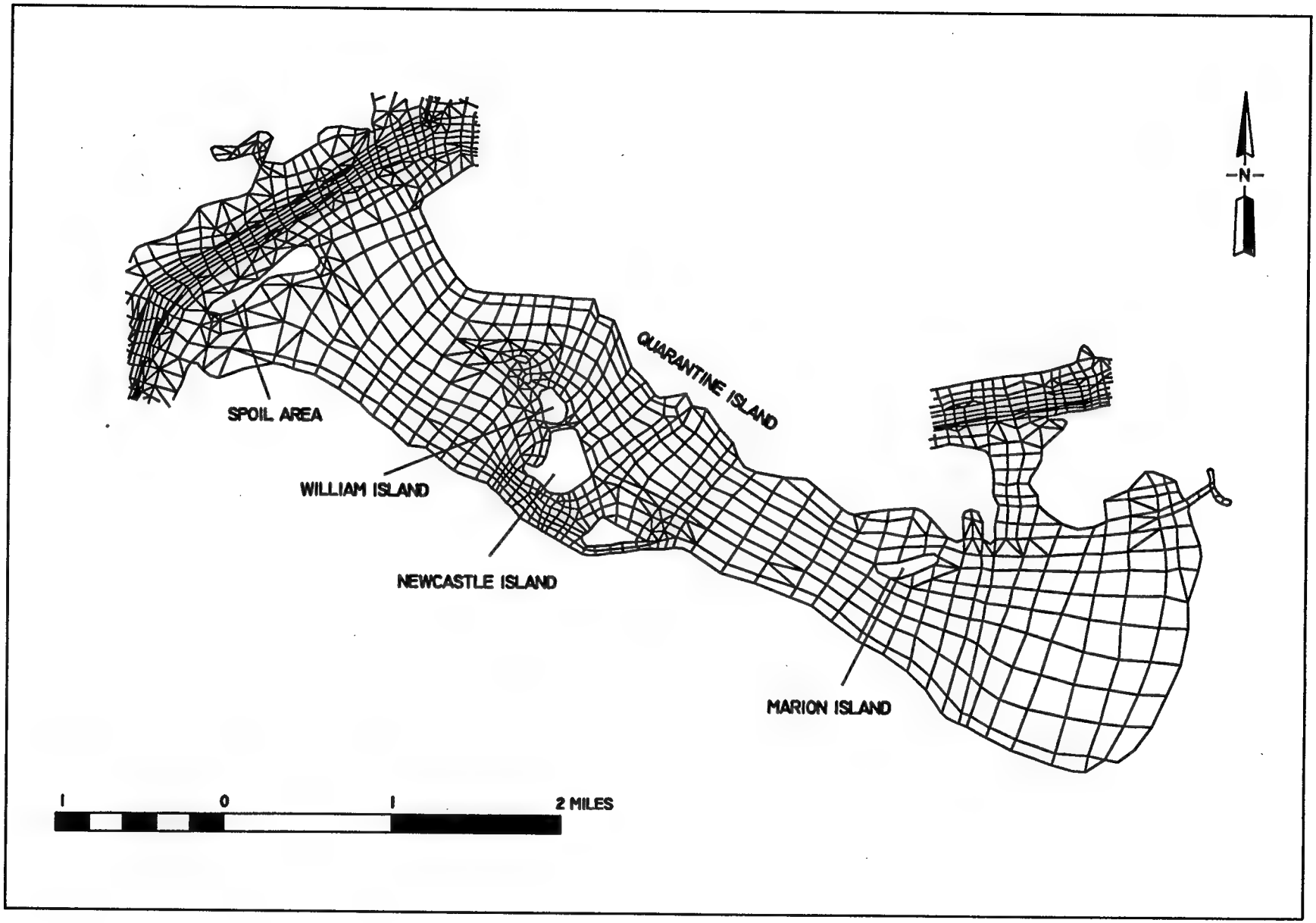

Figure 13. Numerical mesh at Mill Cove, existing condition (to convert scale to kilometers, multiply by 1.6)

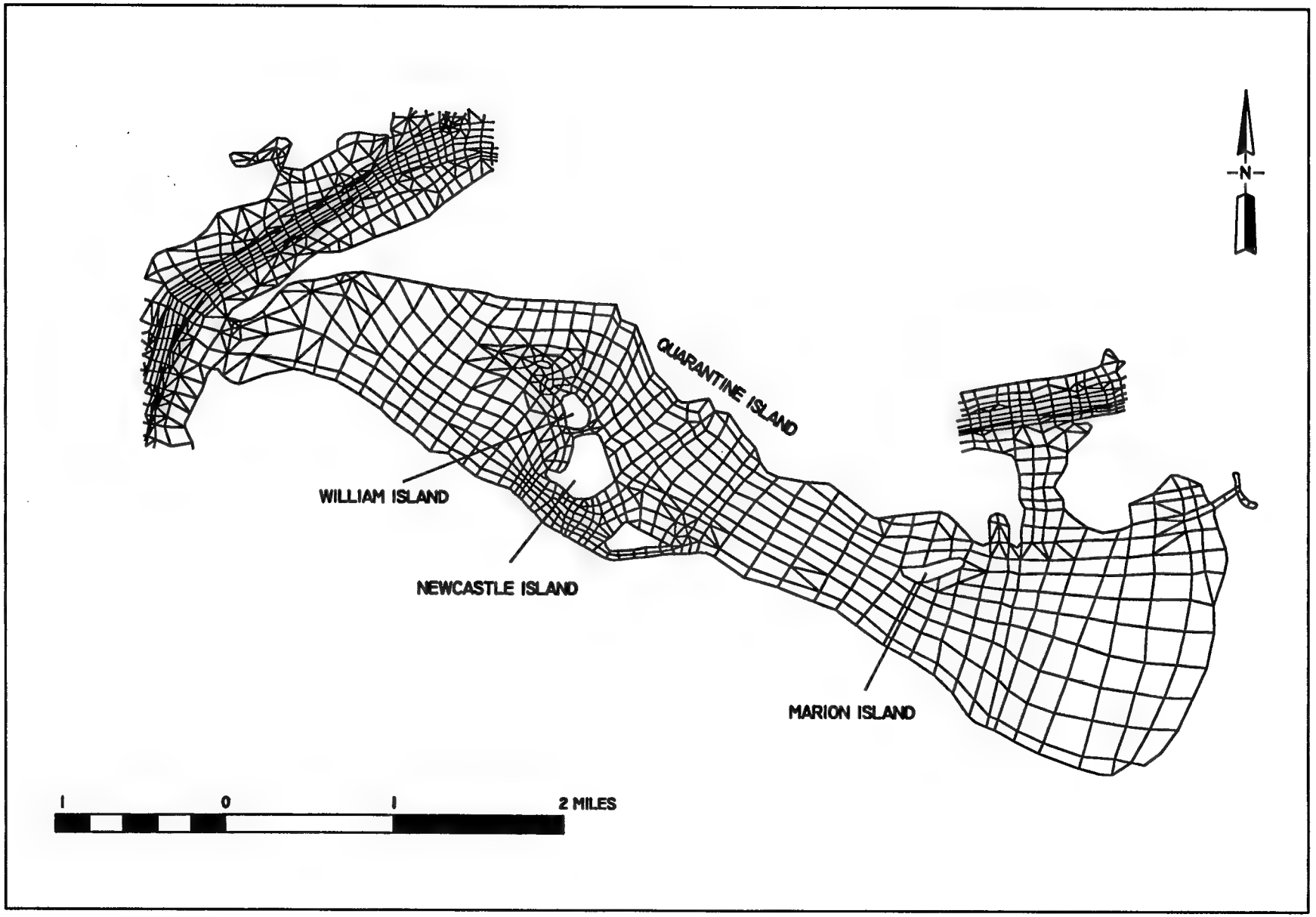

Figure 14. Numerical mesh at Mill Cove, Plan 1 (to convert scale to kilometers, multiply by 1.6)

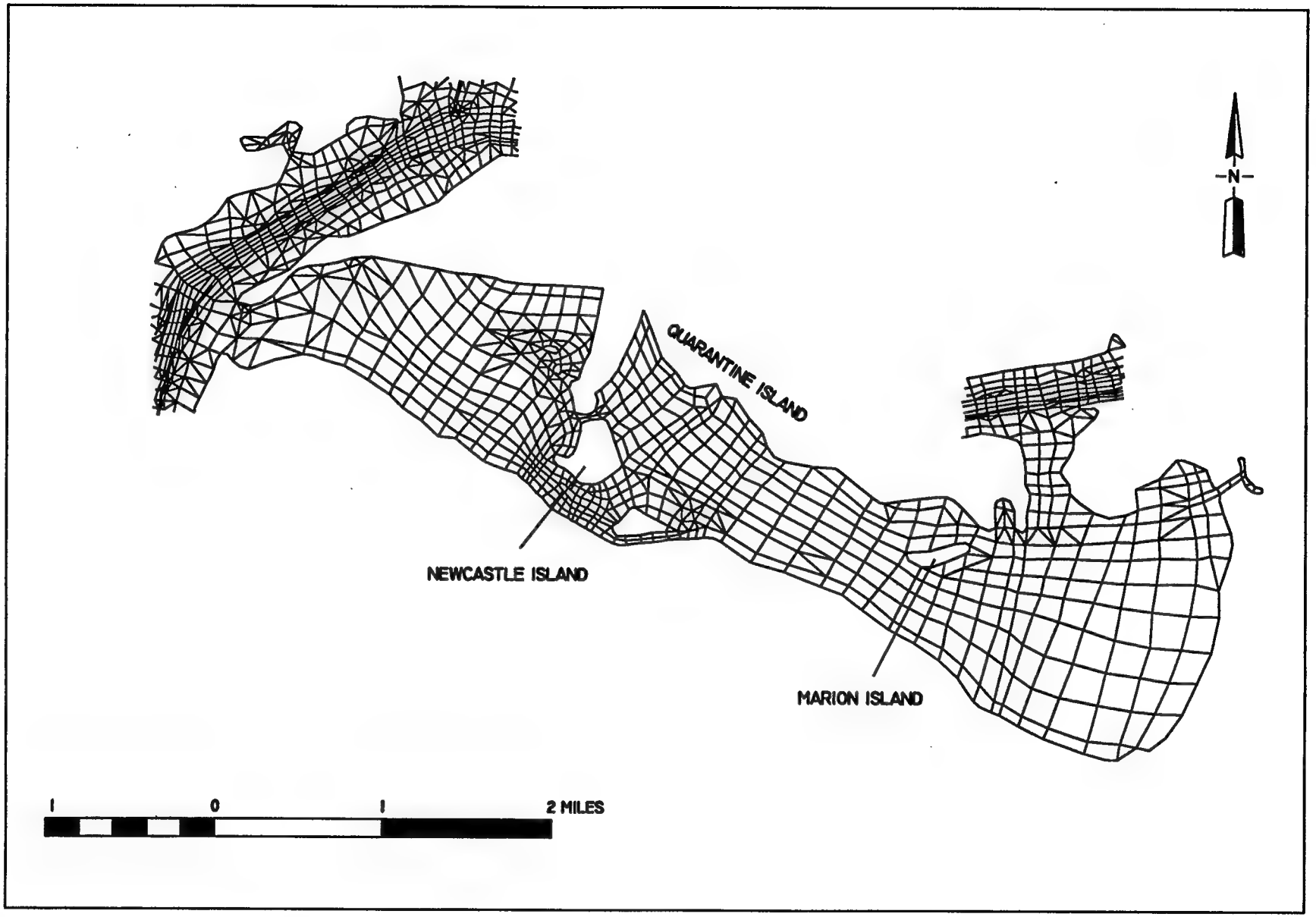

Figure 15. Numerical mesh at Mill Cove, Plan 2 (to convert scale to kilometers, multiply by 1.6)

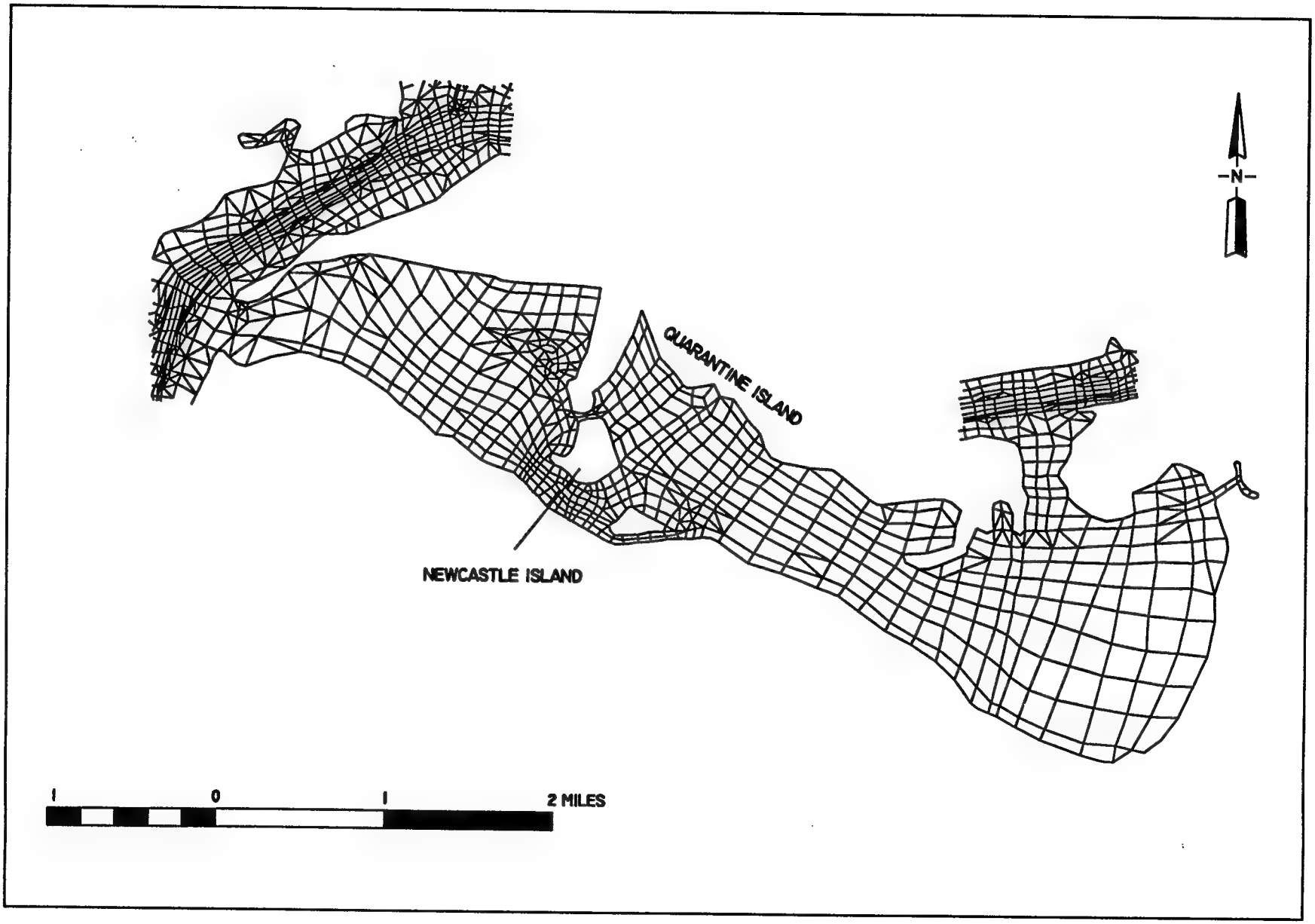

Figure 16. Numerical mesh at Mill Cove, Plan 3 (to convert scale to kilometers, multiply by 1.6)

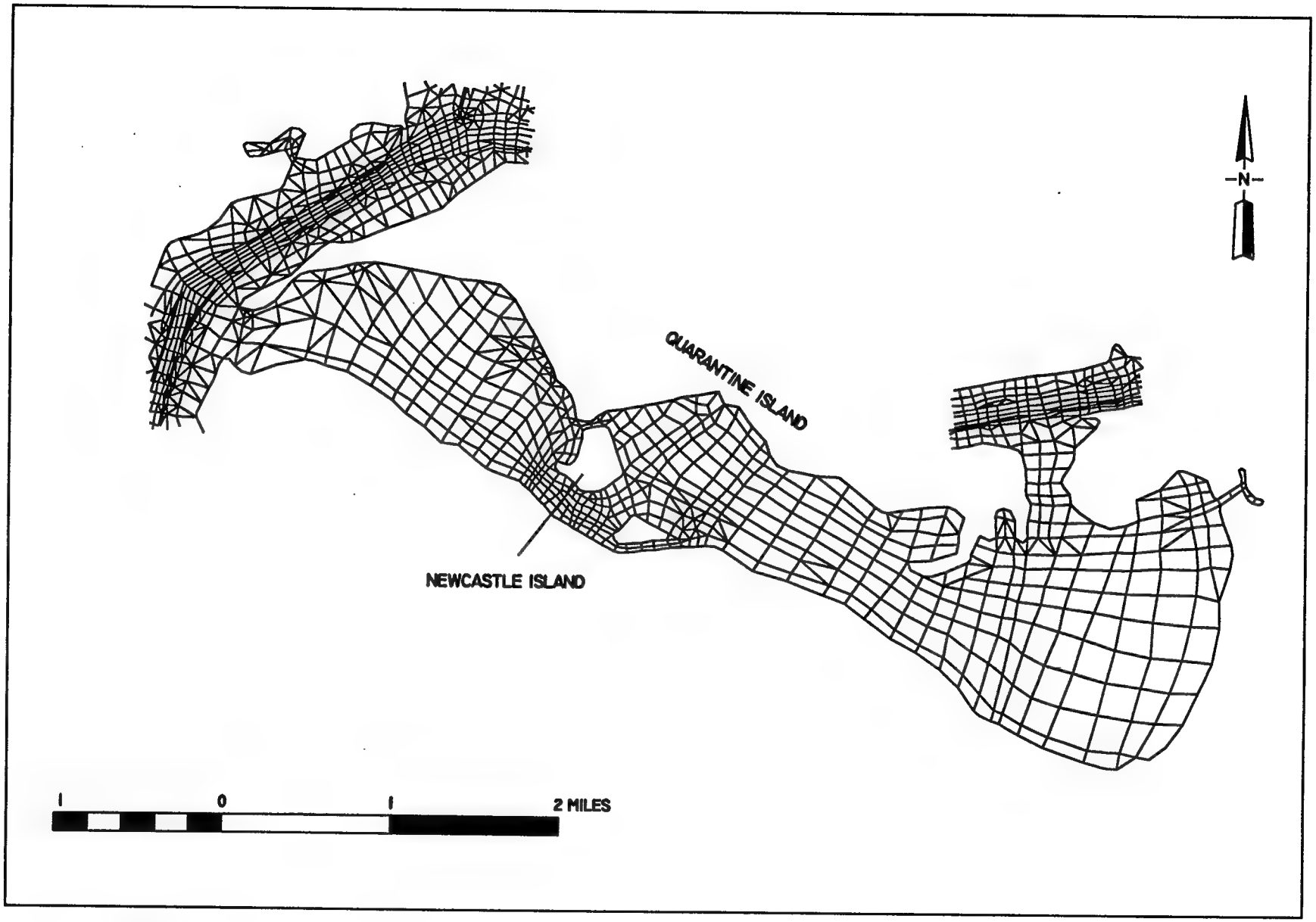

Figure 17. Numerical mesh at Mill Cove, Plan 4 (to convert scale to kilometers, multiply by 1.6)

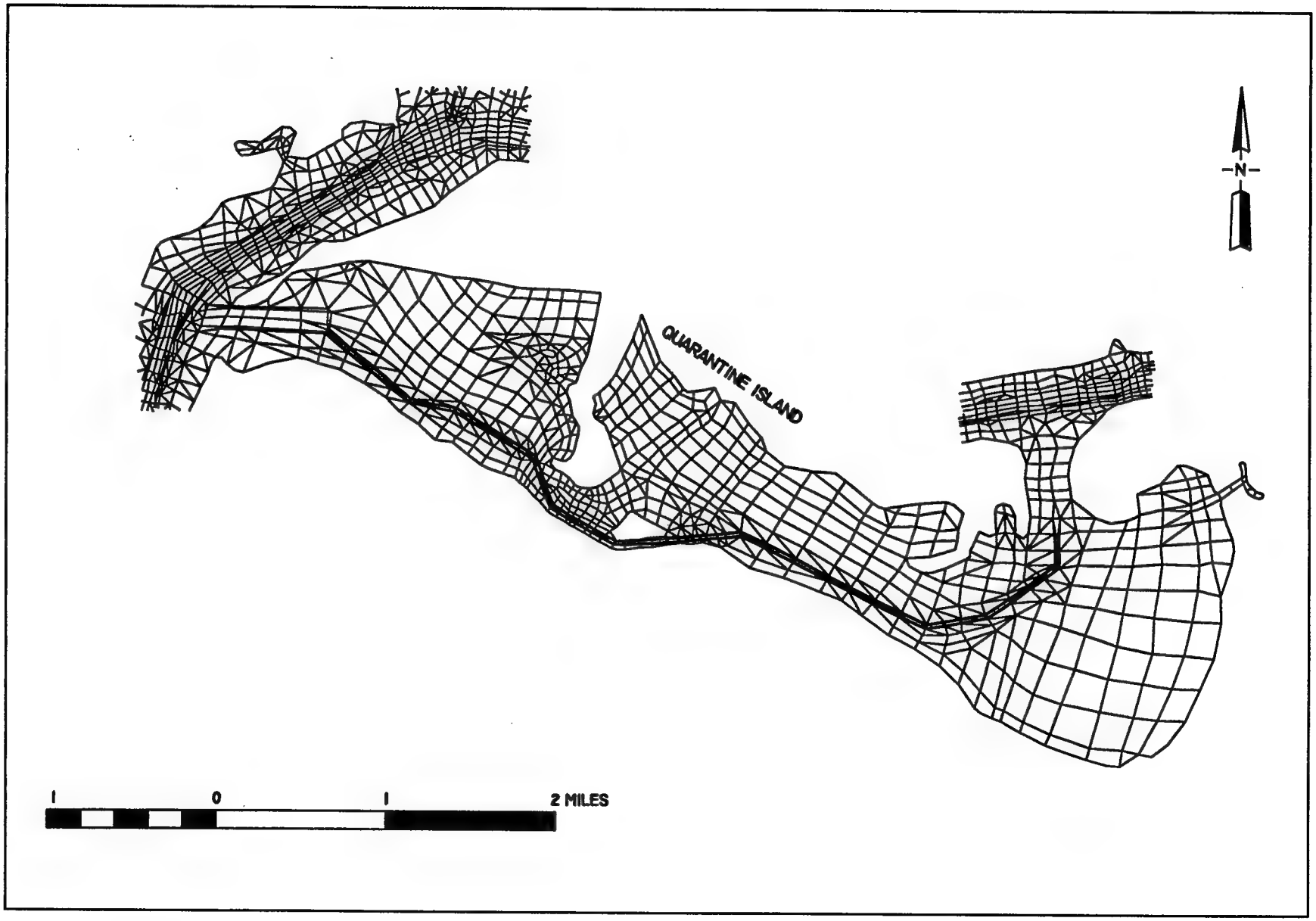

Figure 18. Numerical mesh at Mill Cove, Plan 5 (to convert scale to kilometers, multiply by 1.6)

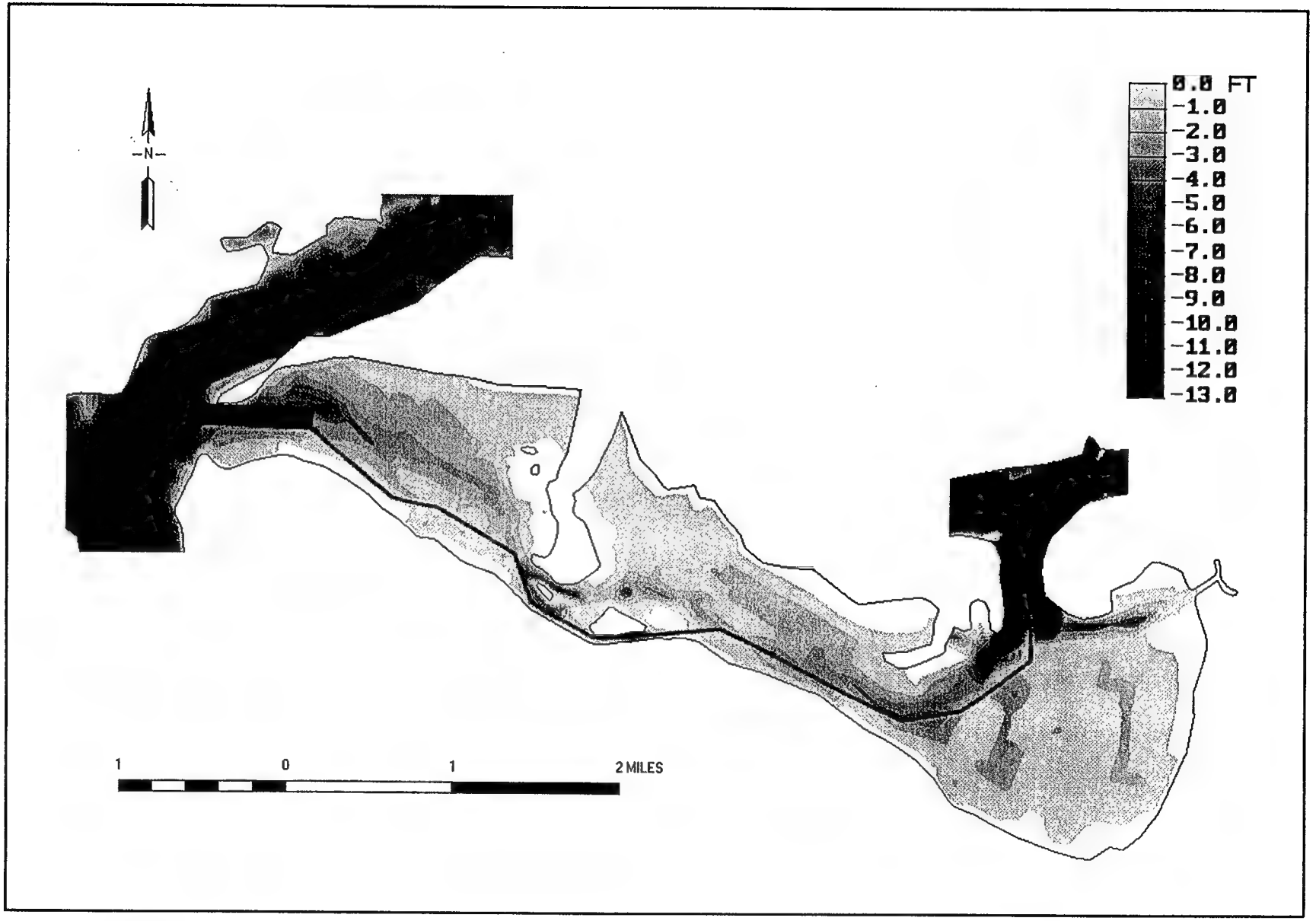

Figure 19. Depth contour map of Mill Cove, Plan 5 (to convert scale to kilometers, multiply by 1.6)

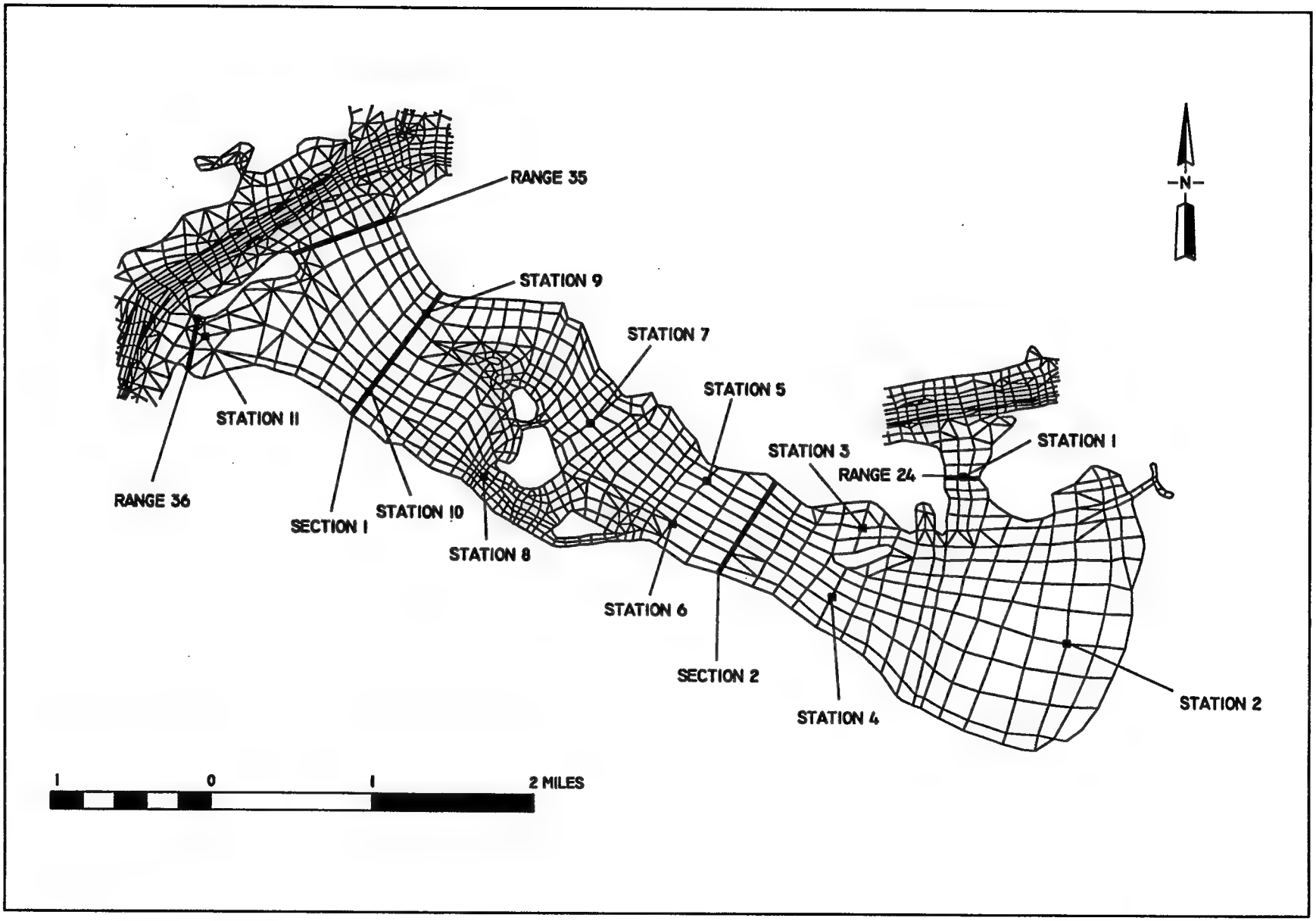

Figure 20. Location of stations (time-history nodes), ranges, and sections in the Mill Cove area (to convert scale to kilometers, multiply by 1.6)

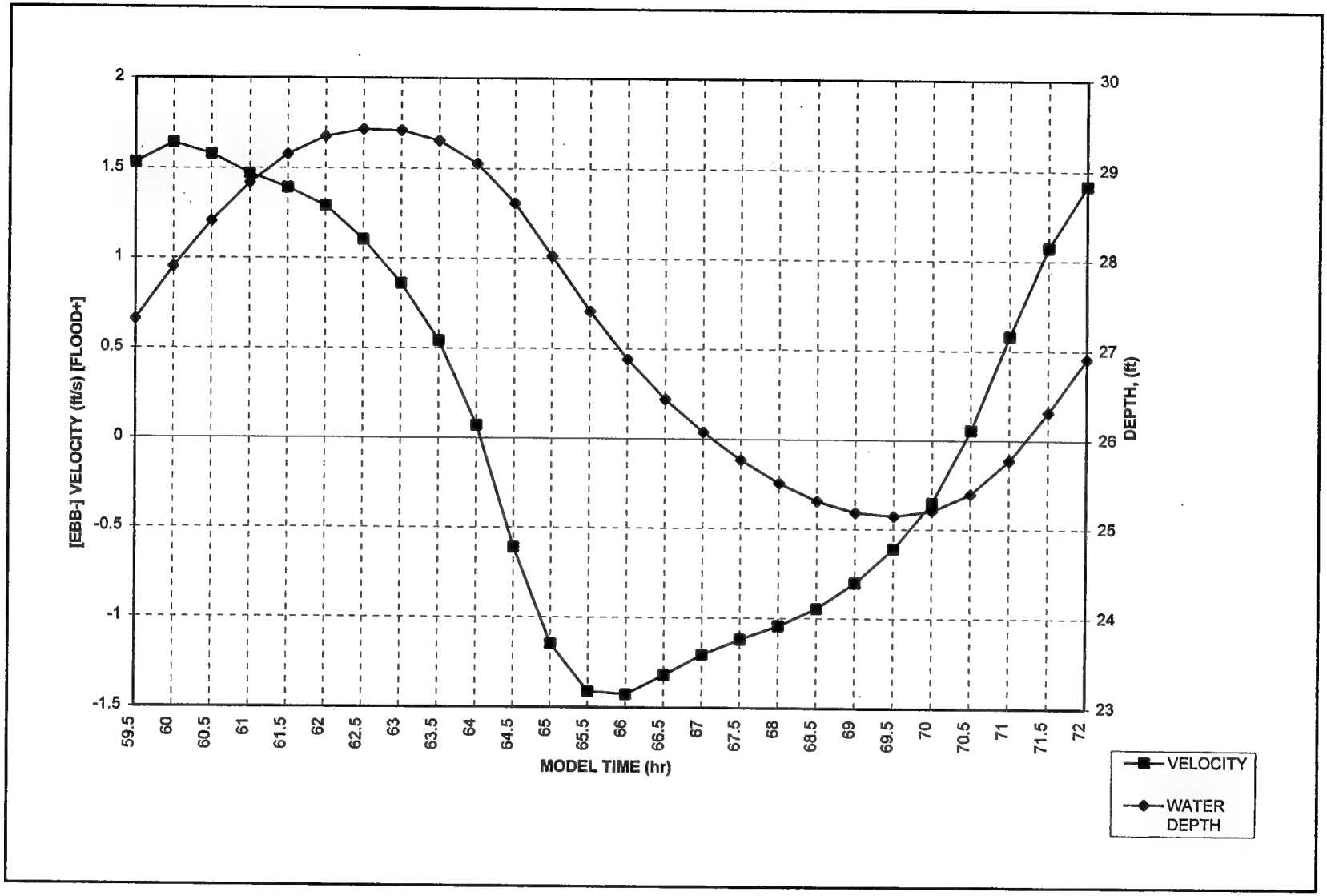

Figure 21. Velocity magnitude and depth for existing condition (base) at station 1(to convert velocities to meters per second, multiply by 0.3048)

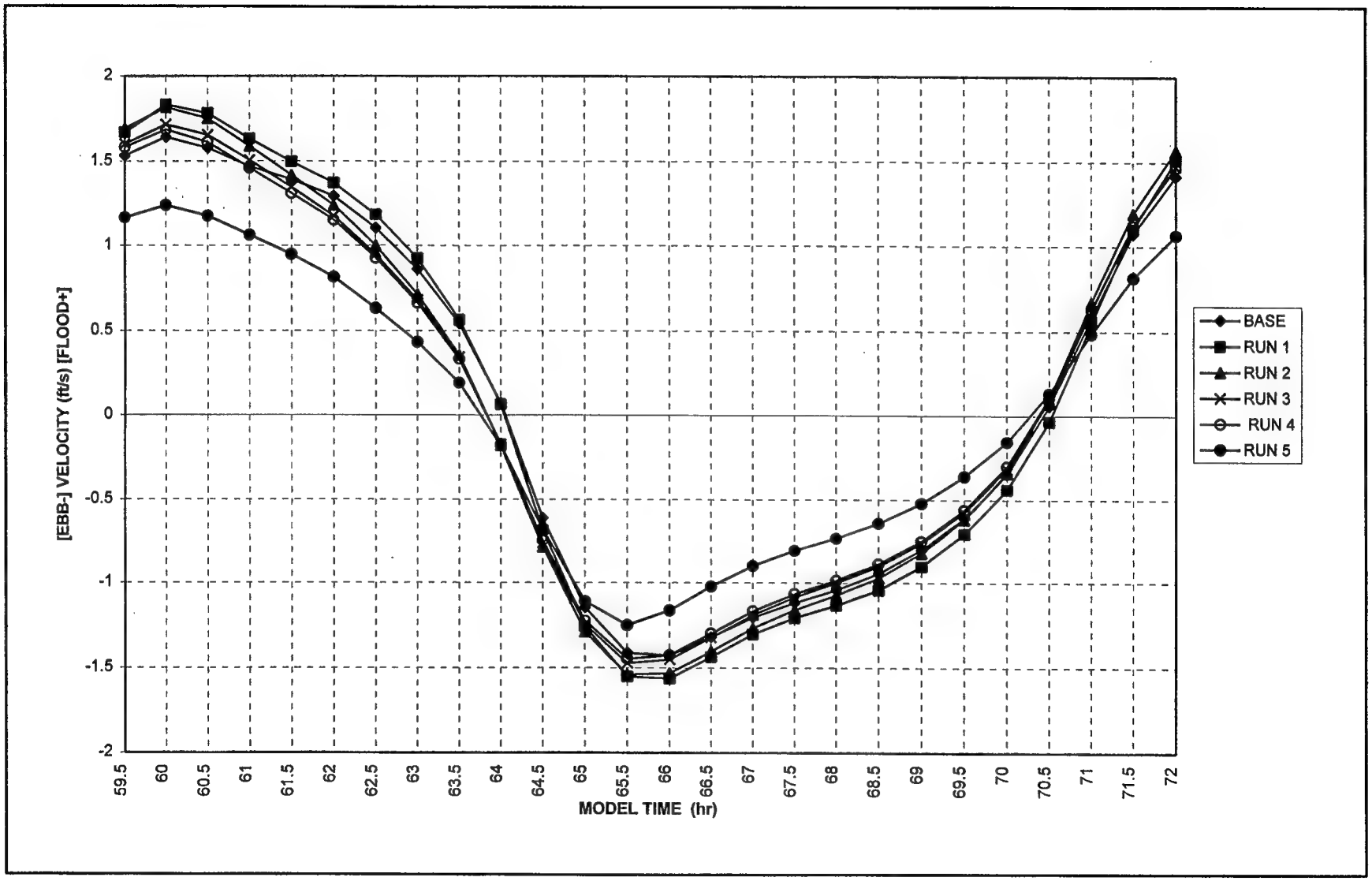

Figure 22. Velocity magnitude at station 1(to convert velocities to meters per second, multiply by 0.3048)

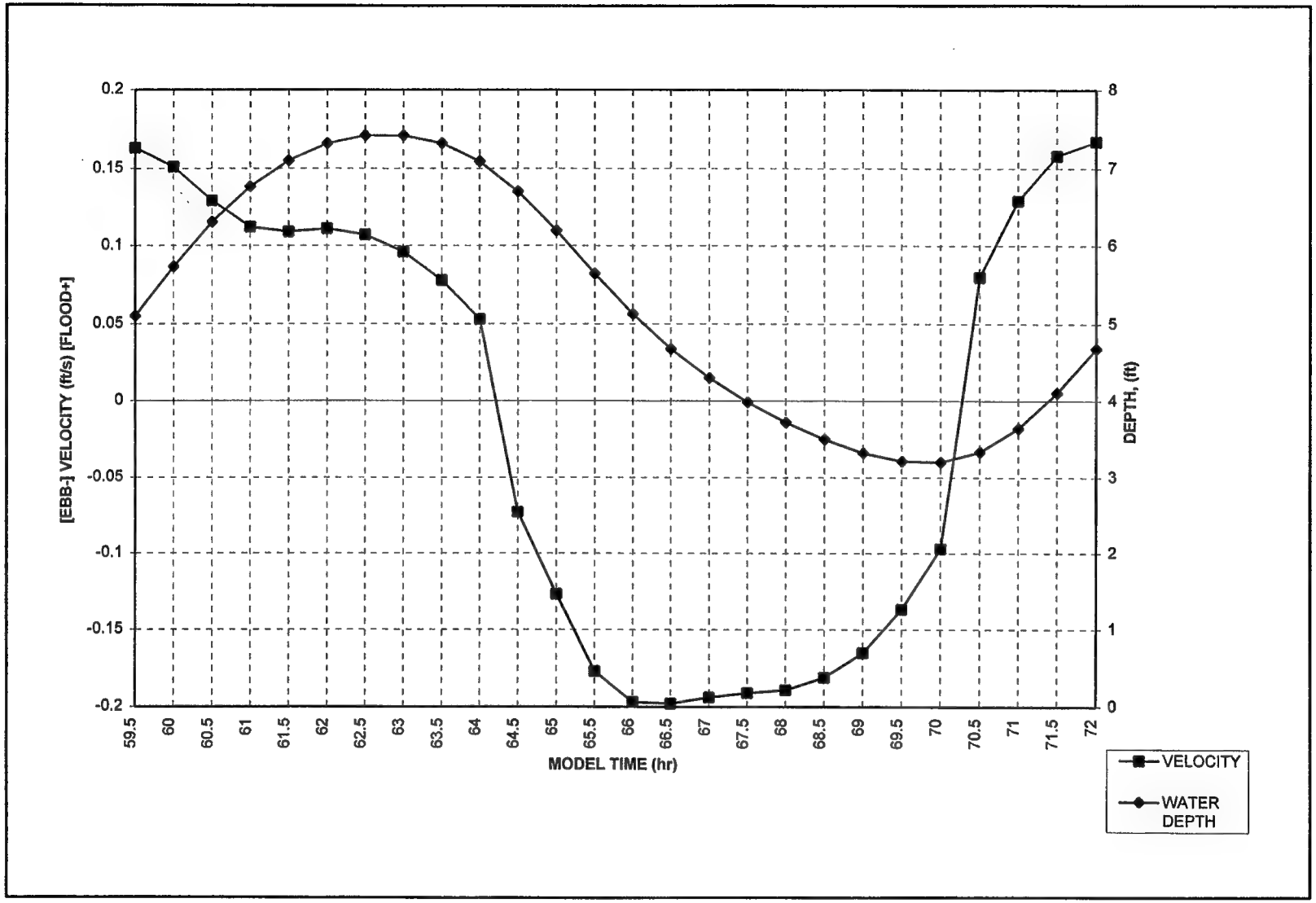

Figure 23. Velocity magnitude and depth for existing (base) condition at station 2 (to convert velocities to meters per second, multiply by 0.3048)

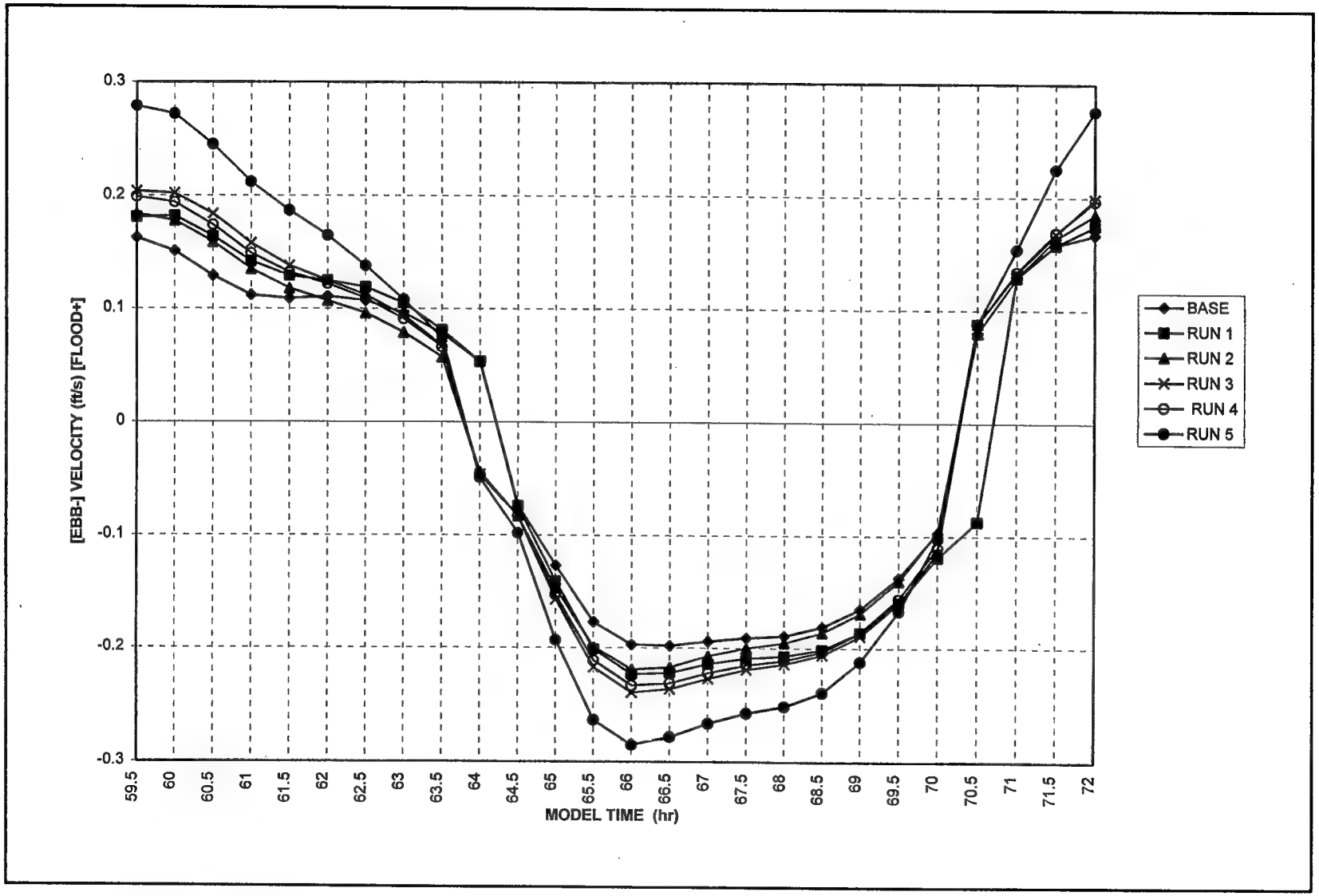

Figure 24. Velocity magnitude at station 2 (to convert velocities to meters per second, multiply by 0.3048)

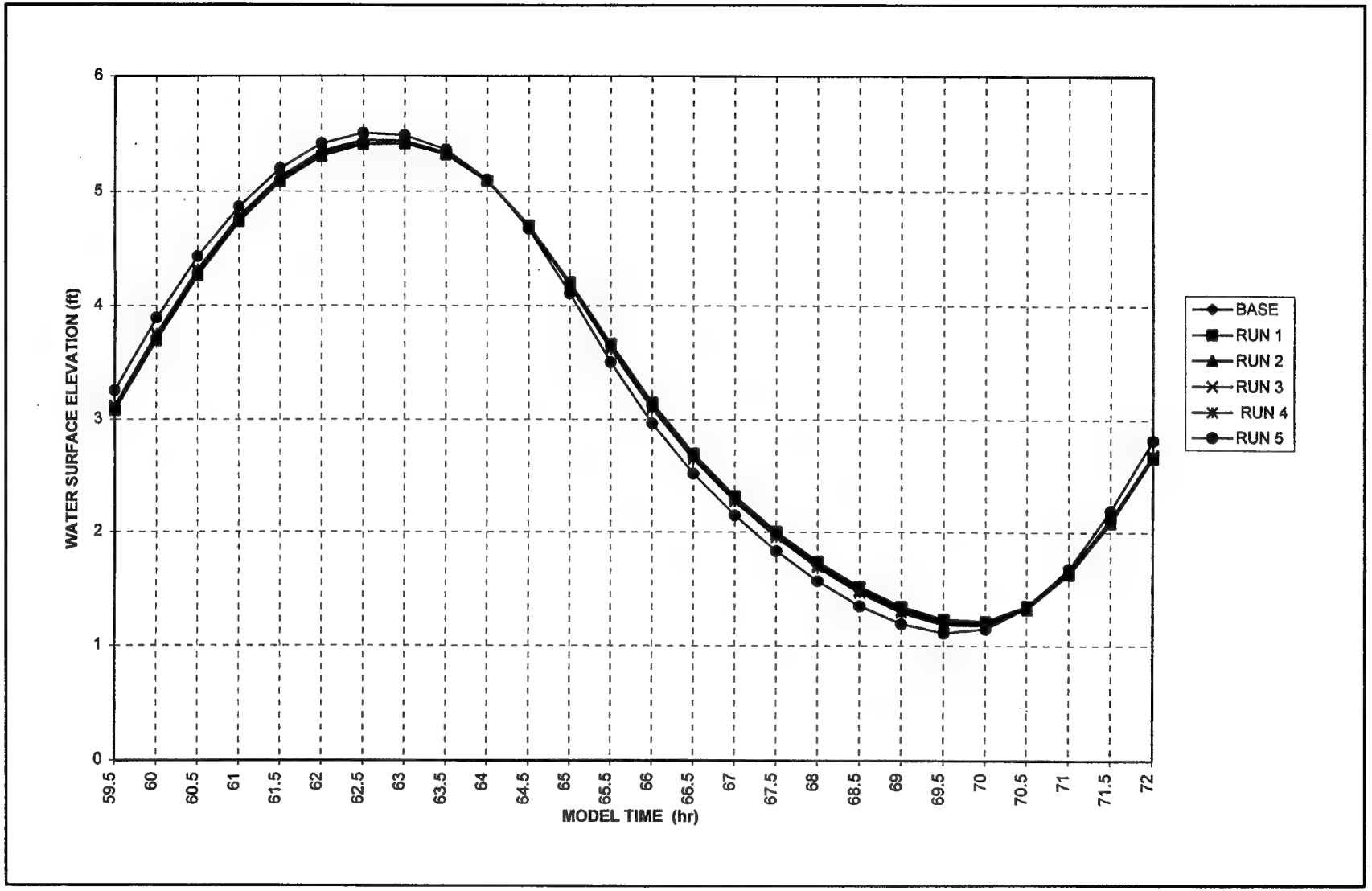

Figure 25. Water surface elevation at station 2 (to convert velocities to meters per second, multiply by 0.3048)

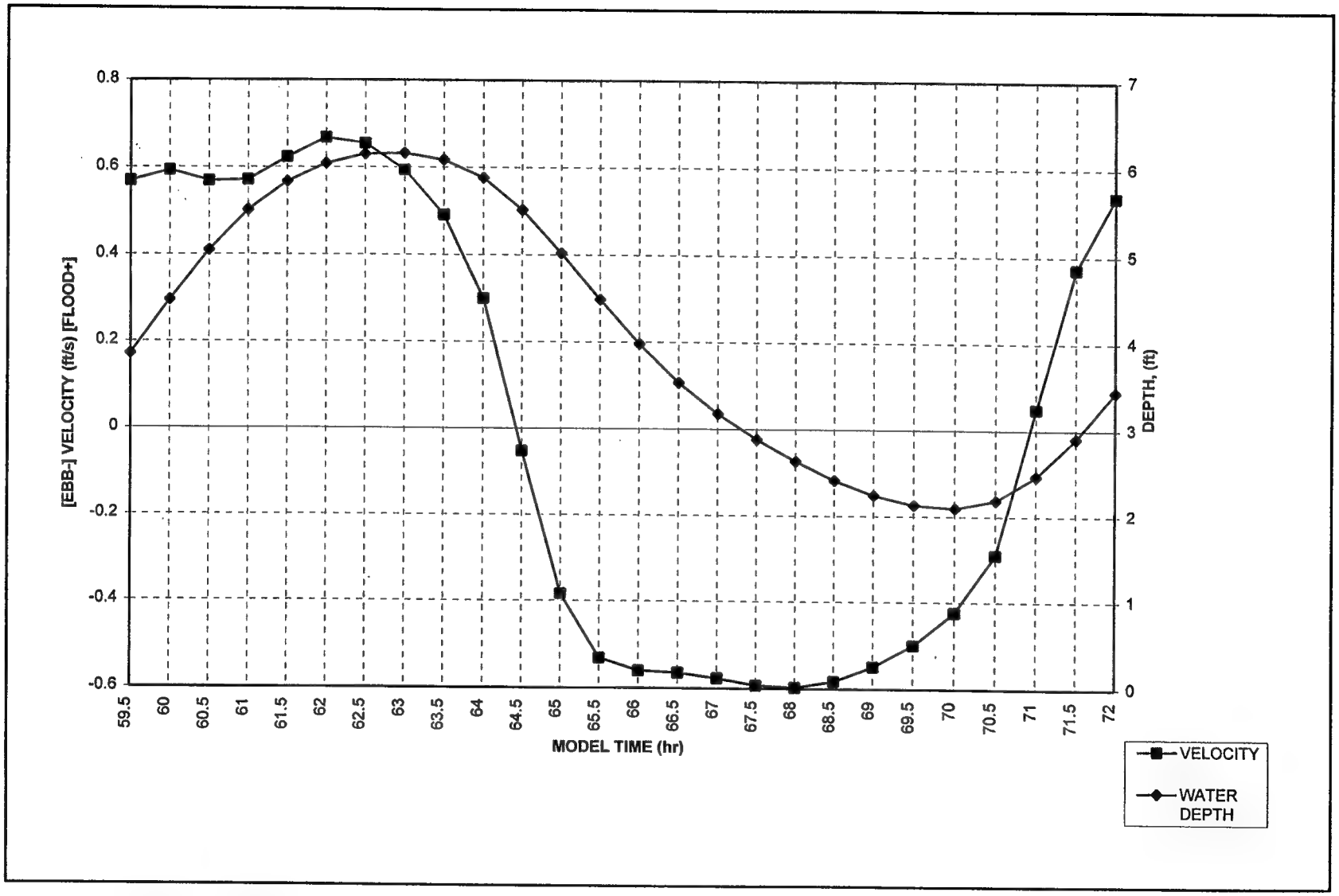

Figure 26. Velocity magnitude and depth for existing condition (base) at station 3 (to convert velocities to meters per second, multiply by 0.3048)

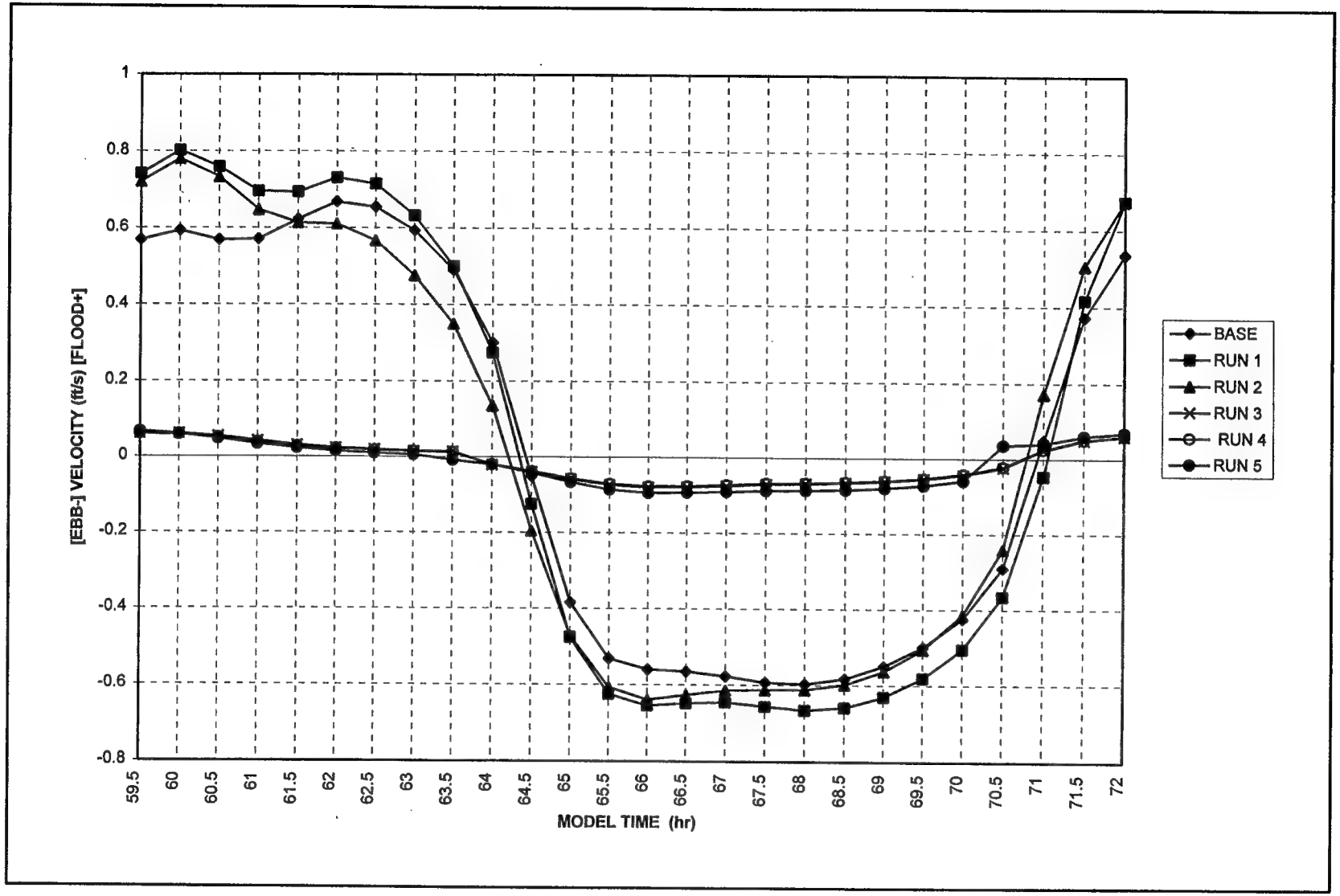

Figure 27. Velocity magnitude at station 3 (to convert velocities to meters per second, multiply by 0.3048)

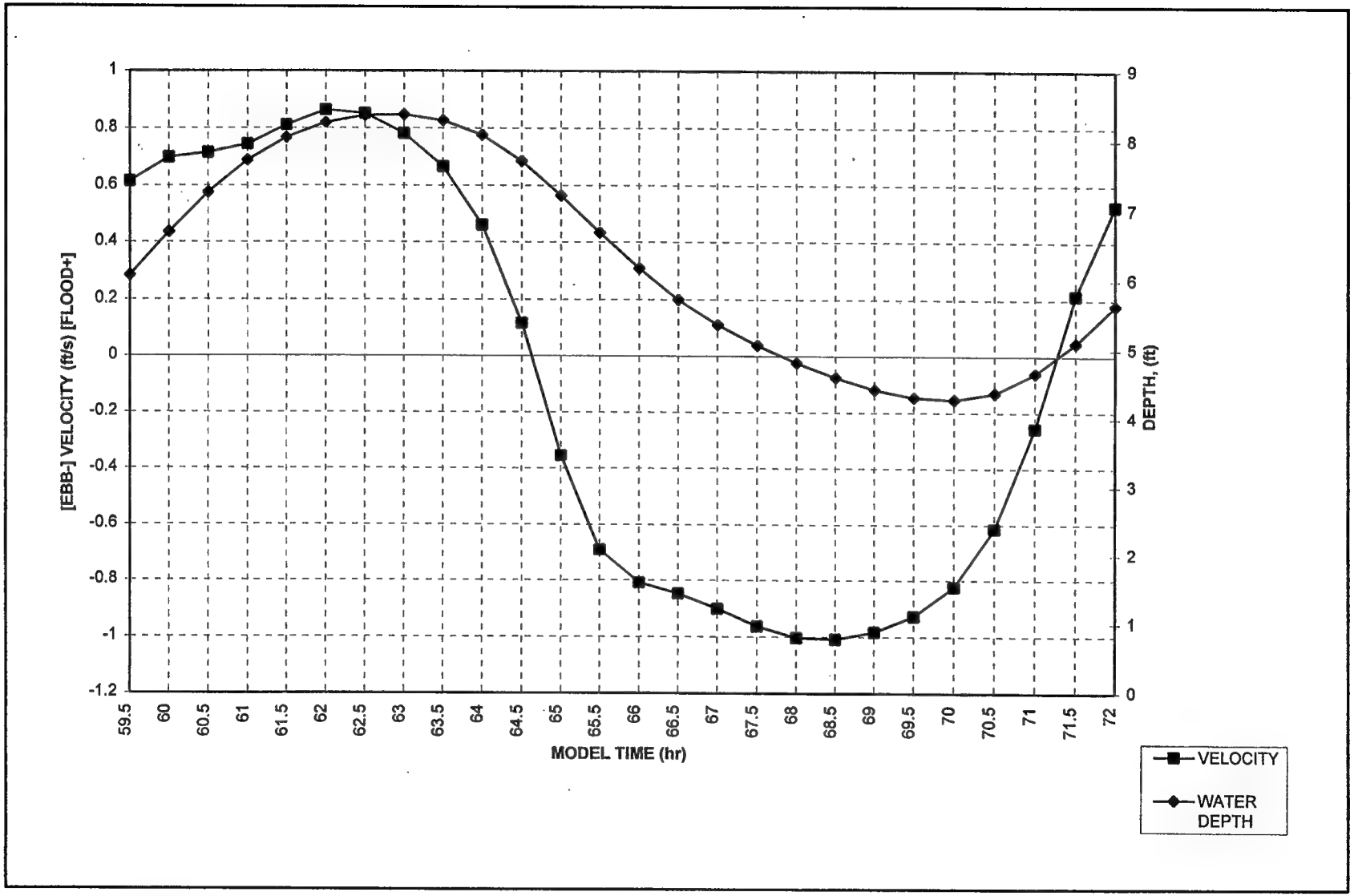

Figure 28. Velocity magnitude and depth for existing condition (base) at station 4 (to convert velocities to meters per second, multiply by 0.3048)

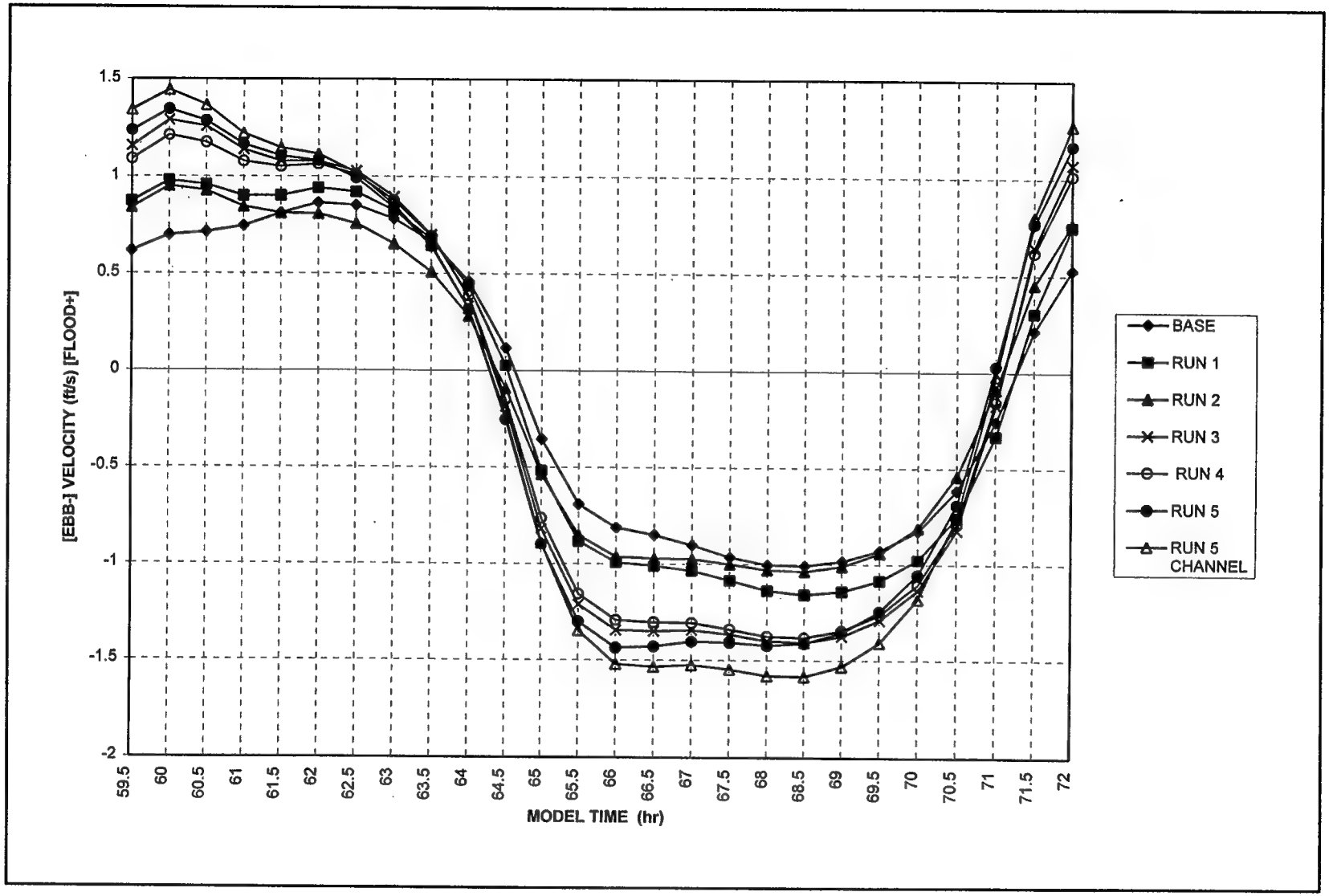

Figure 29. Velocity magnitude at station 4 (to convert velocities to meters per second, multiply by 0.3048)

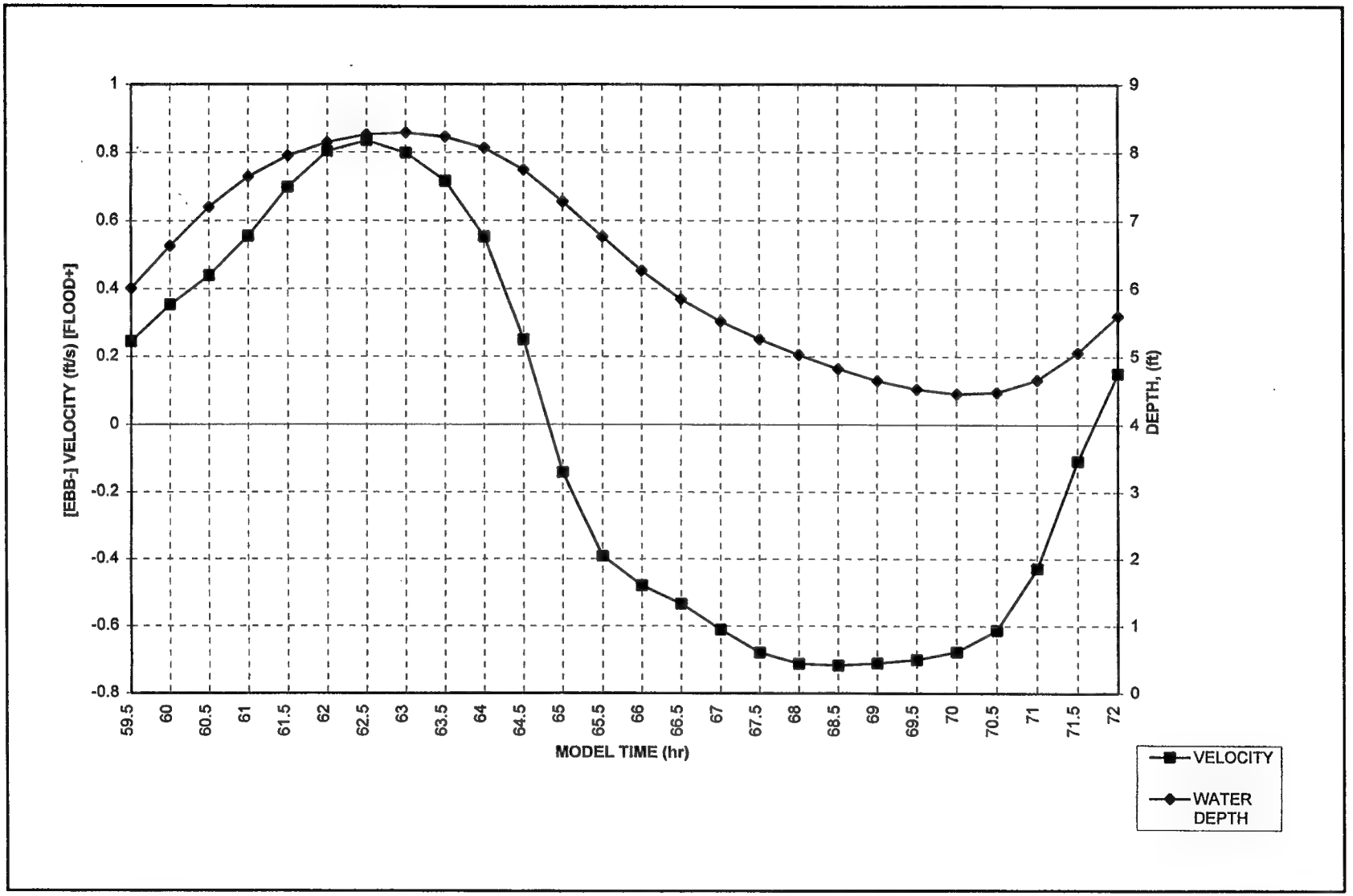

Figure 30. Velocity magnitude and depth for existing condition (base) at station 5 (to convert velocities to meters per second, multiply by 0.3048)

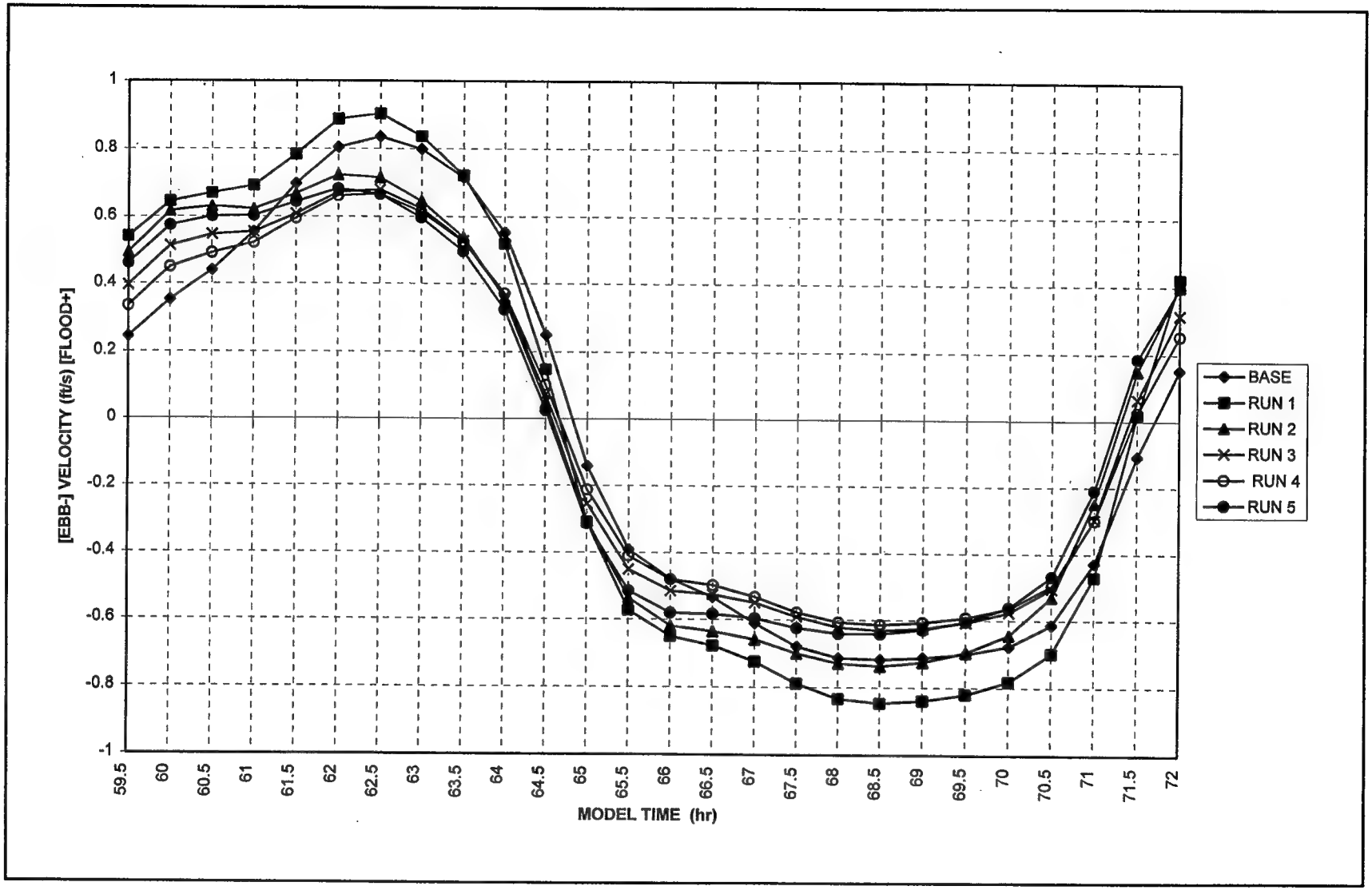

Figure 31. Velocity magnitude at station 5 (to convert velocities to meters per second, multiply by 0.3048)

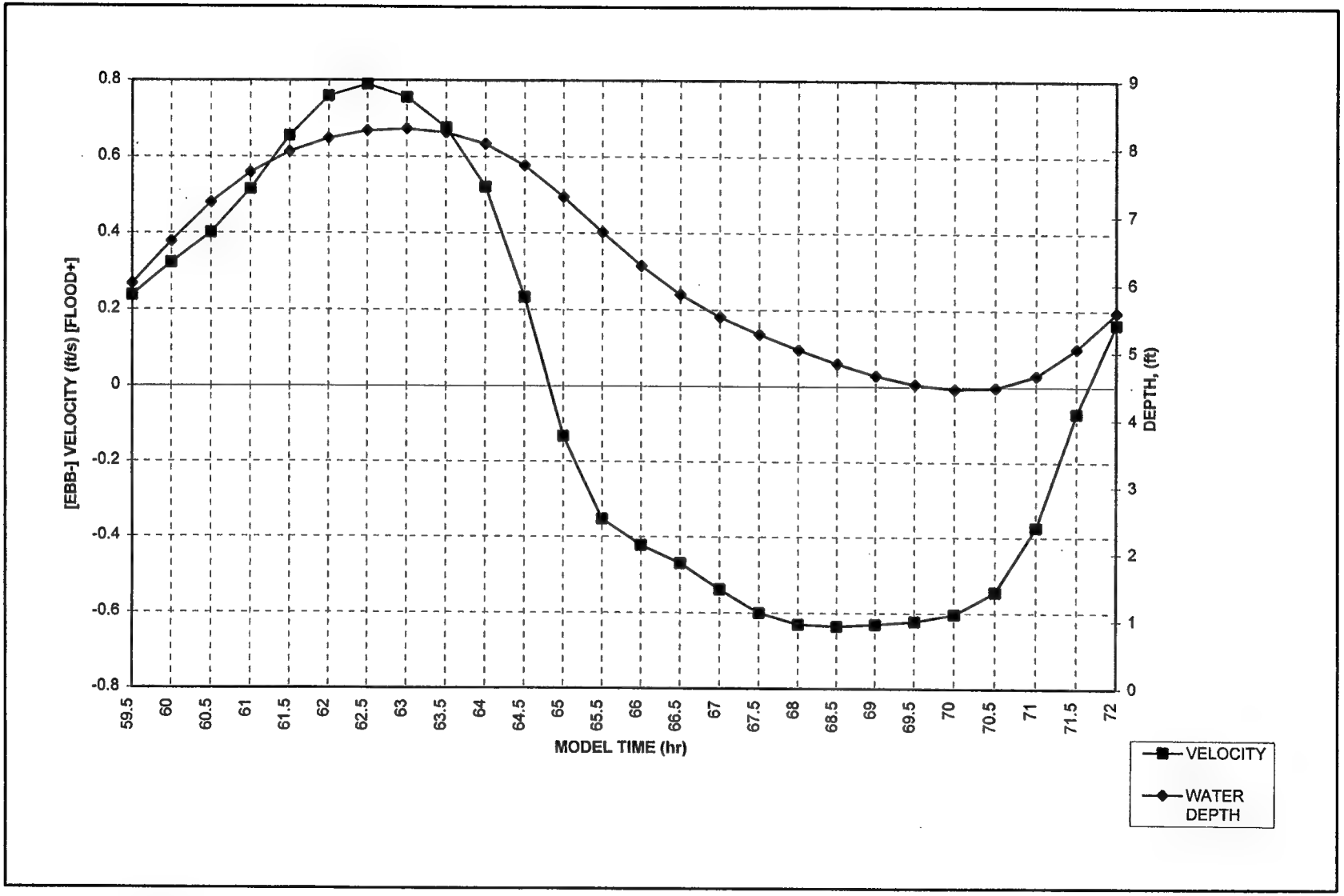

Figure 32. Velocity magnitude and depth for existing condition (base) at station 6 (to convert velocities to meters per second, multiply by 0.3048)

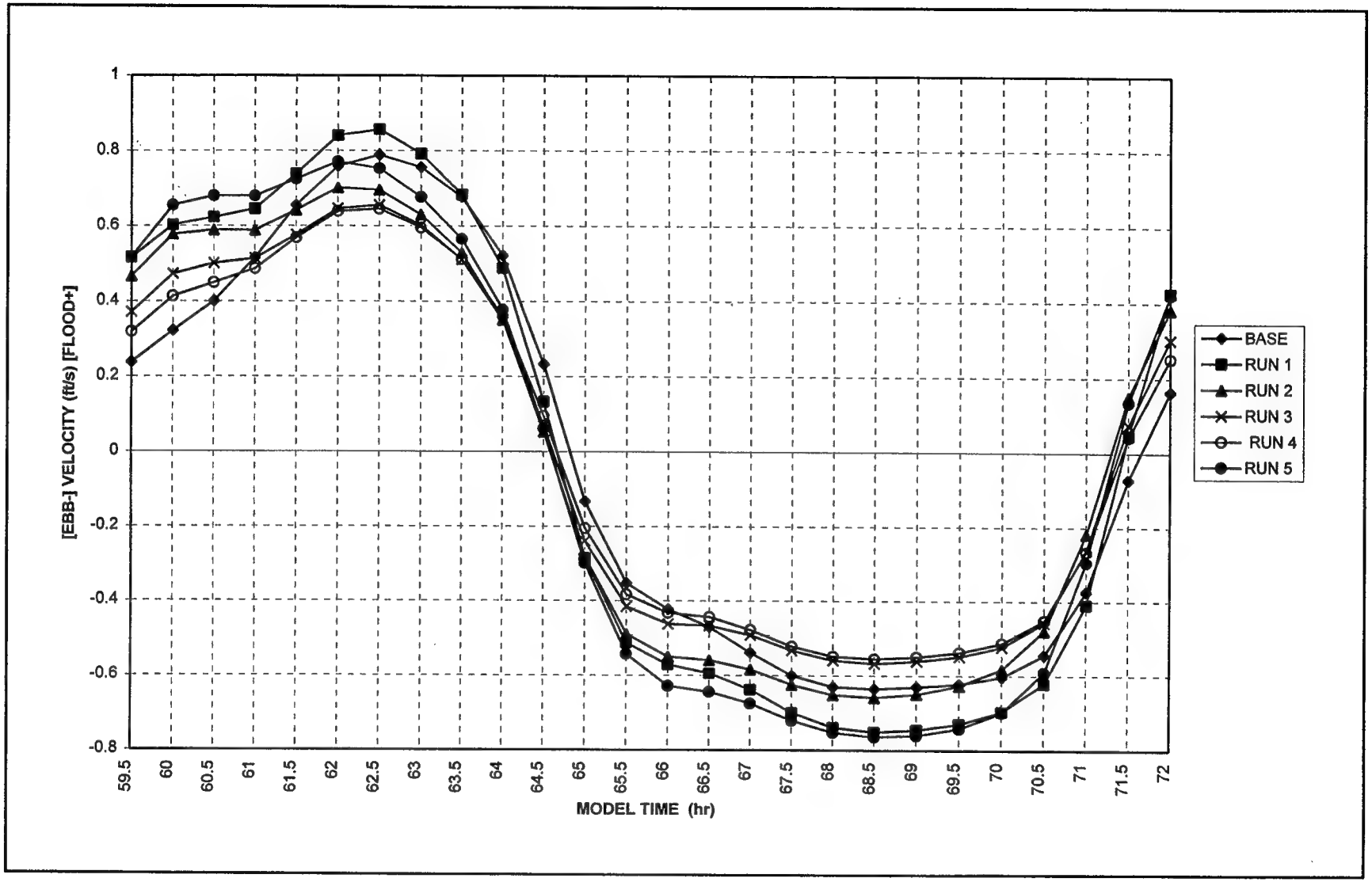

Figure 33. Velocity magnitude at station 6 (to convert velocities to meters per second, multiply by 0.3048)

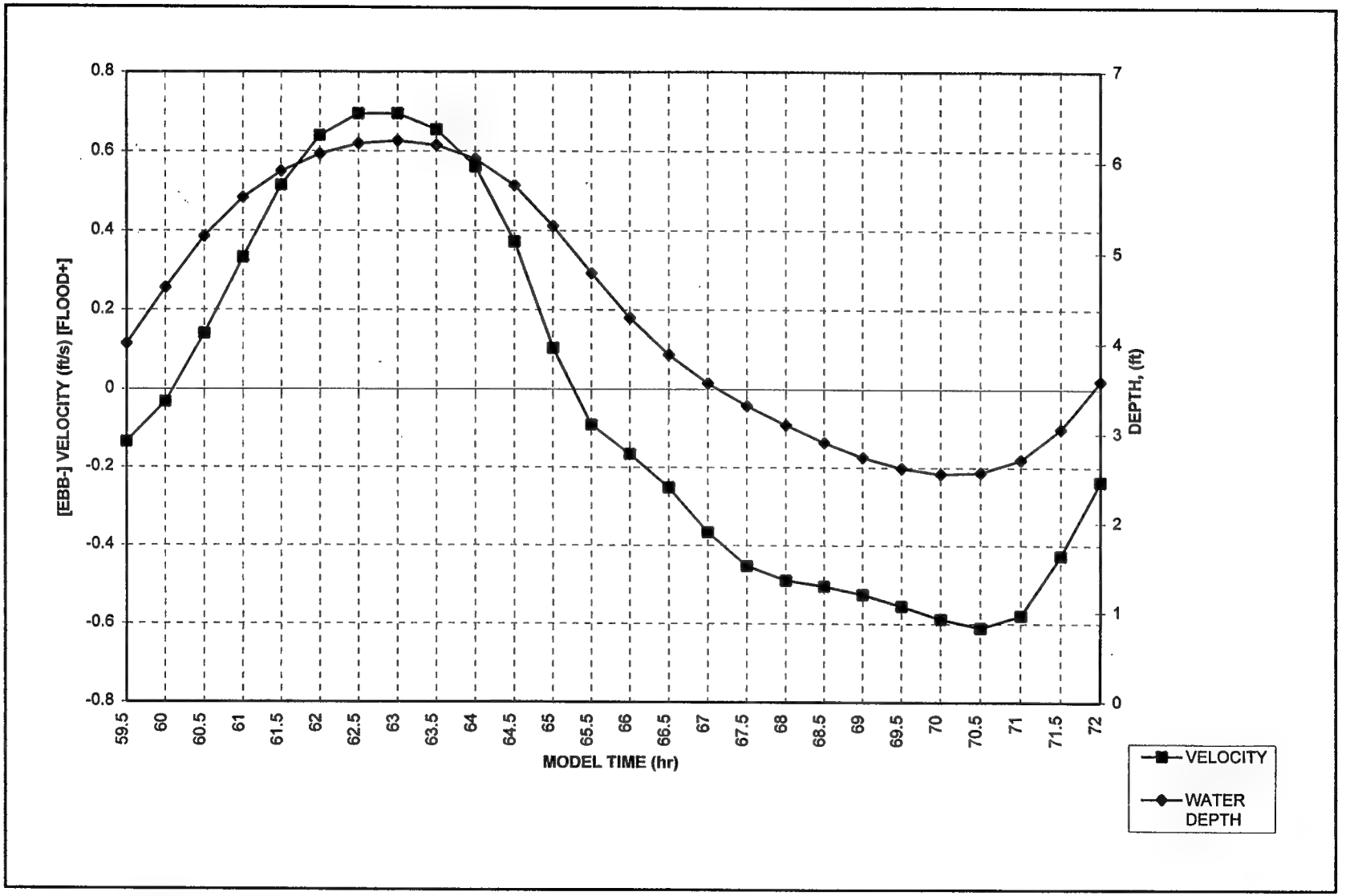

Figure 34. Velocity magnitude and depth for existing condition (base) at station 7 (to convert velocities to meters per second, multiply by 0.3048)

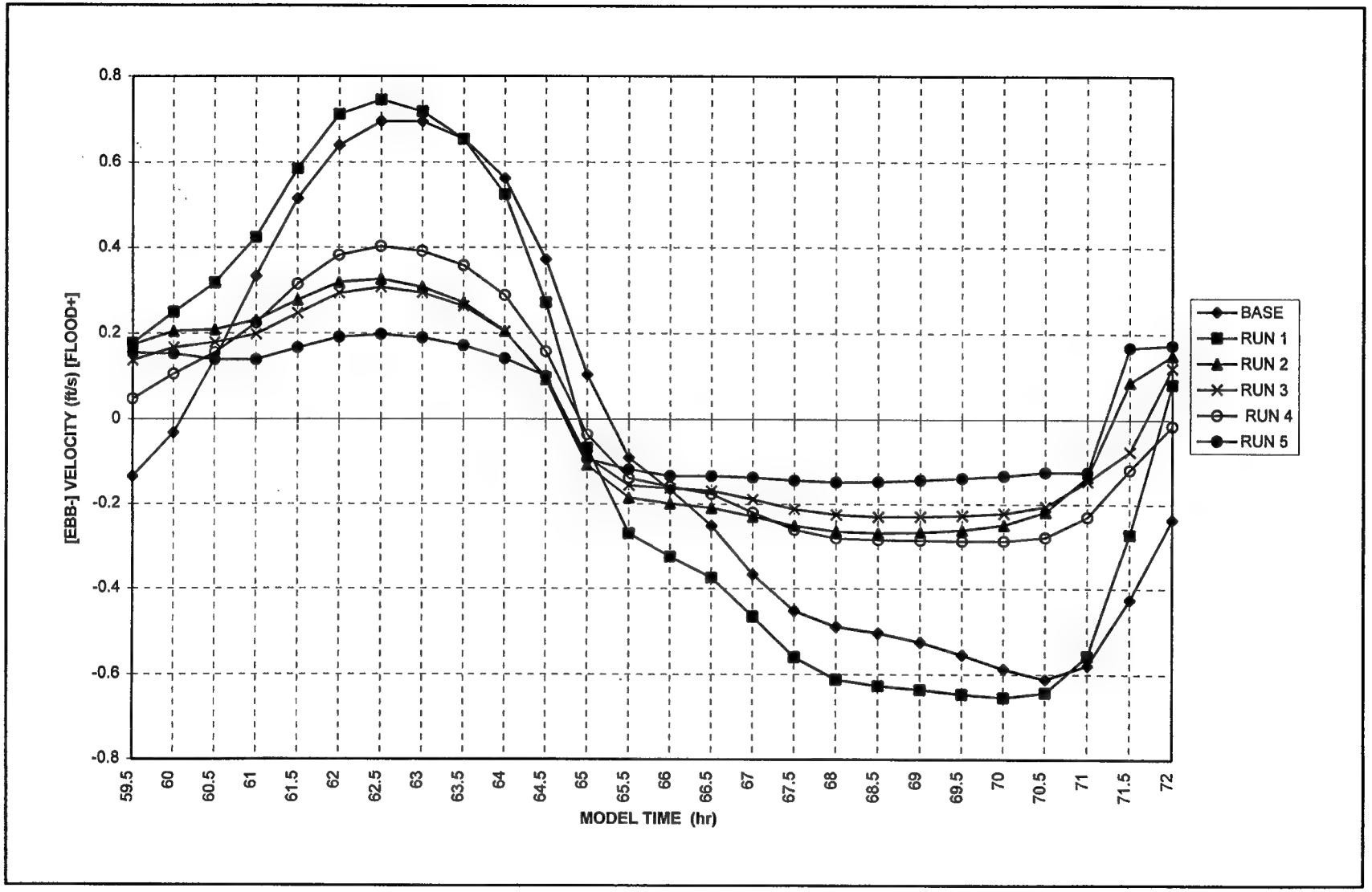

Figure 35. Velocity magnitude at station 7 (to convert velocities to meters per second, multiply by 0.3048)

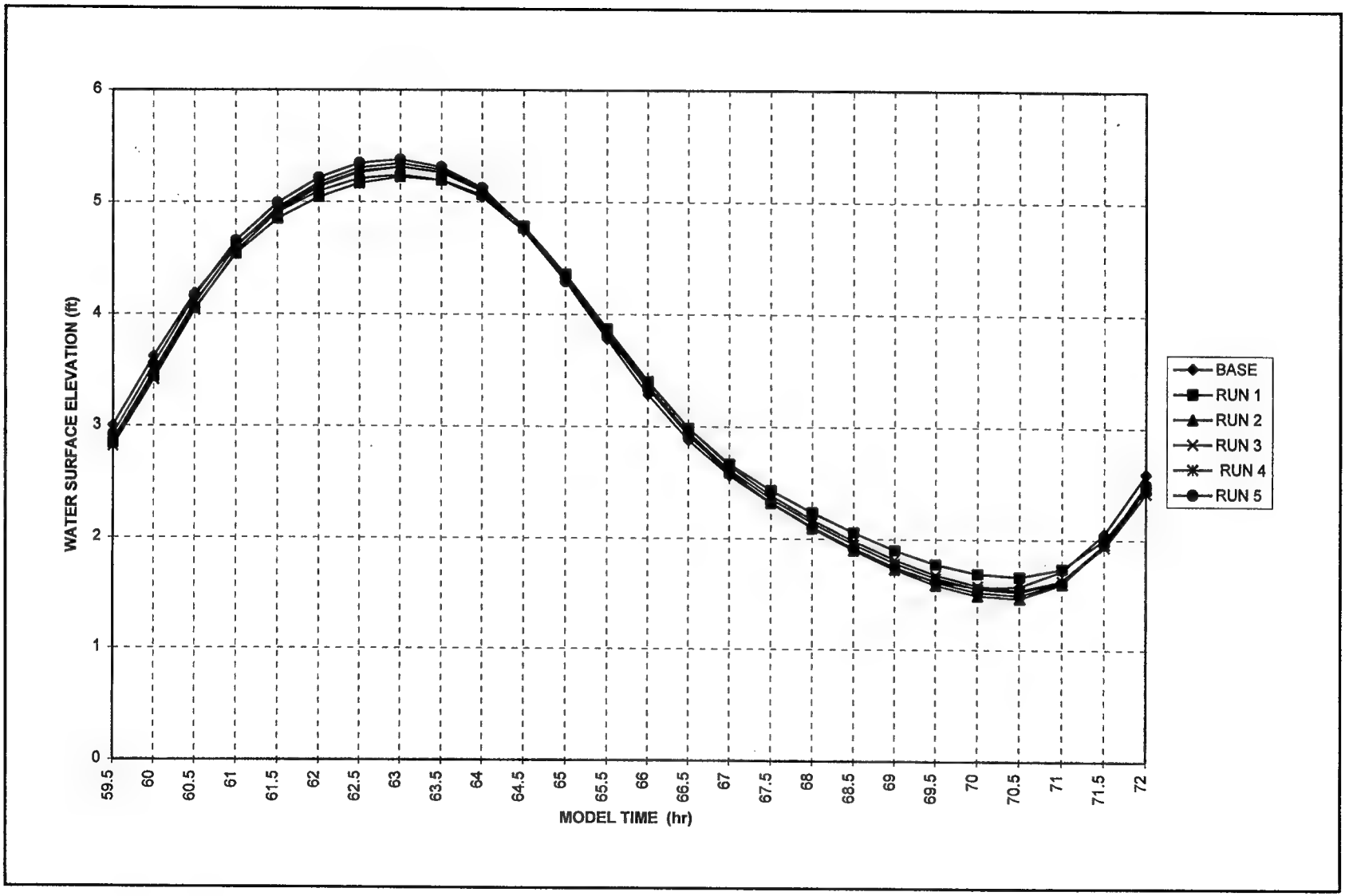

Figure 36. Water surface elevation at station 7 (to convert velocities to meters per second, multiply by 0.3048)

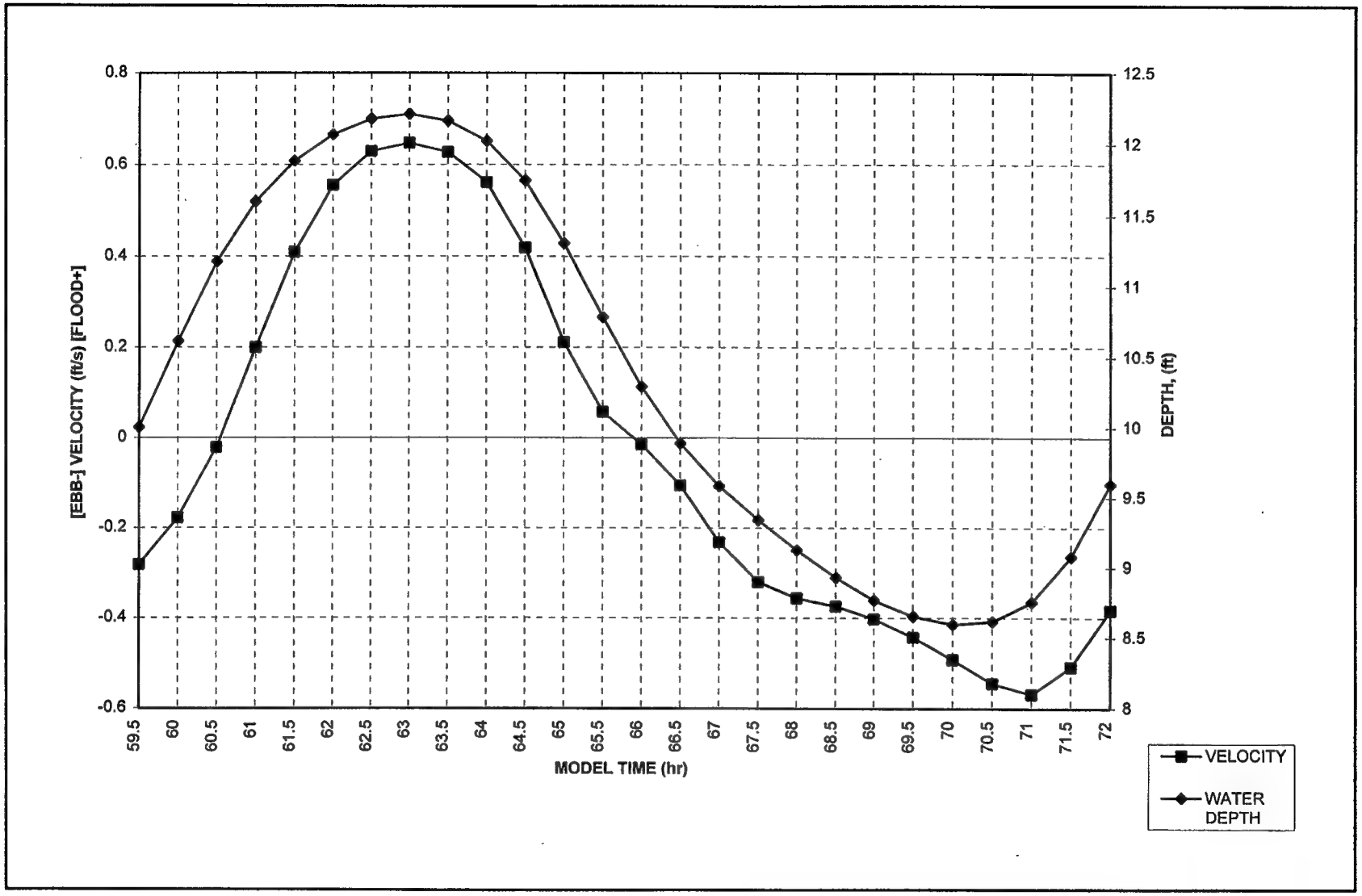

Figure 37. Velocity magnitude and depth for existing condition (base) at station 8 (to convert velocities to meters per second, multiply by 0.3048)

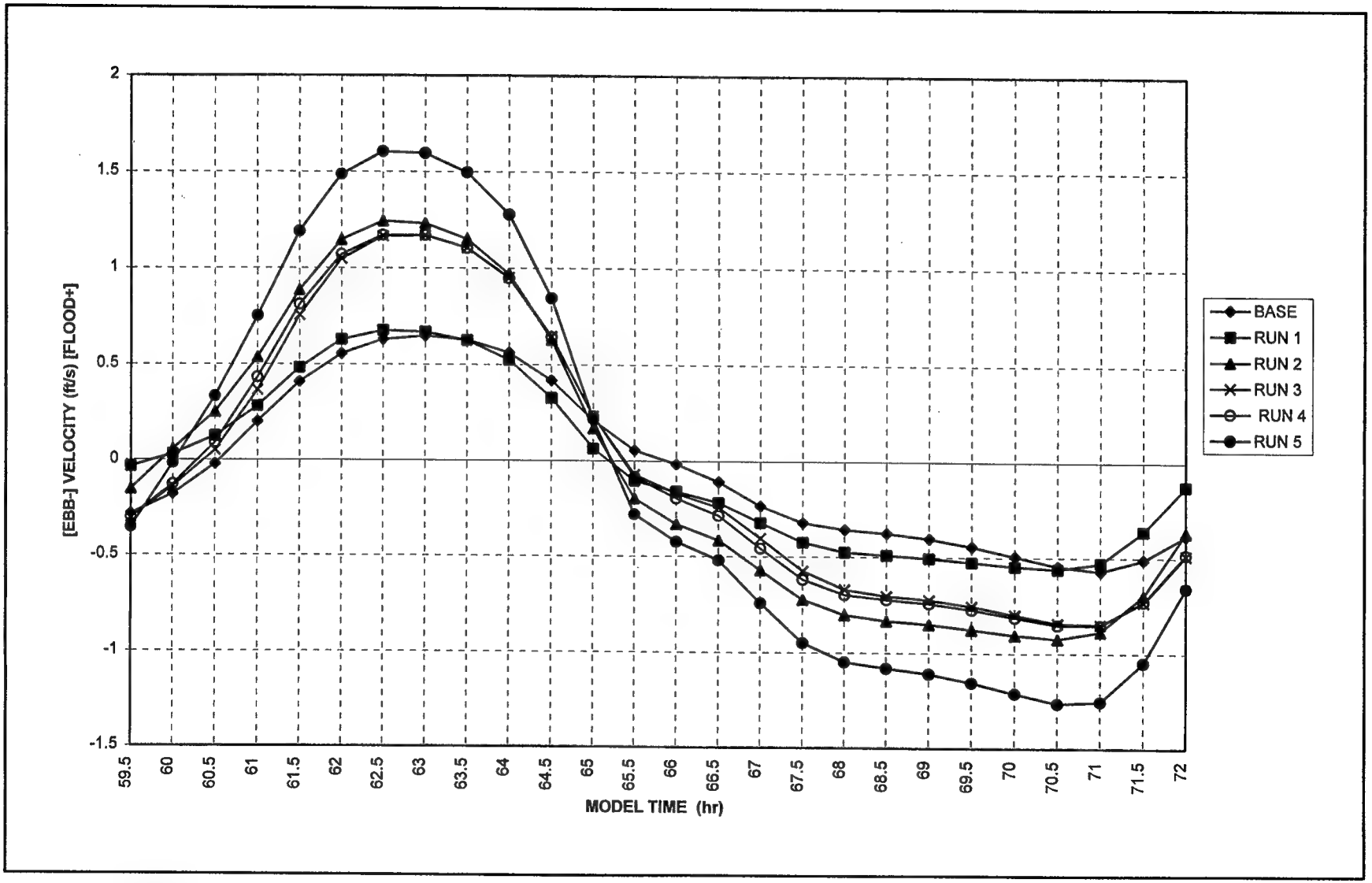

Figure 38. Velocity magnitude at station 8 (to convert velocities to meters per second, multiply by 0.3048)

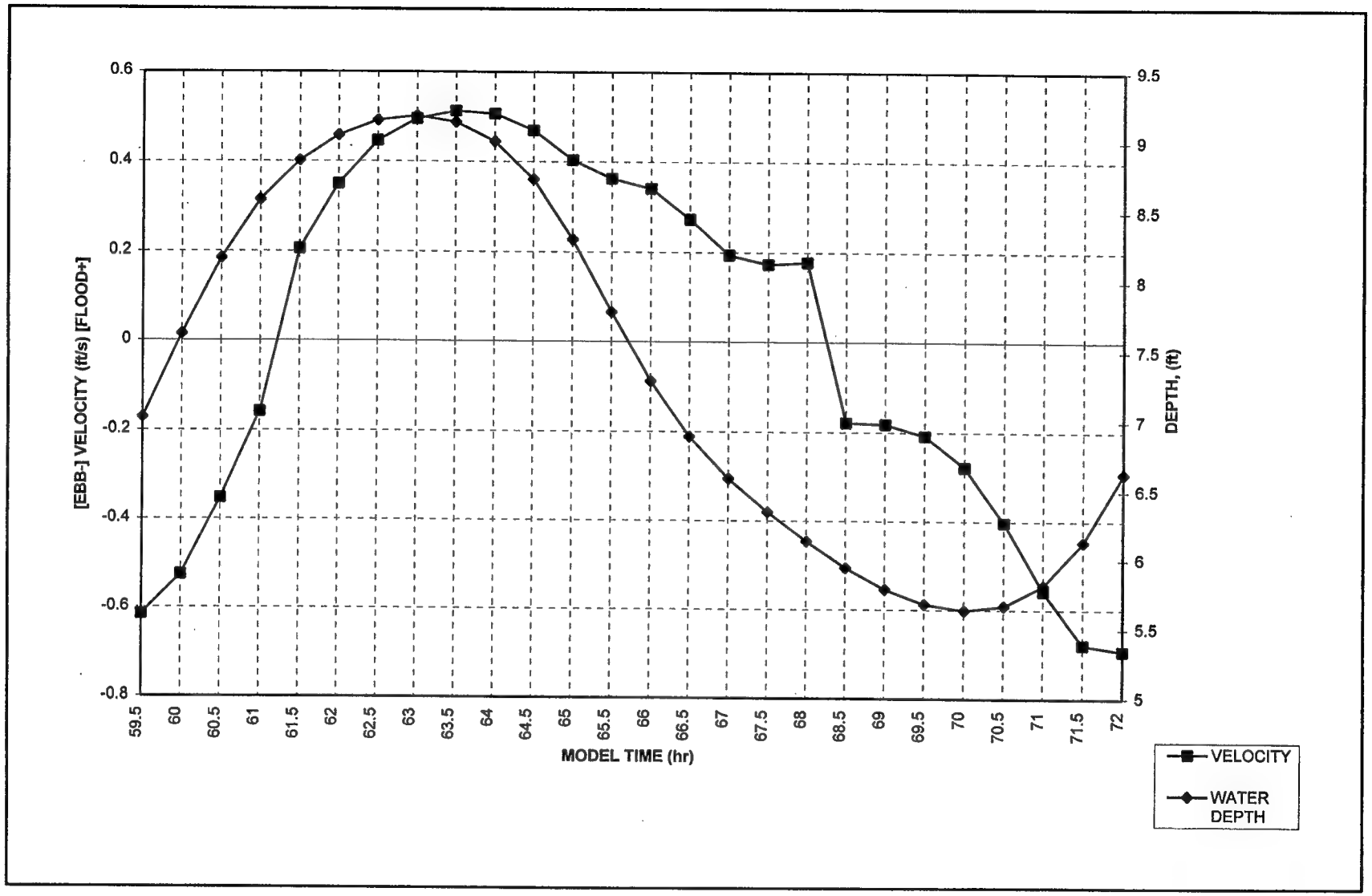

Figure 39. Velocity magnitude and depth for existing condition (base) at station 9 (to convert velocities to meters per second, multiply by 0.3048)

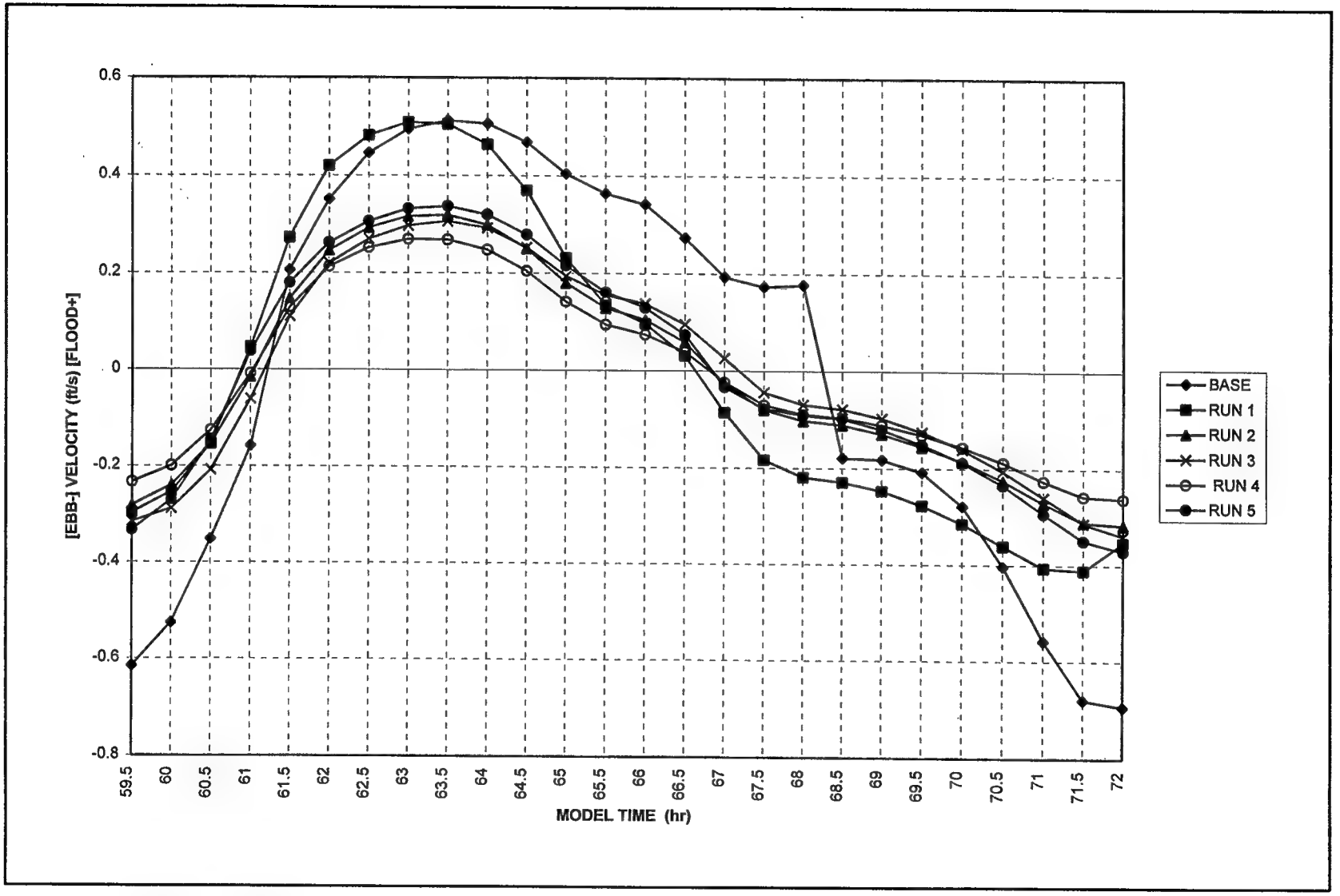

Figure 40. Velocity magnitude at station 9 (to convert velocities to meters per second, multiply by 0.3048)

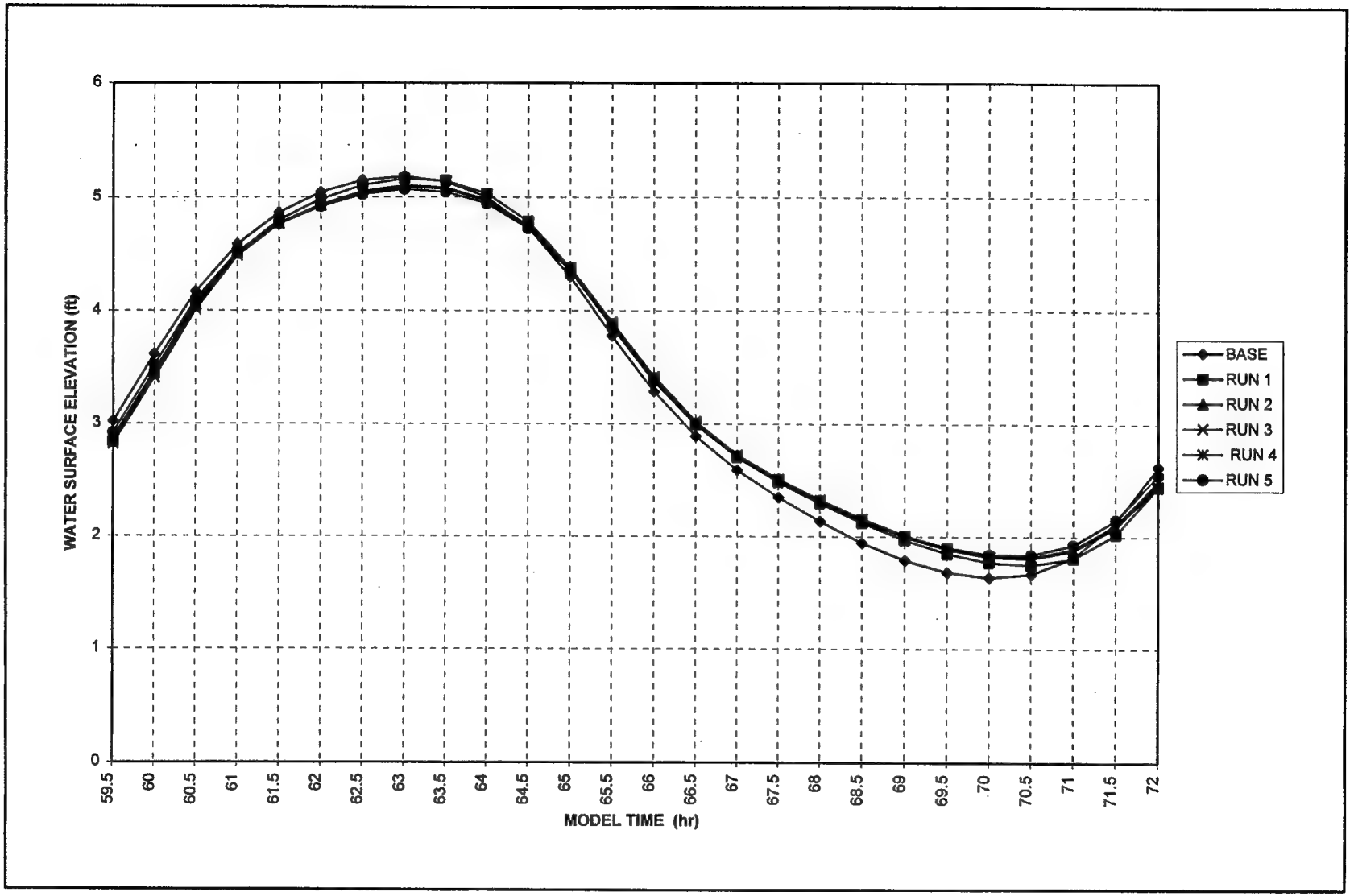

Figure 41. Water surface elevation at station 9 (to convert velocities to meters per second, multiply by 0.3048)

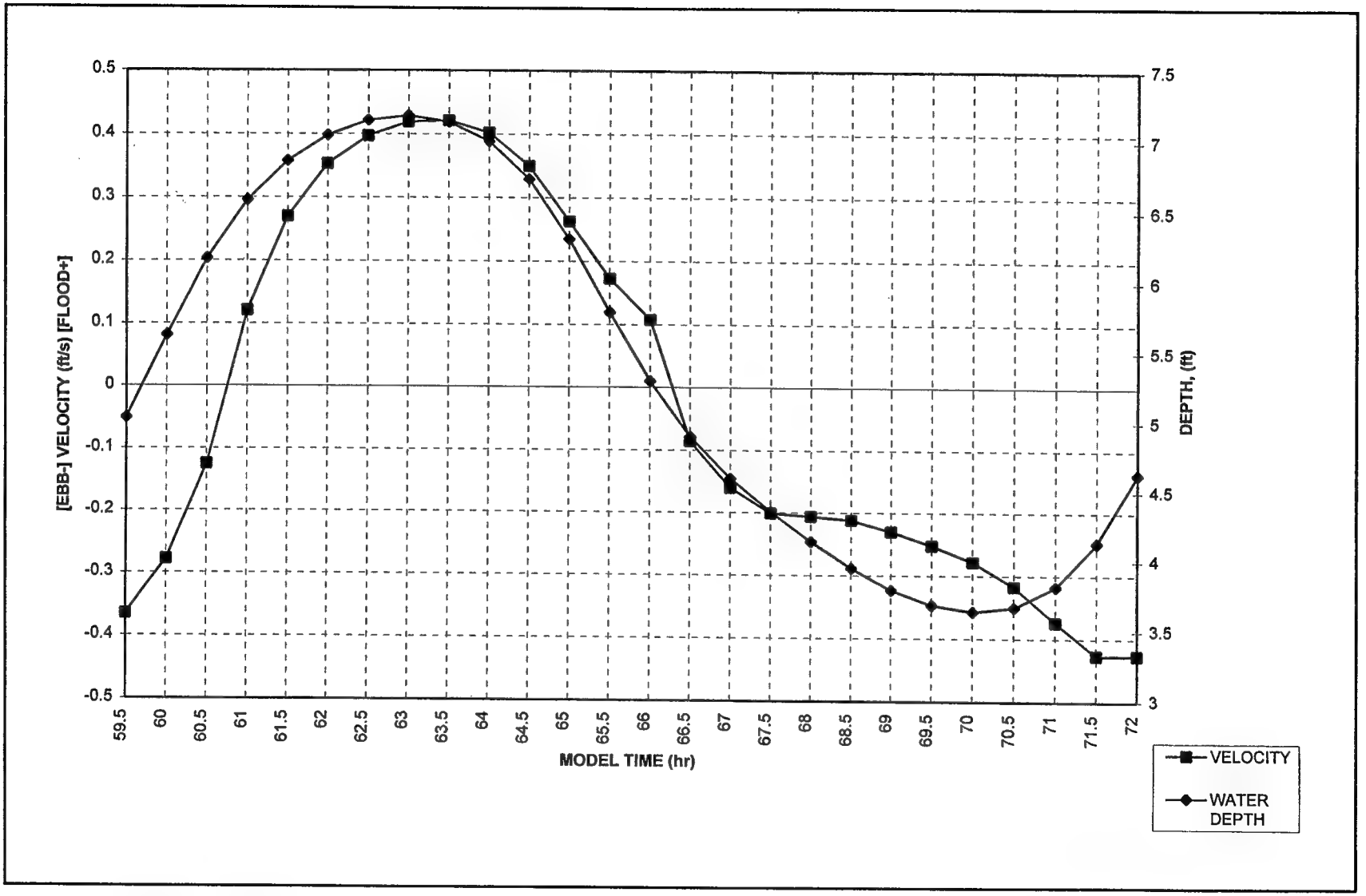

Figure 42. Velocity magnitude and depth for existing condition (base) at station 10 (to convert velocities to meters per second, multiply by 0.3048)

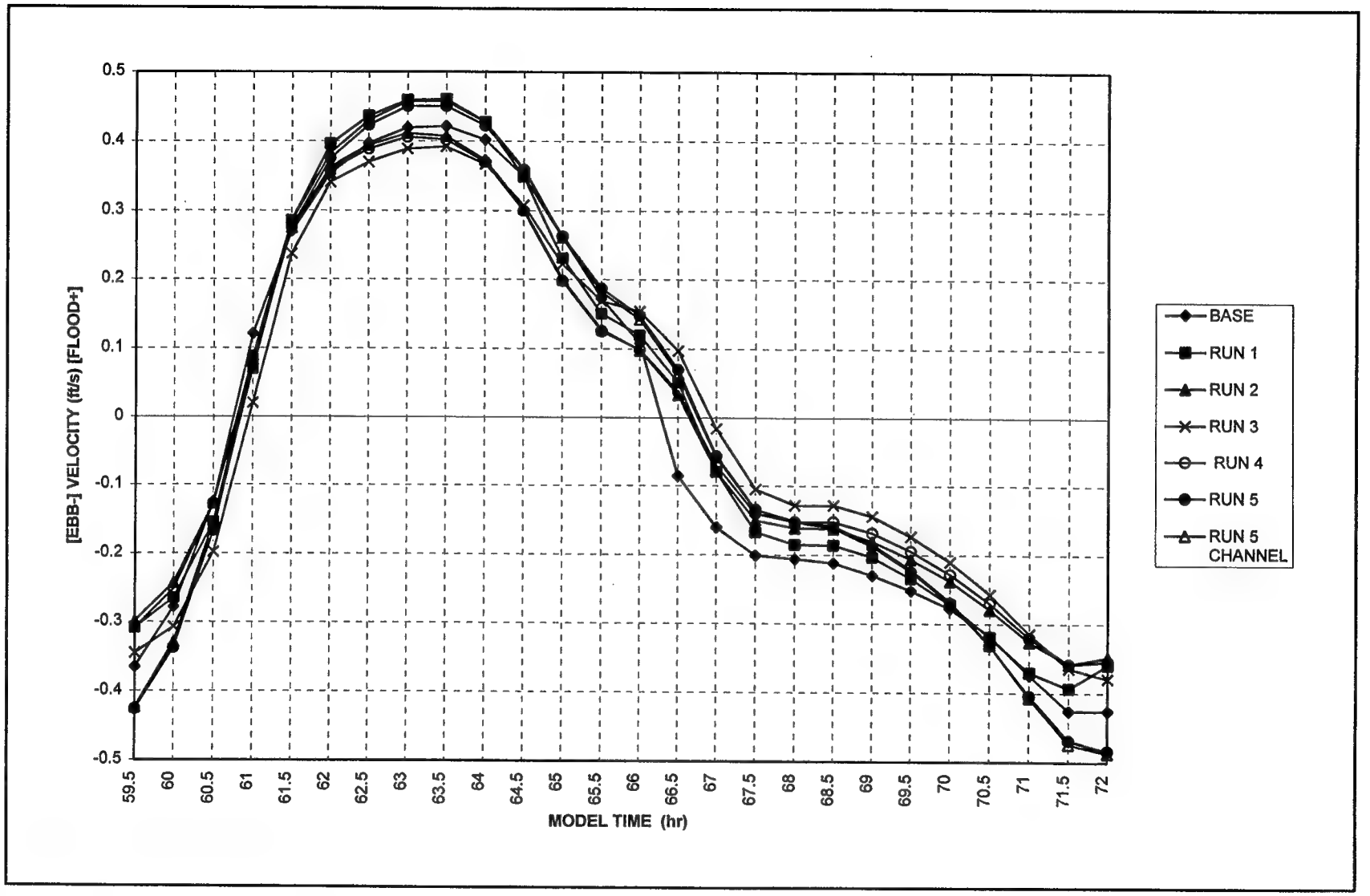

Figure 43. Velocity magnitude at station 10 (to convert velocities to meters per second, multiply by 0.3048)

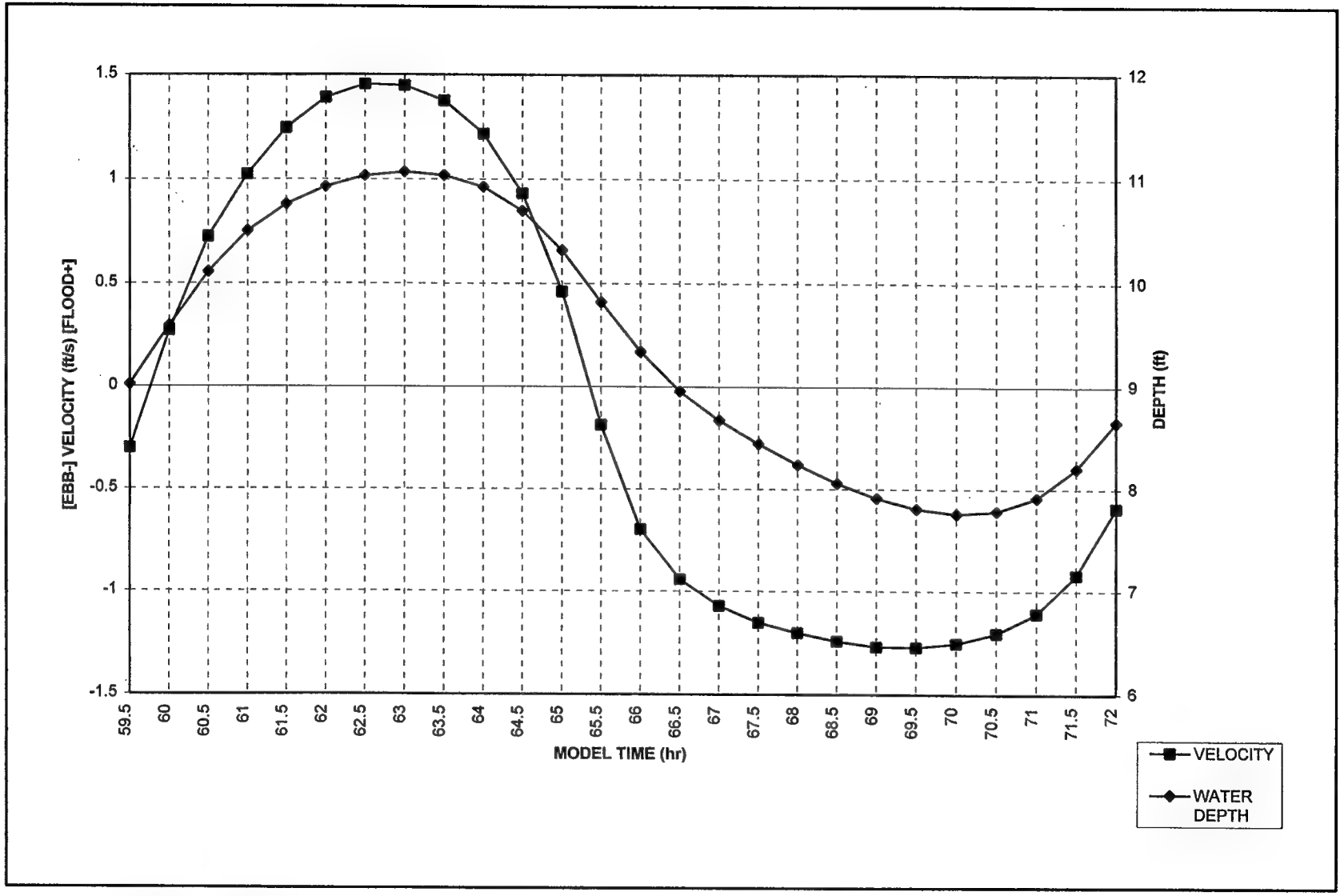

Figure 44. Velocity magnitude and depth for existing condition (base) at station 11 (to convert velocities to meters per second, multiply by 0.3048)

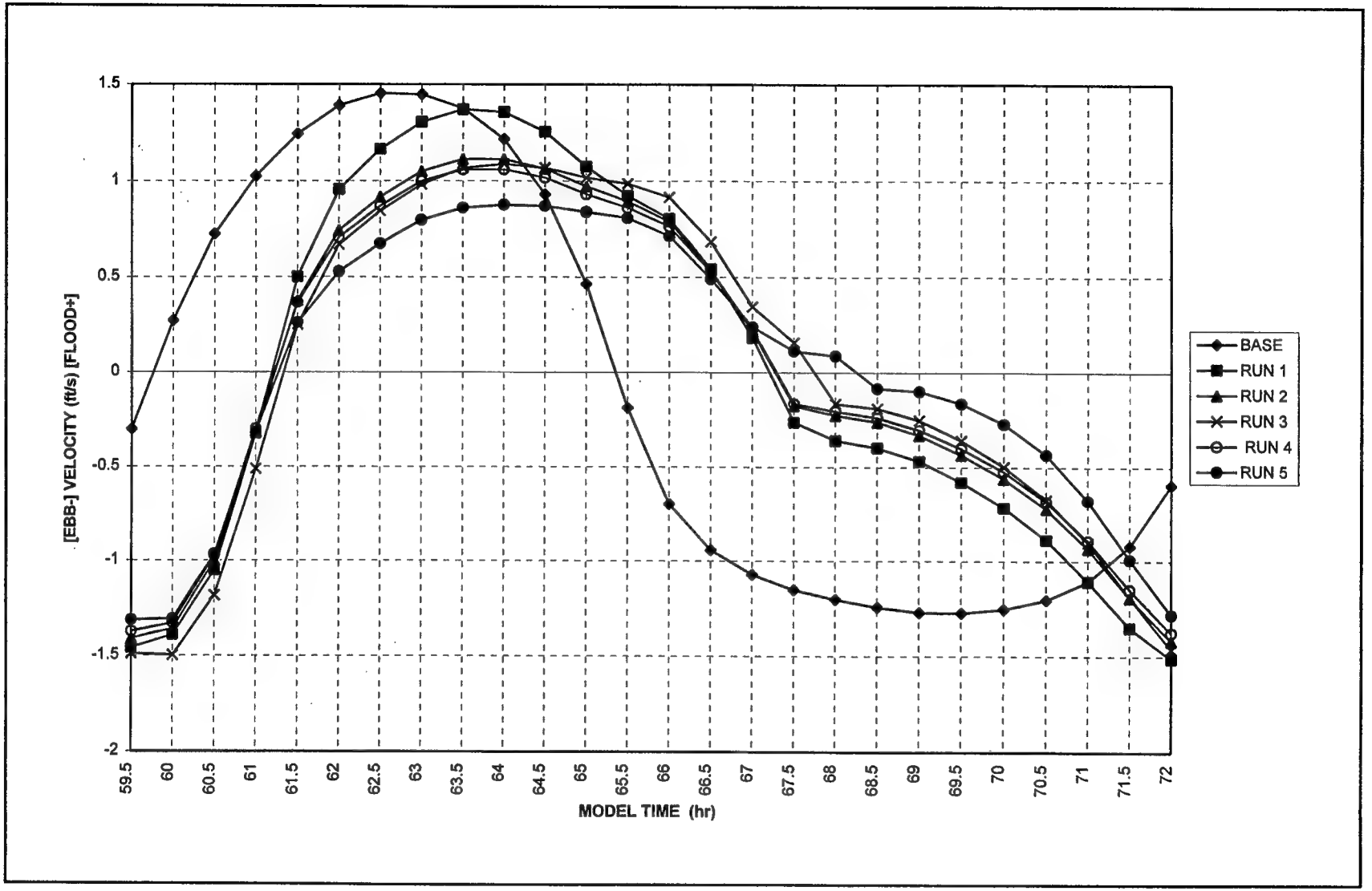

Figure 45. Velocity magnitude at station 11 (to convert velocities to meters per second, multiply by 0.3048)

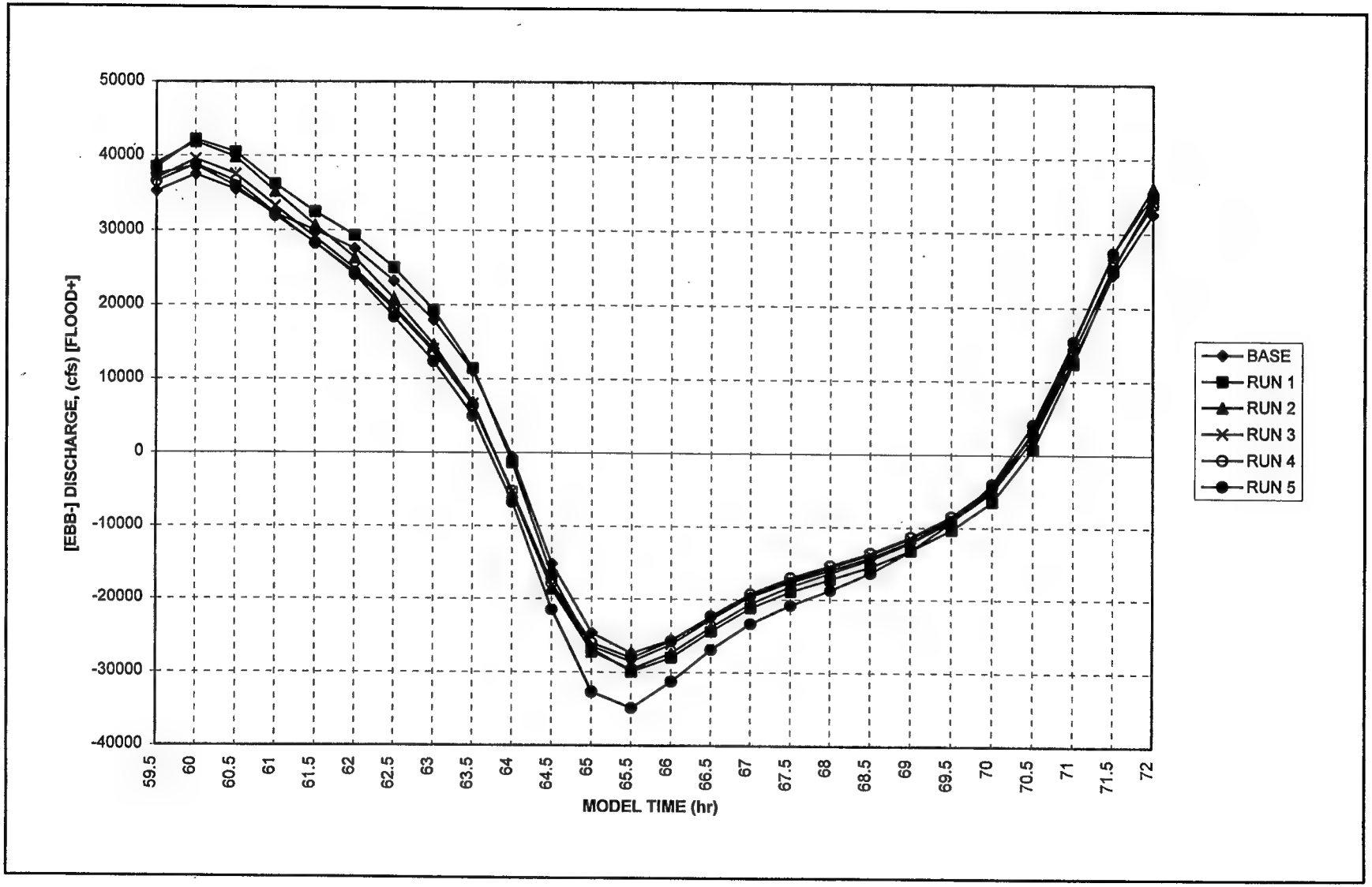

Figure 46. Water discharge at range 24 (ebb discharge is out of Mill Cove) (to convert discharge to cu m/sec, multiply by 0.0283)

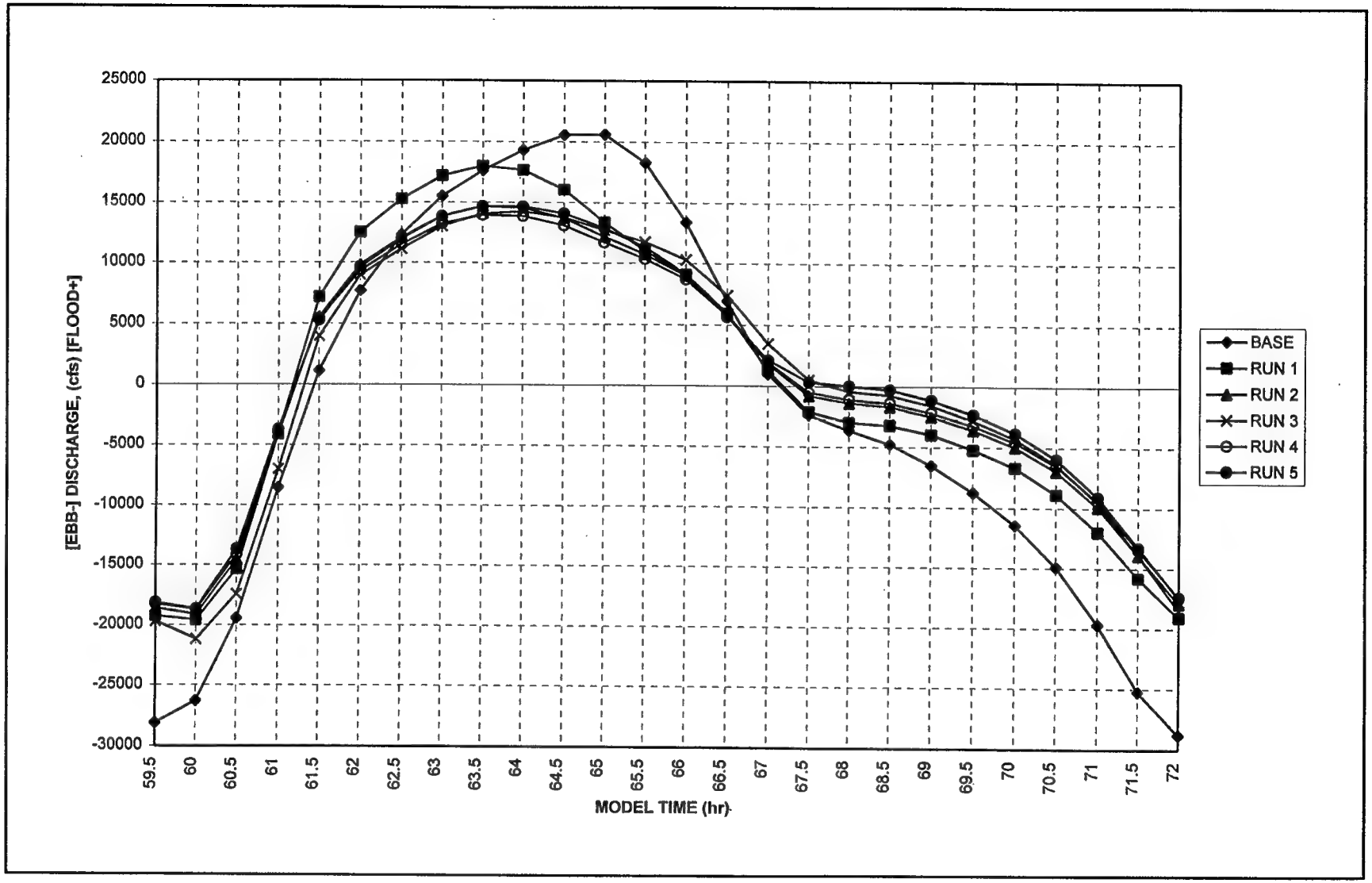

Figure 47. Water discharge at ranges 35+36 (ebb discharge is into Mill Cove) (to convert discharge to cu m/sec, multiply by 0.0283)

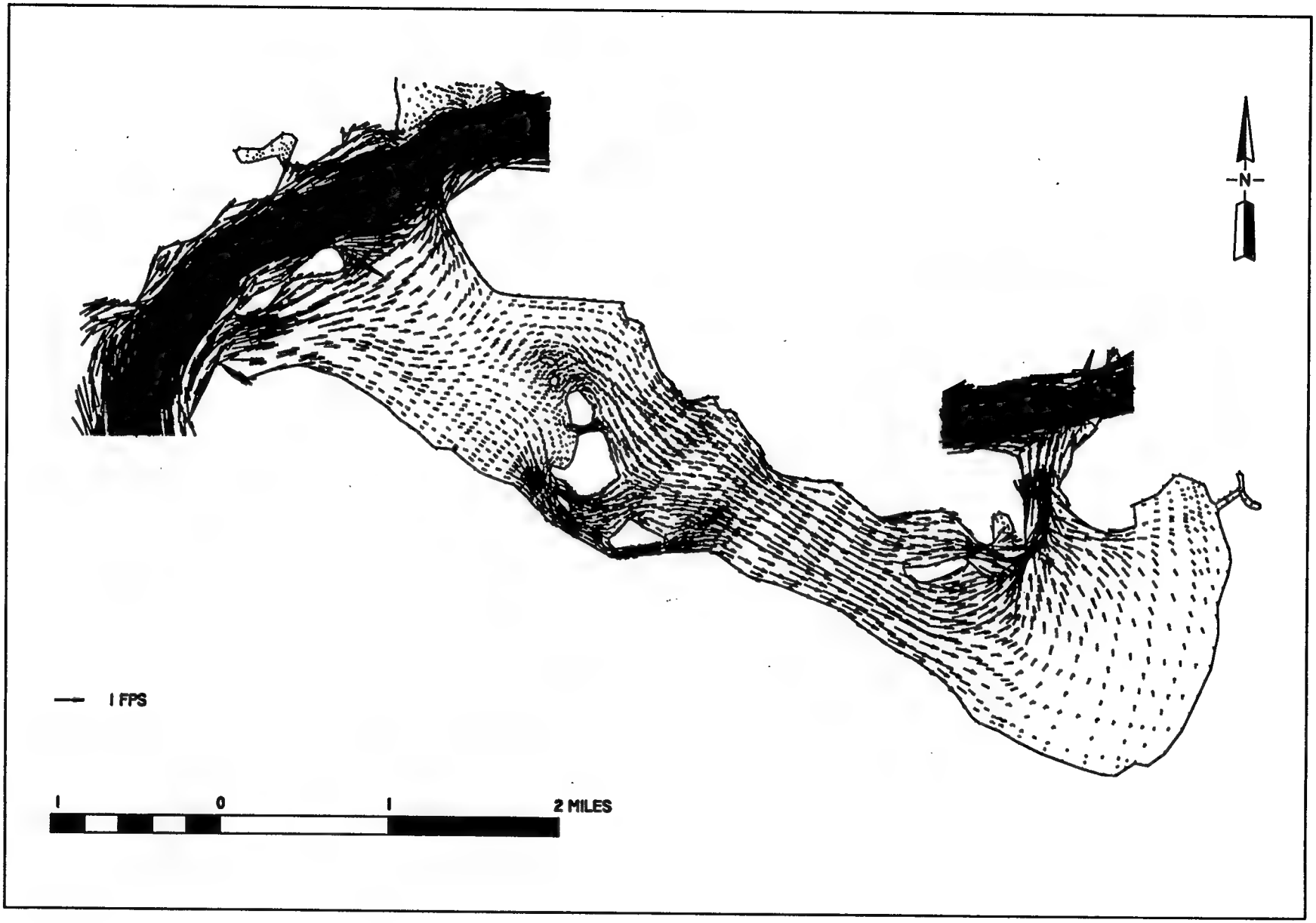

Figure 48. Ebb velocity vectors at Mill Cove, existing condition (to convert scale to kilometers, multiply by 1.6)

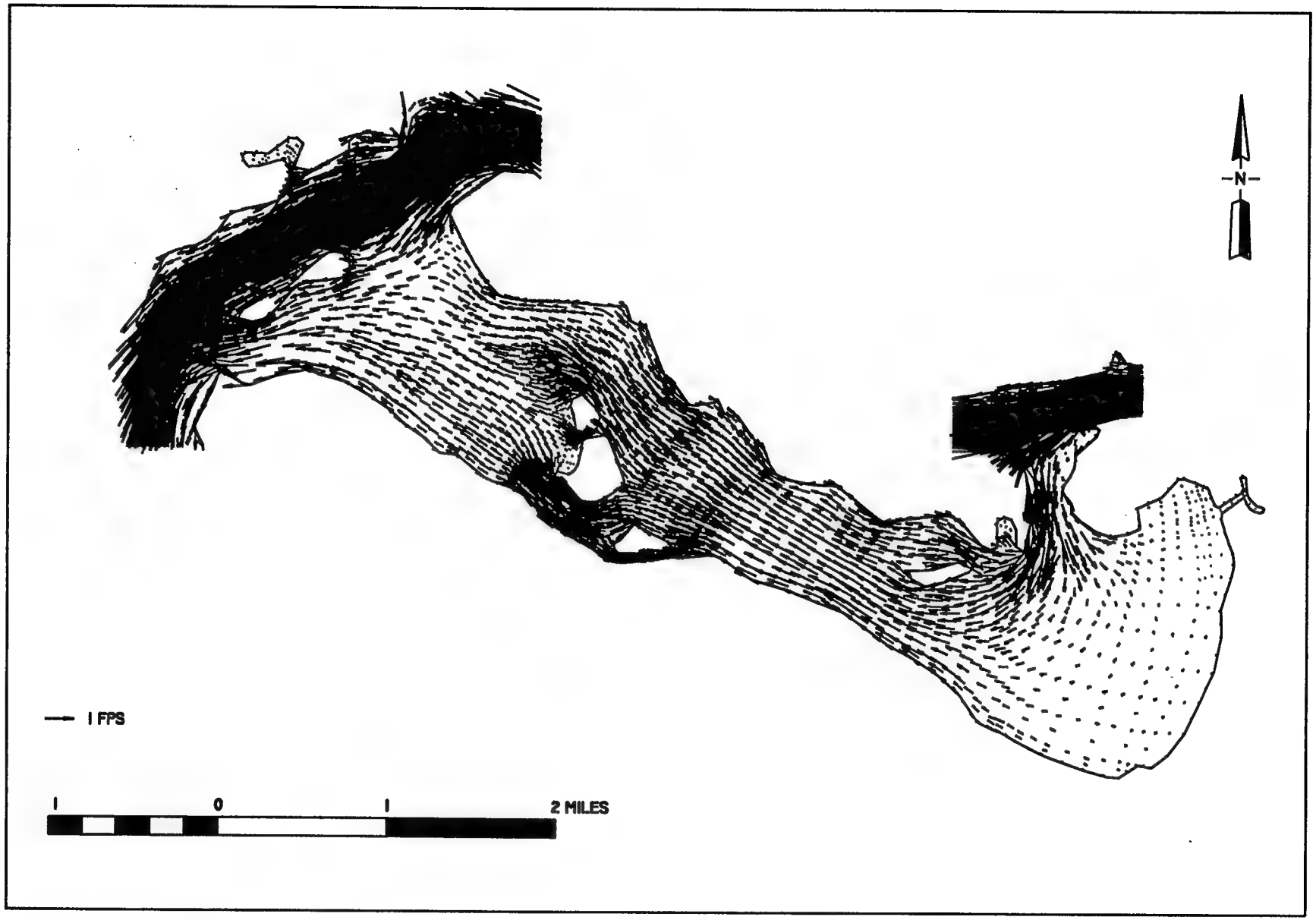

Figure 49. Flood velocity vectors at Mill Cove, existing conditions (to convert scale to kilometers, multiply by 1.6)

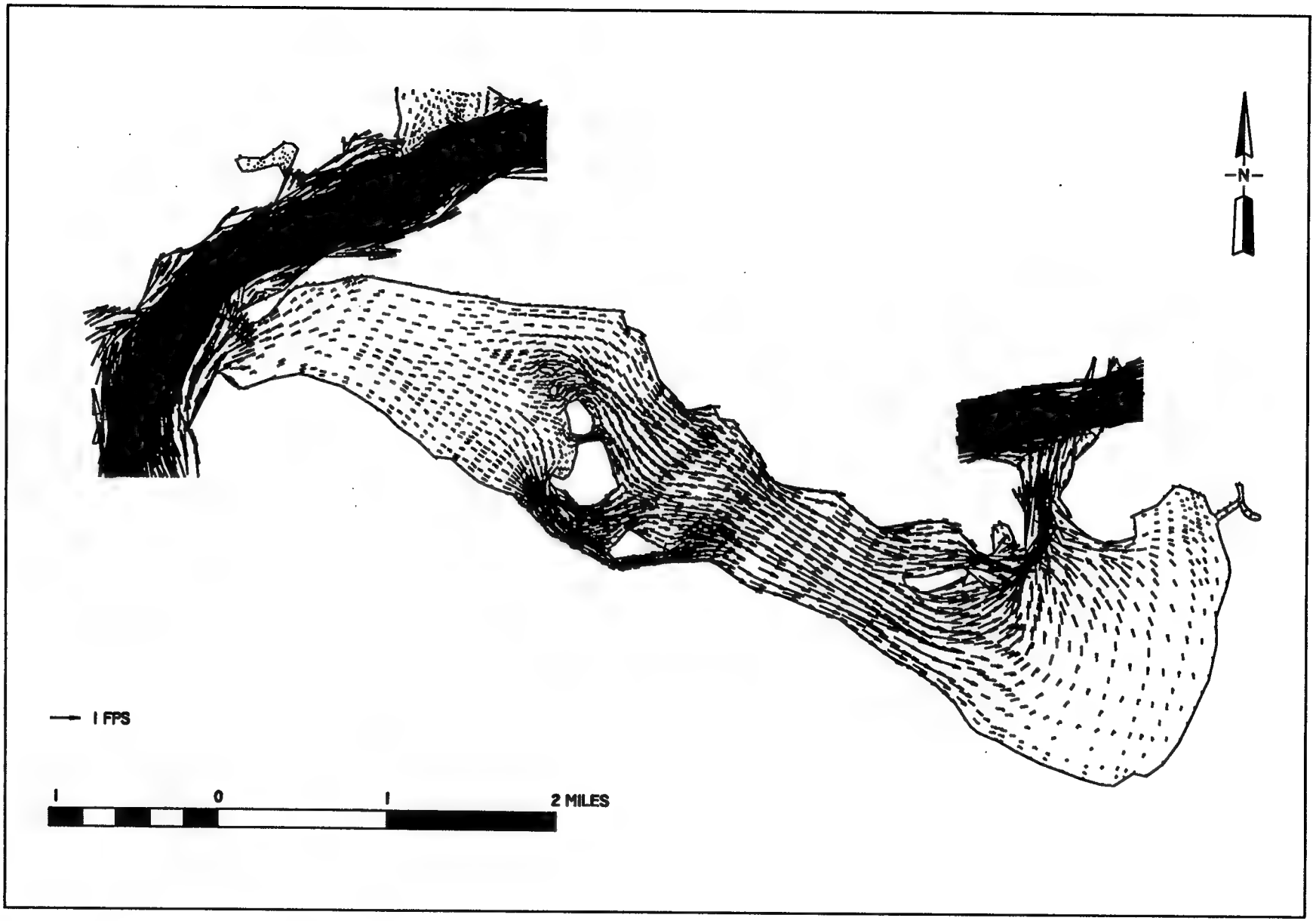

Figure 50. Ebb velocity vectors at Mill Cove, Plan 1 (to convert scale to kilometers, multiply by 1.6)

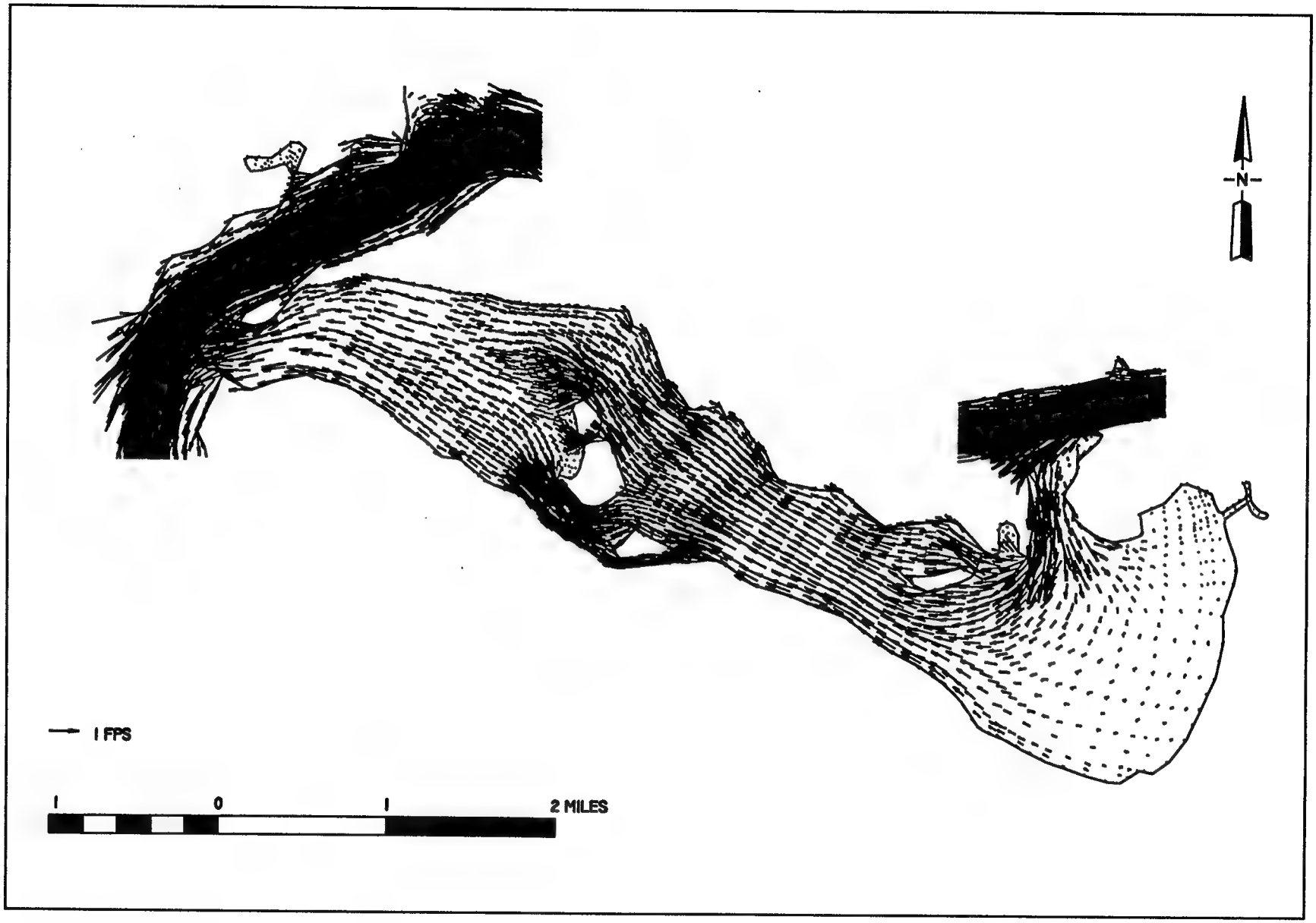

Figure 51. Flood velocity vectors at Mill Cove, Plan 1 (to convert scale to kilometers, multiply by 1.6)

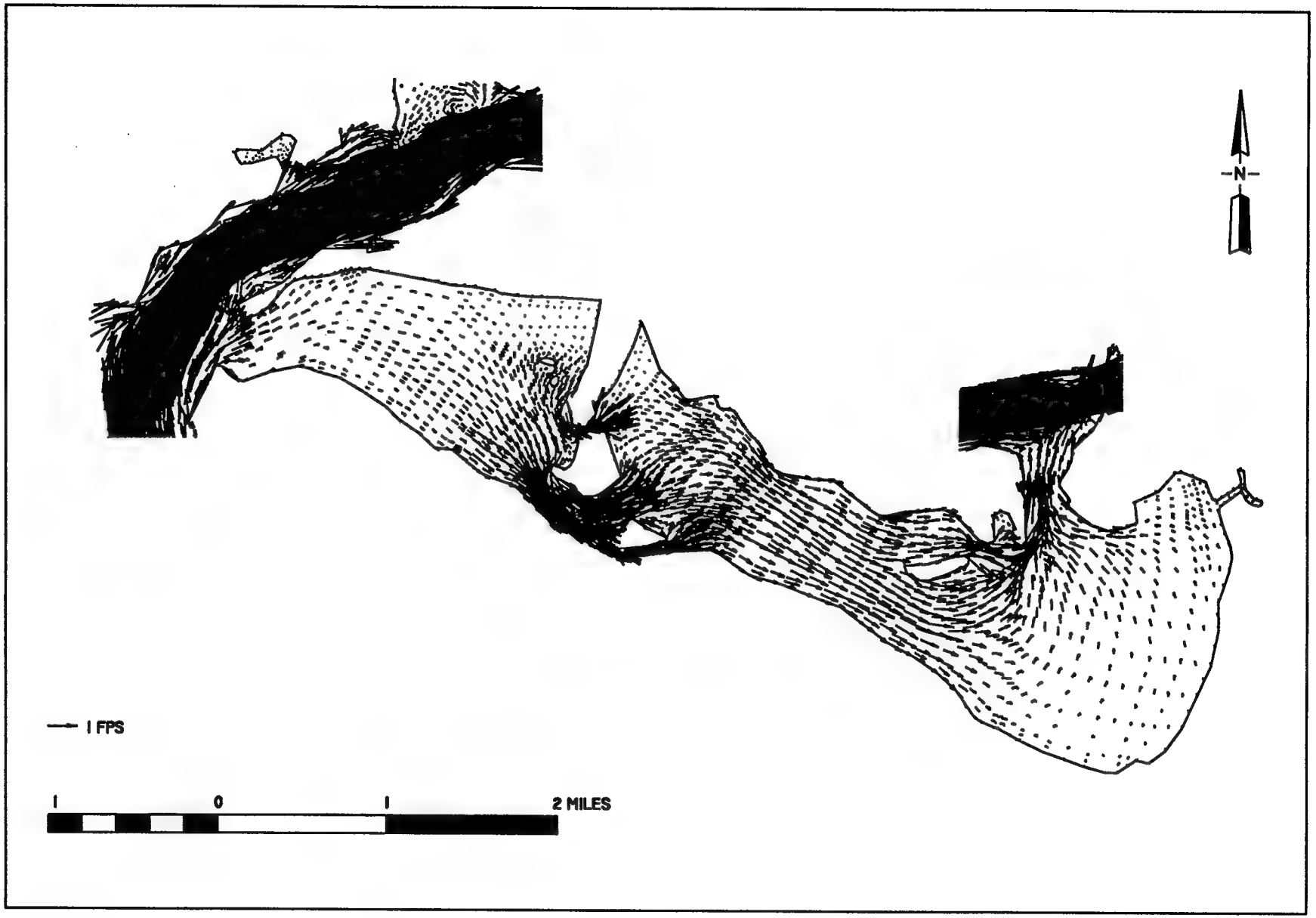

Figure 52. Ebb velocity vectors at Mill Cove, Plan 2 (to convert scale to kilometers, multiply by 1.6)

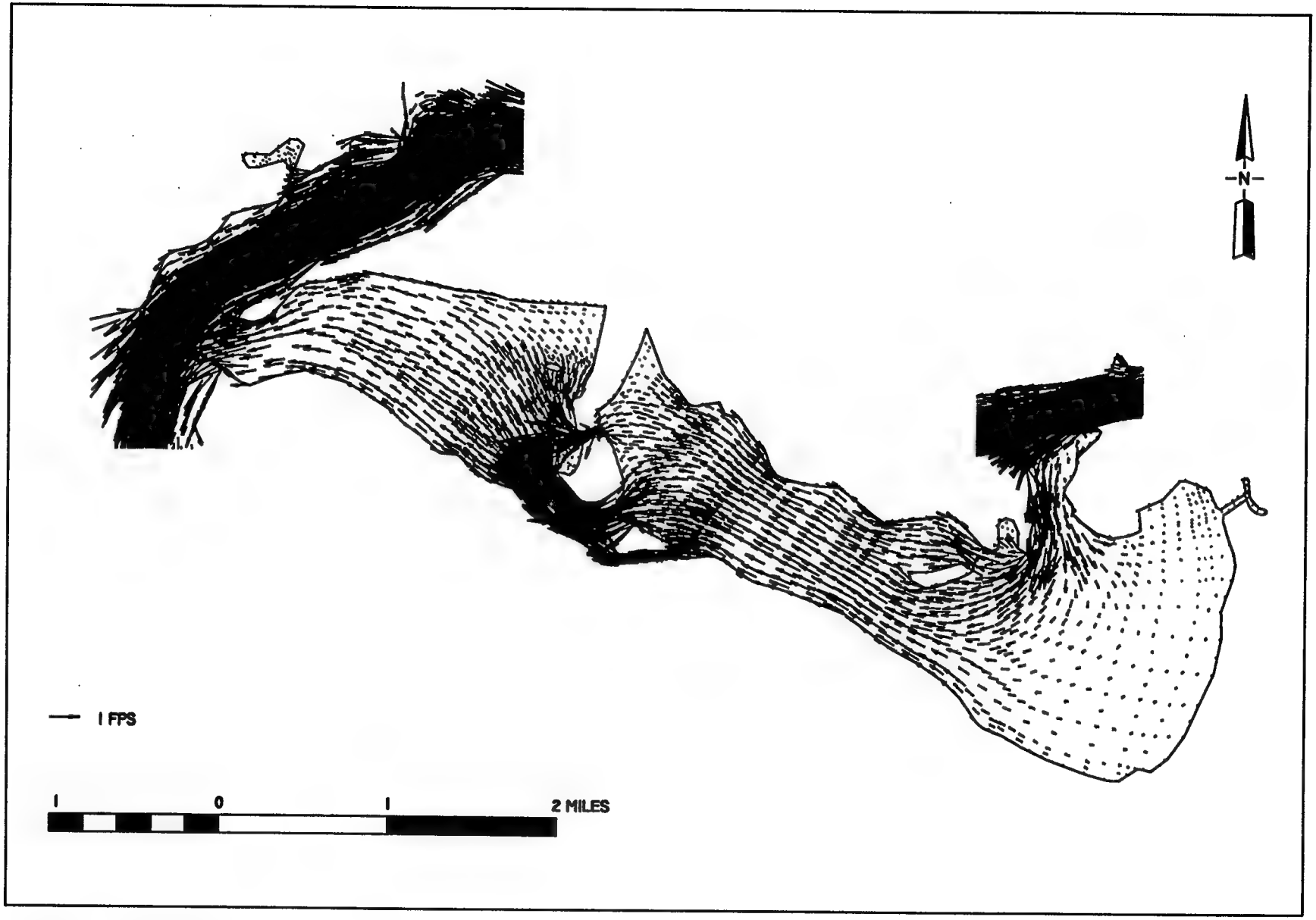

Figure 53. Flood velocity vectors at Mill Cove, Plan 2 (to convert scale to kilometers, multiply by 1.6)

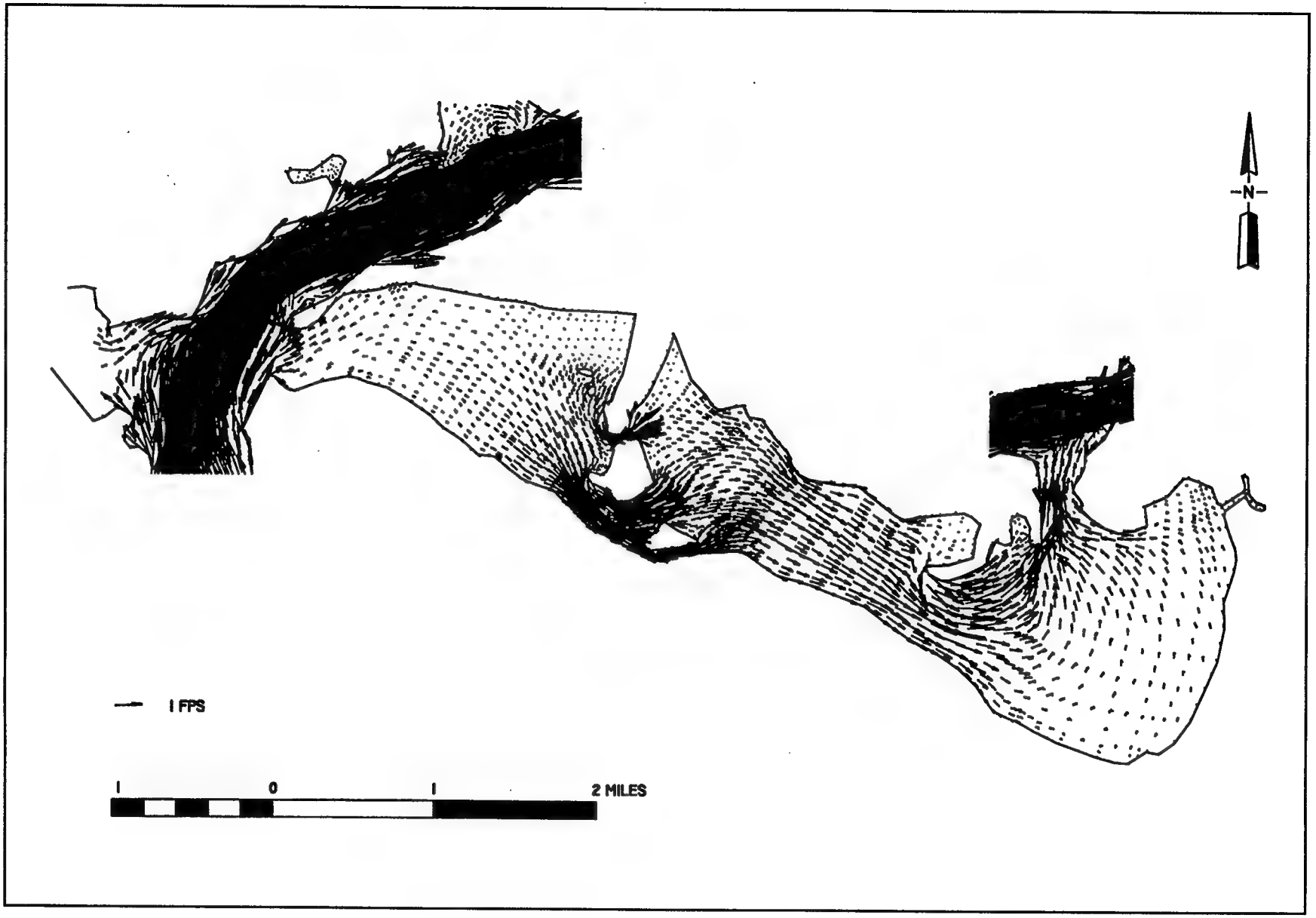

Figure 54. Ebb velocity vectors at Mill Cove, Plan 3 (to convert scale to kilometers, multiply by 1.6)

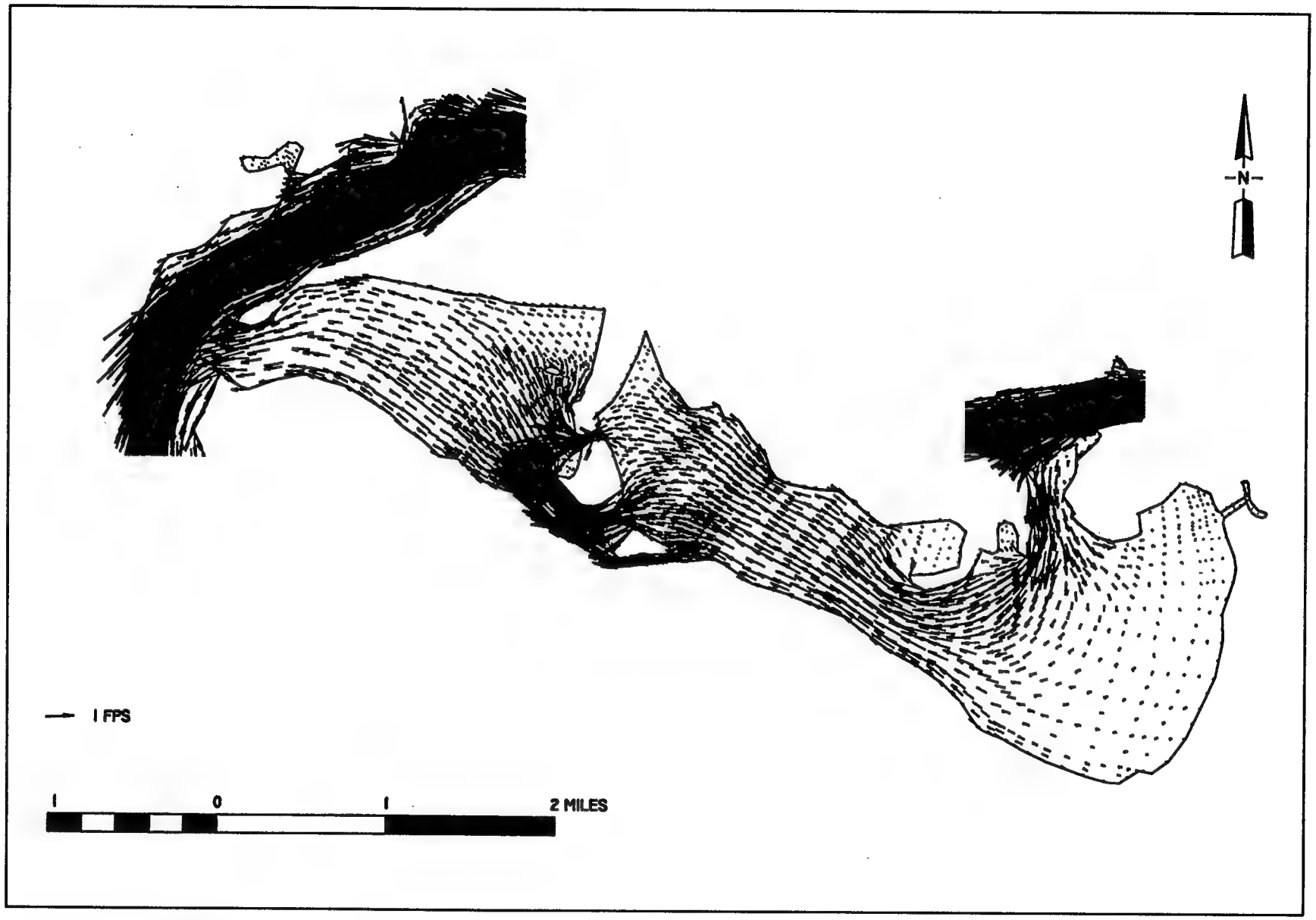

Figure 55. Flood velocity vectors at Mill Cove, Plan 3 (to convert scale to kilometers, multiply by 1.6)

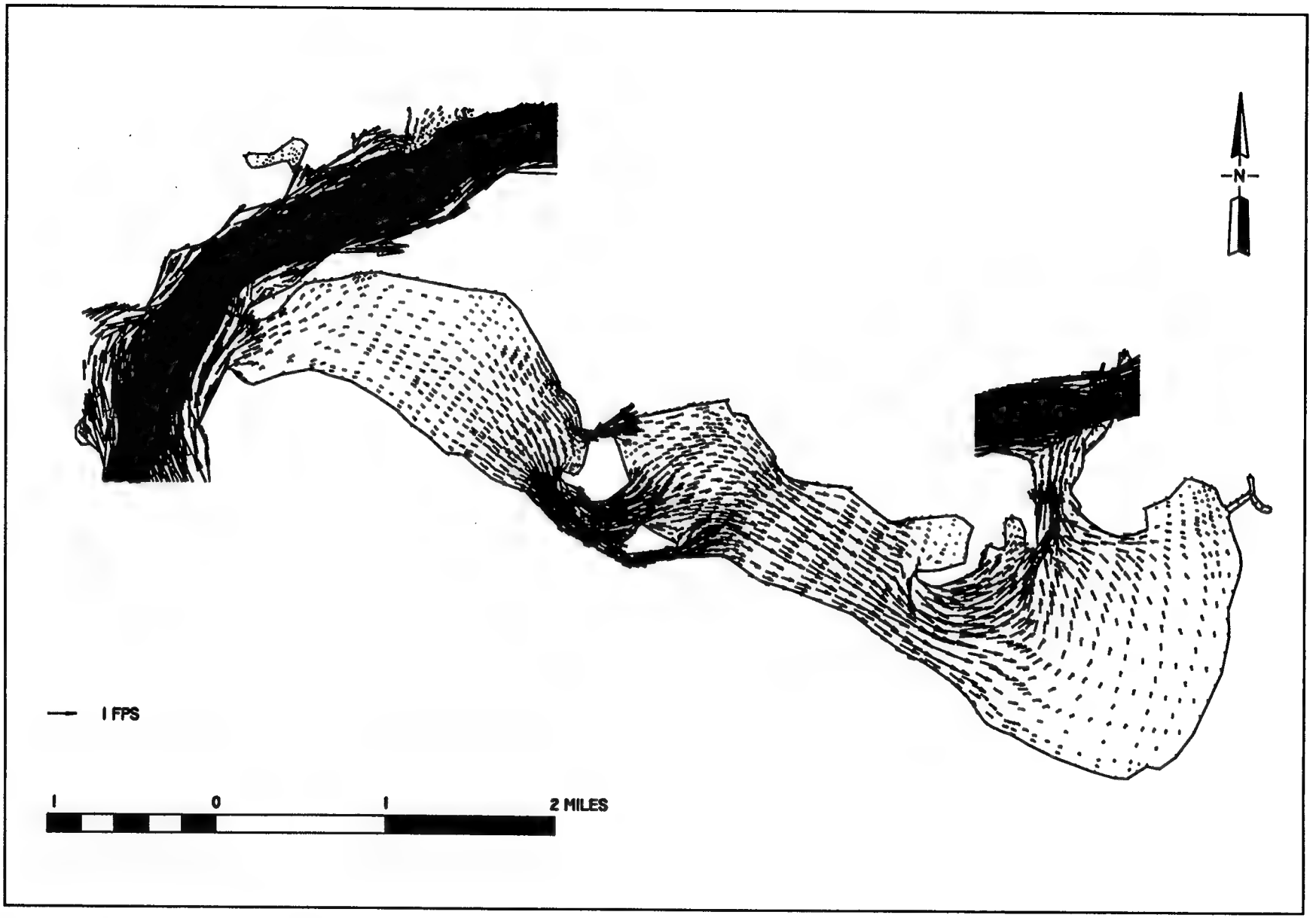

Figure 56. Ebb velocity vectors at Mill Cove, Plan 4 (to convert scale to kilometers, multiply by 1.6)

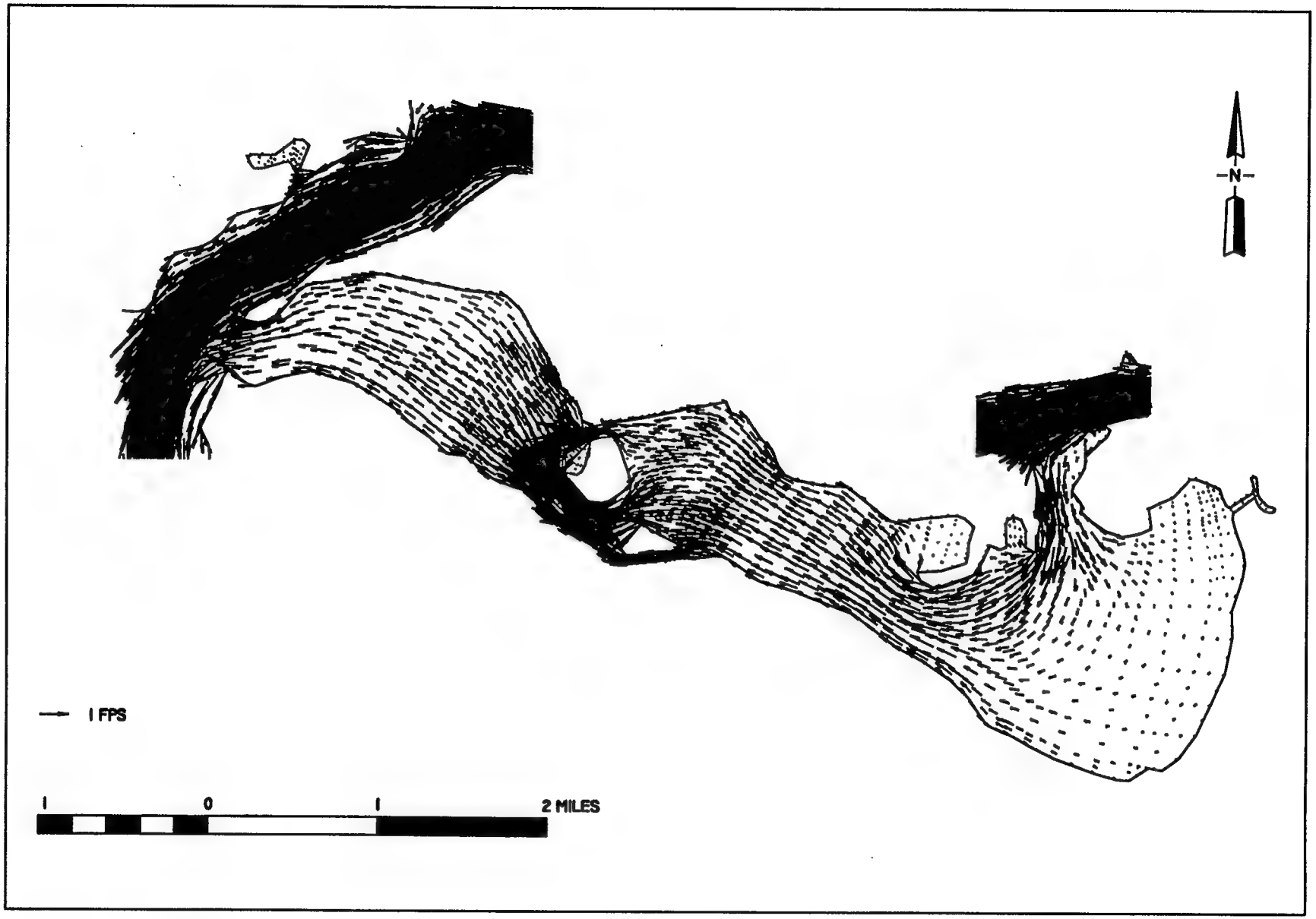

Figure 57. Flood velocity vectors at Mill Cove, Plan 4 (to convert scale to kilometers, multiply by 1.6)

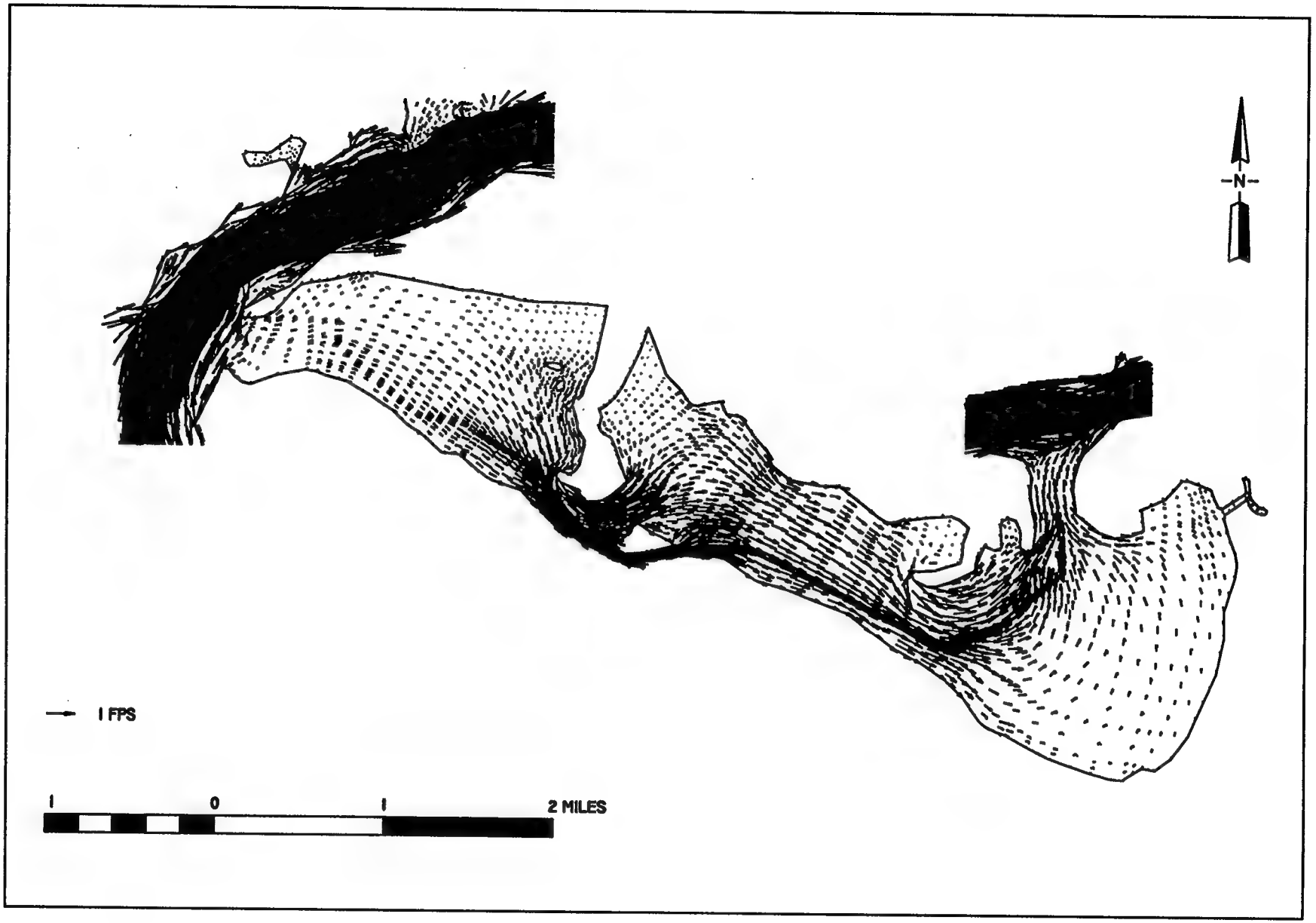

Figure 58. Ebb velocity vectors at Mill Cove, Plan 5 (to convert scale to kilometers, multiply by 1.6)

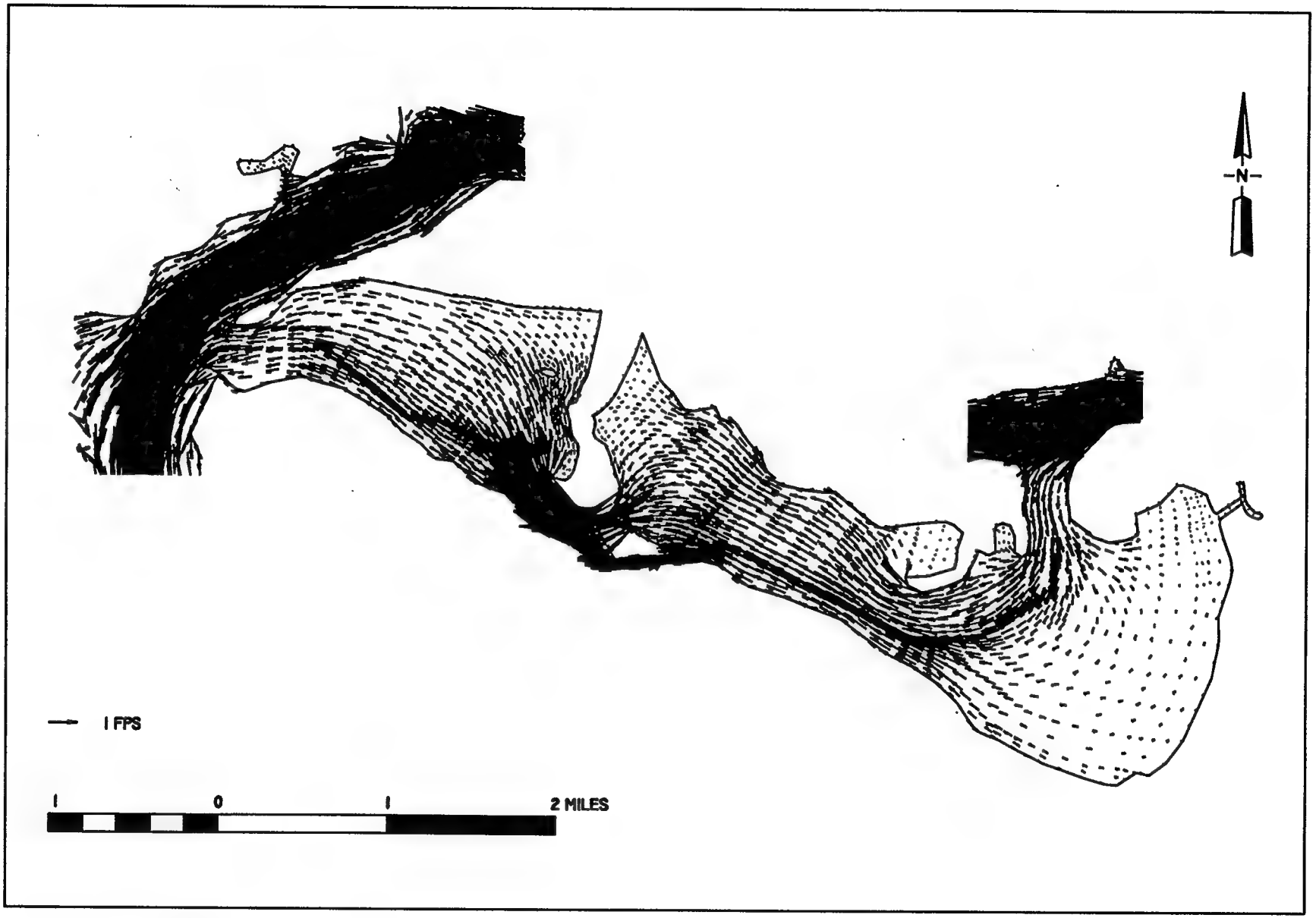

Figure 59. Flood velocity vectors at Mill Cove, Plan 5 (to convert scale to kilometers, multiply by 1.6)

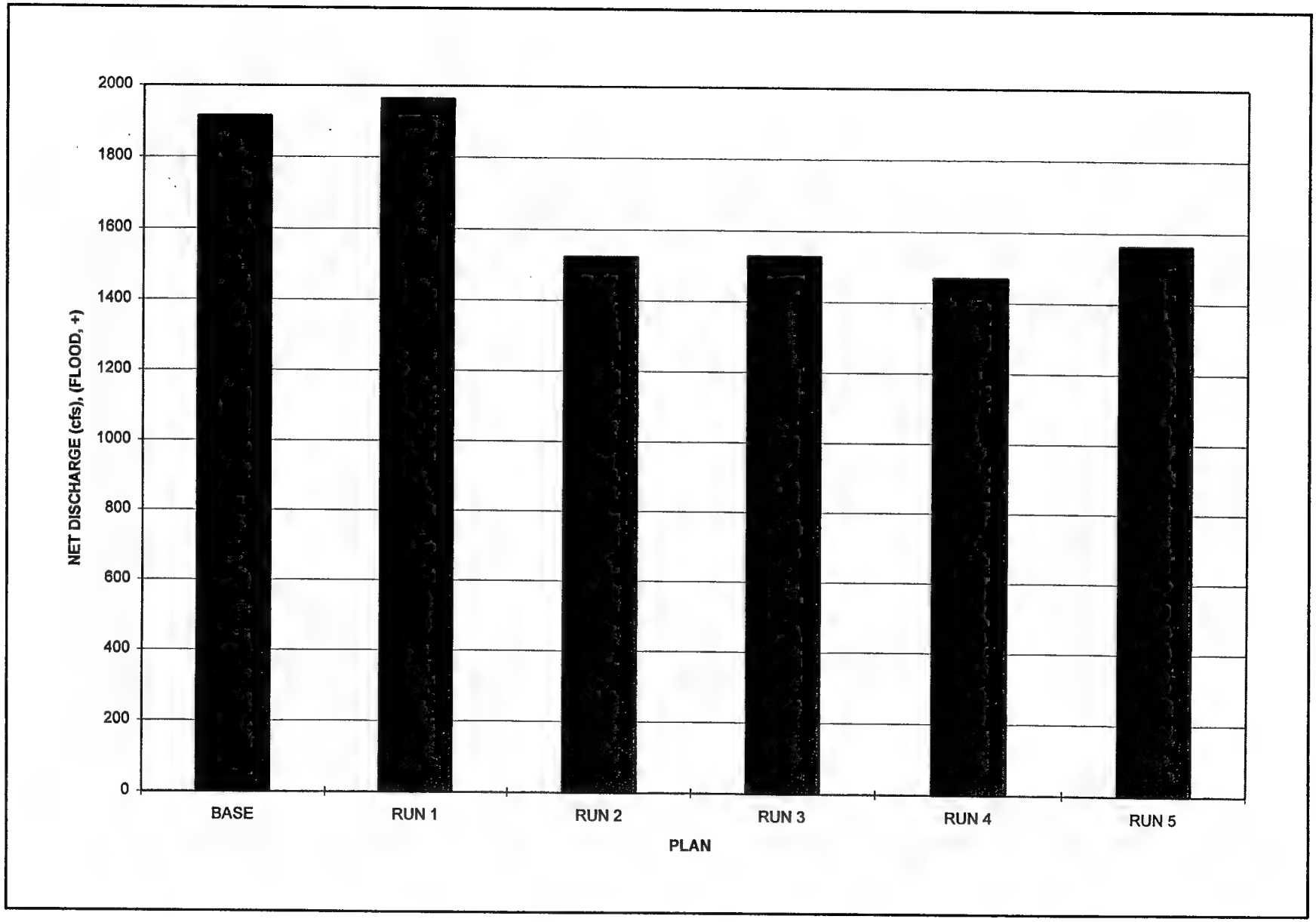

Figure 60. Net discharge at cross section 1 (to convert discharges to cu m/sec, multiply by 0.0283)

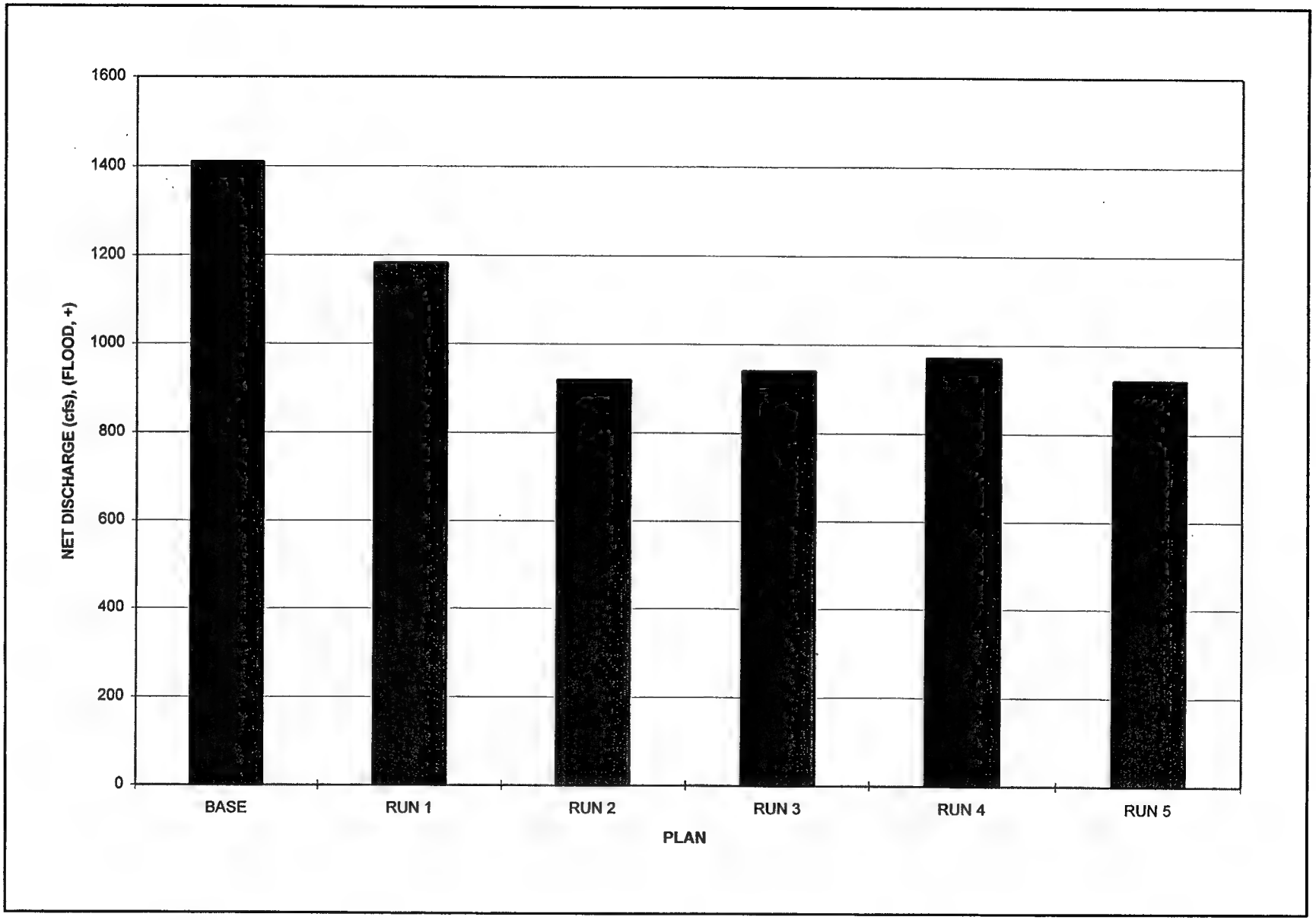

Figure 61. Net discharge at cross section 2 (to convert discharges to cu m/sec, multiply by 0.0283)

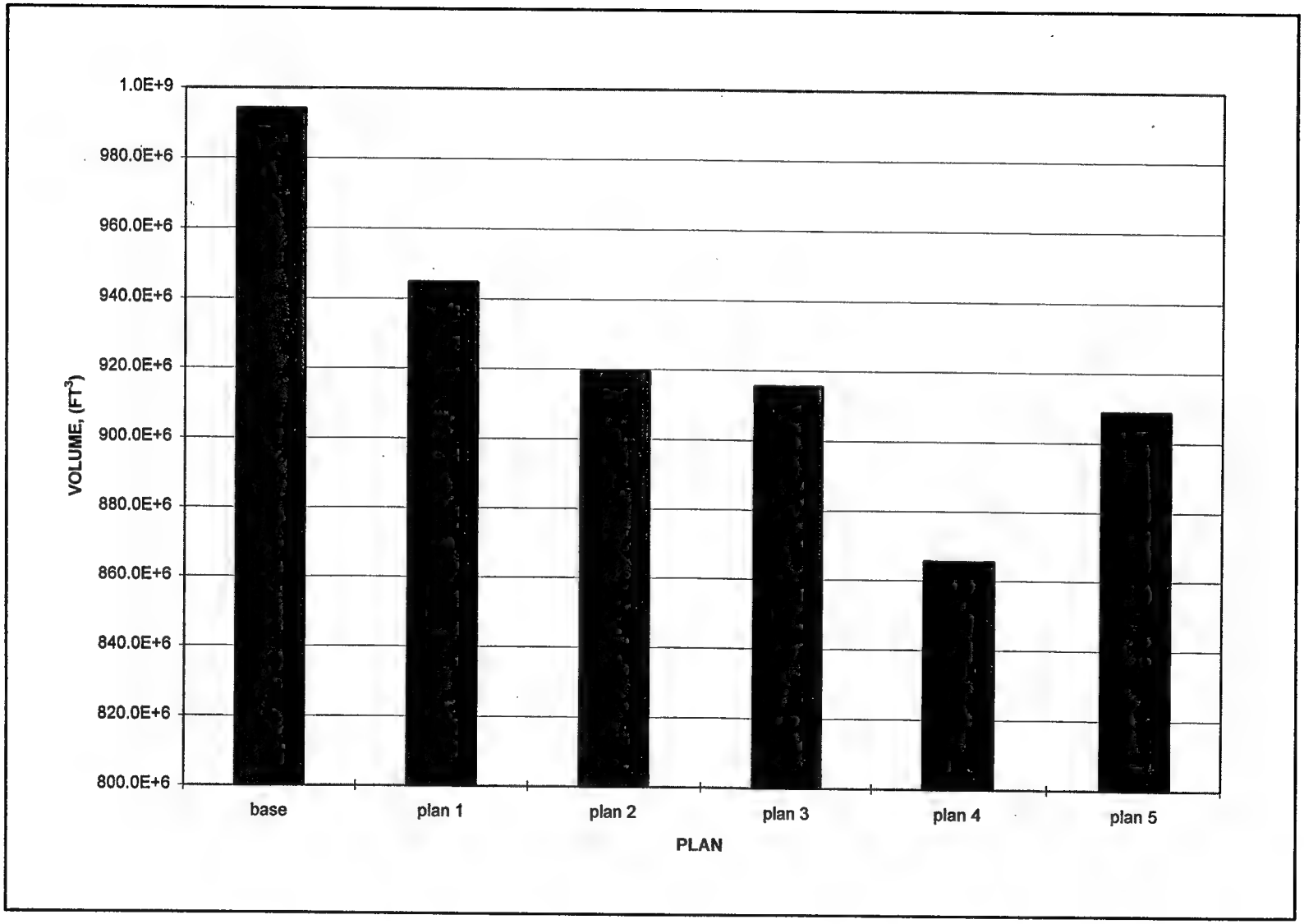

Figure 62. Volume of water in Mill Cove (to convert volumes to cu m, multiply by 0.028)

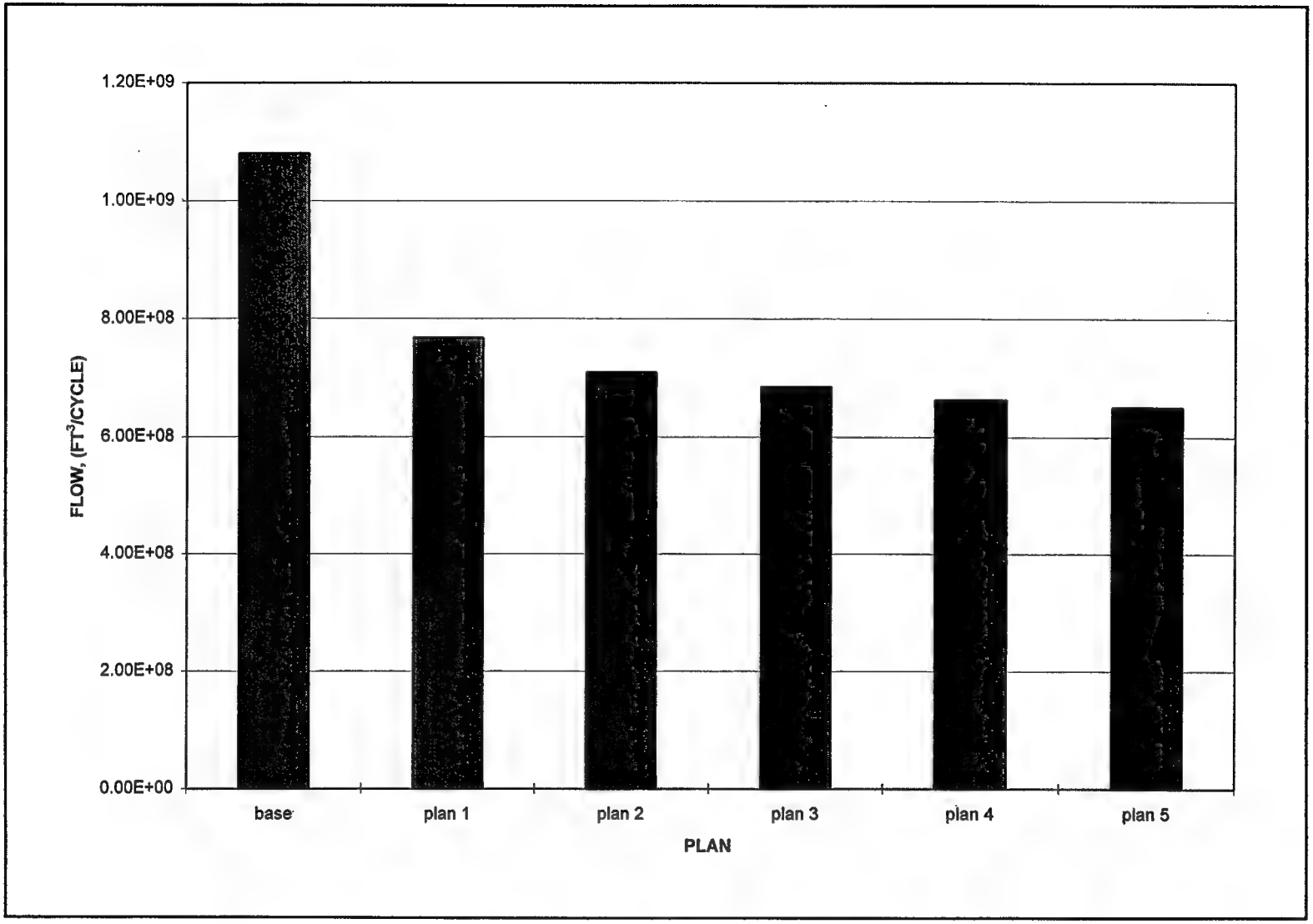

Figure 63. Water flow into Mill Cove during one tidal cycle (to convert flow into cu m, multiply by 0.028)

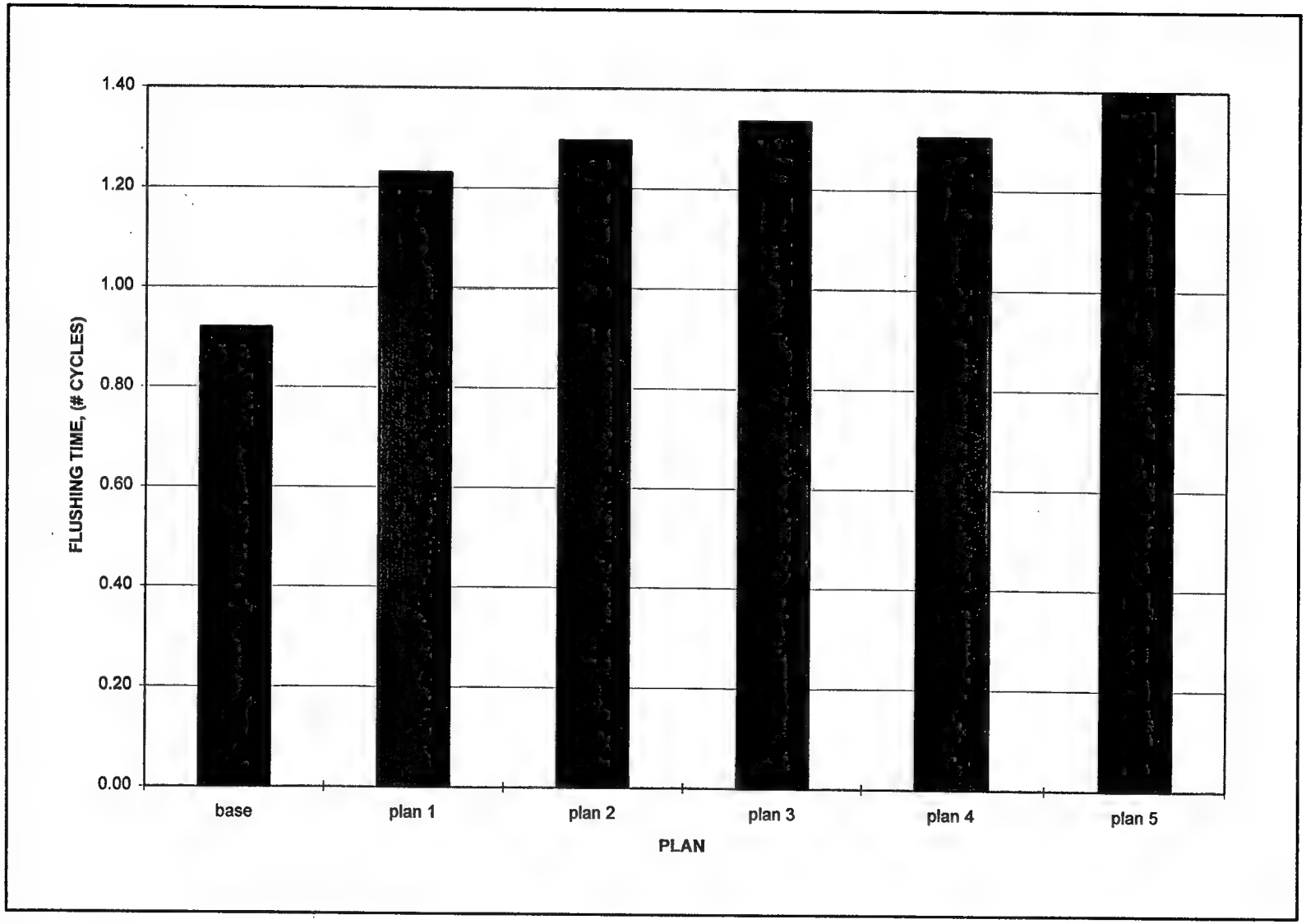

Figure 64. Tidal flushing

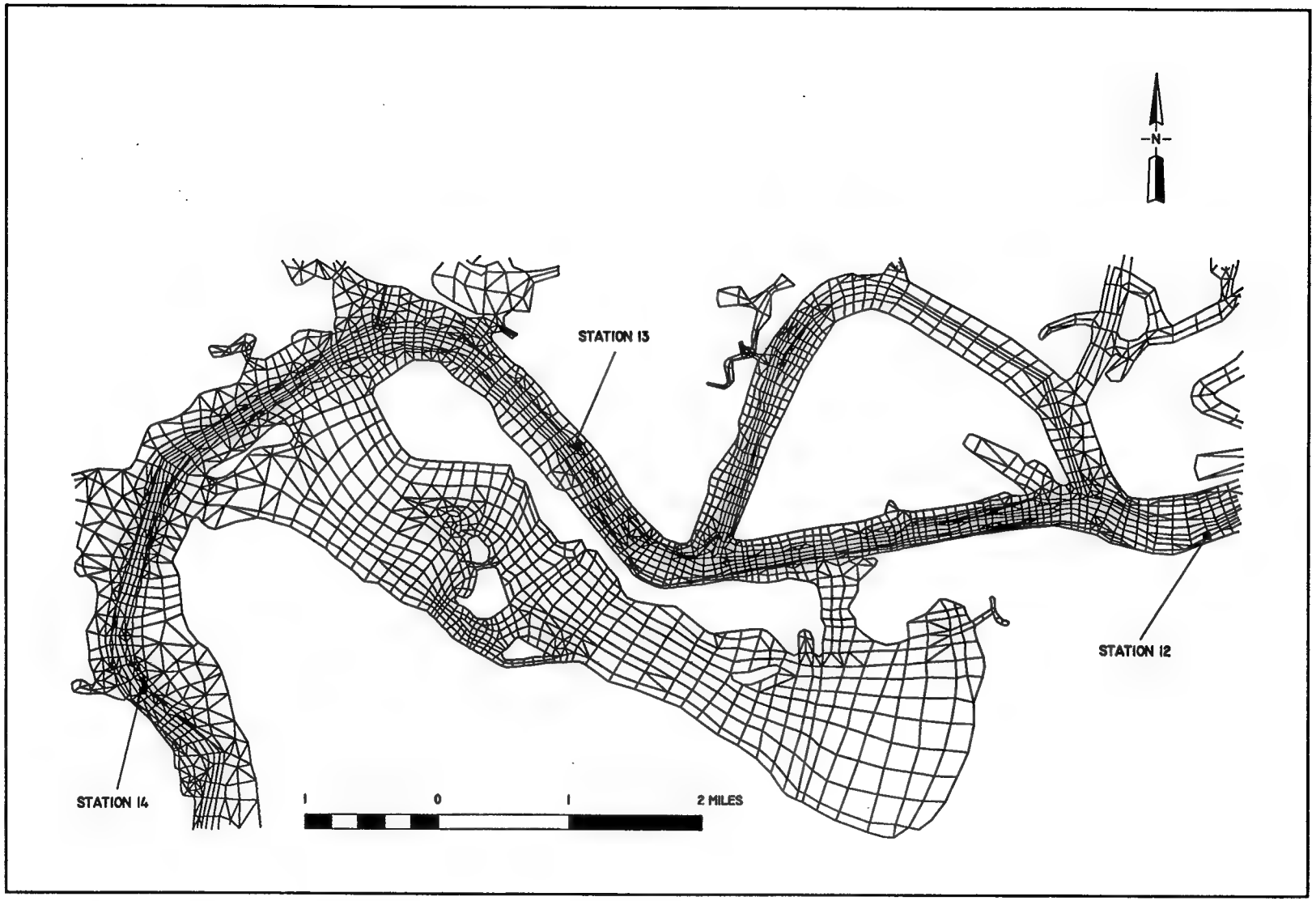

Figure 65. Location of stations in the navigation channel (to convert scale to kilometers, multiply by 1.6)

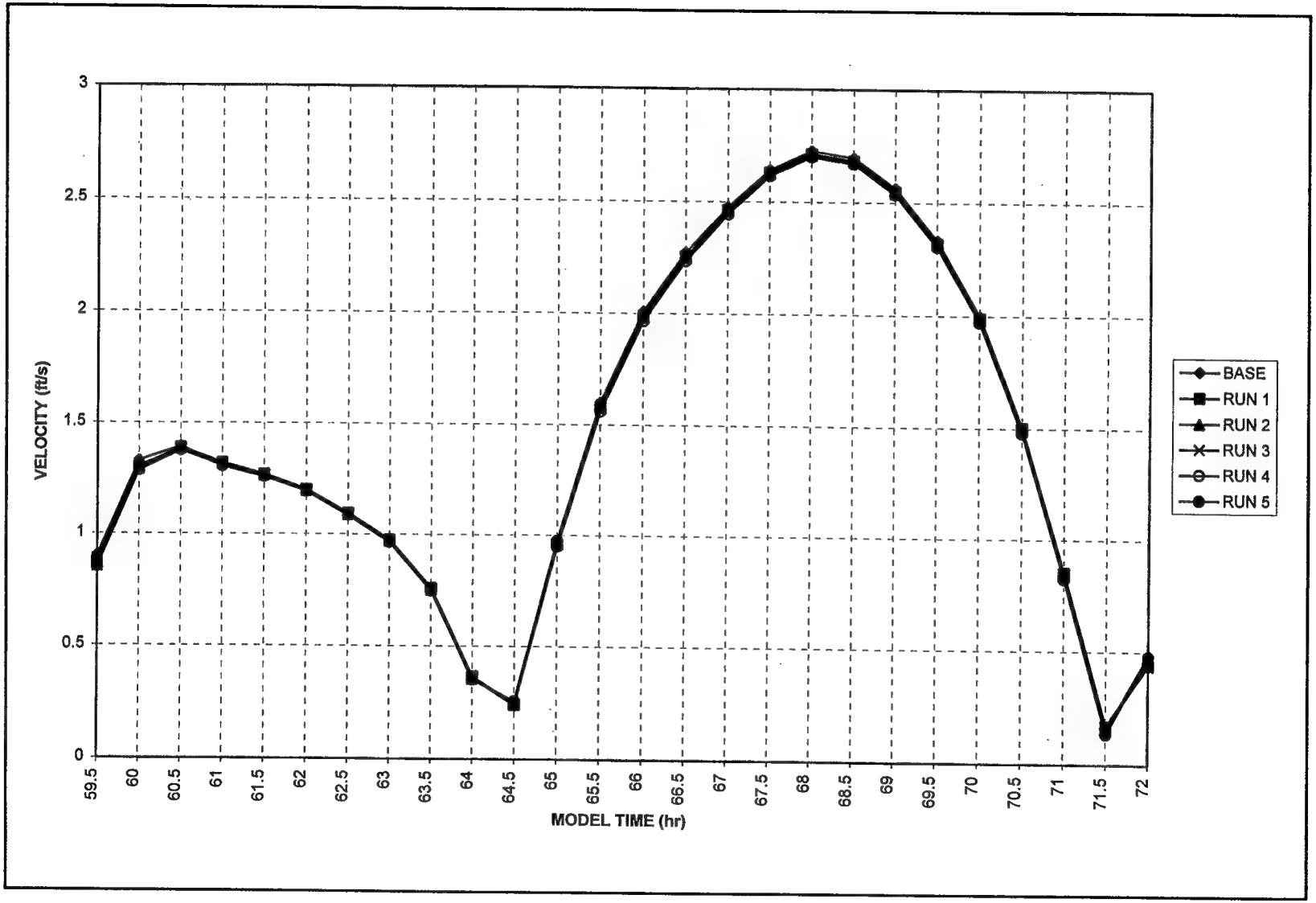

Figure 66. Velocity magnitude at station 12 (to convert velocities to meters per second, multiply by 0.3048)

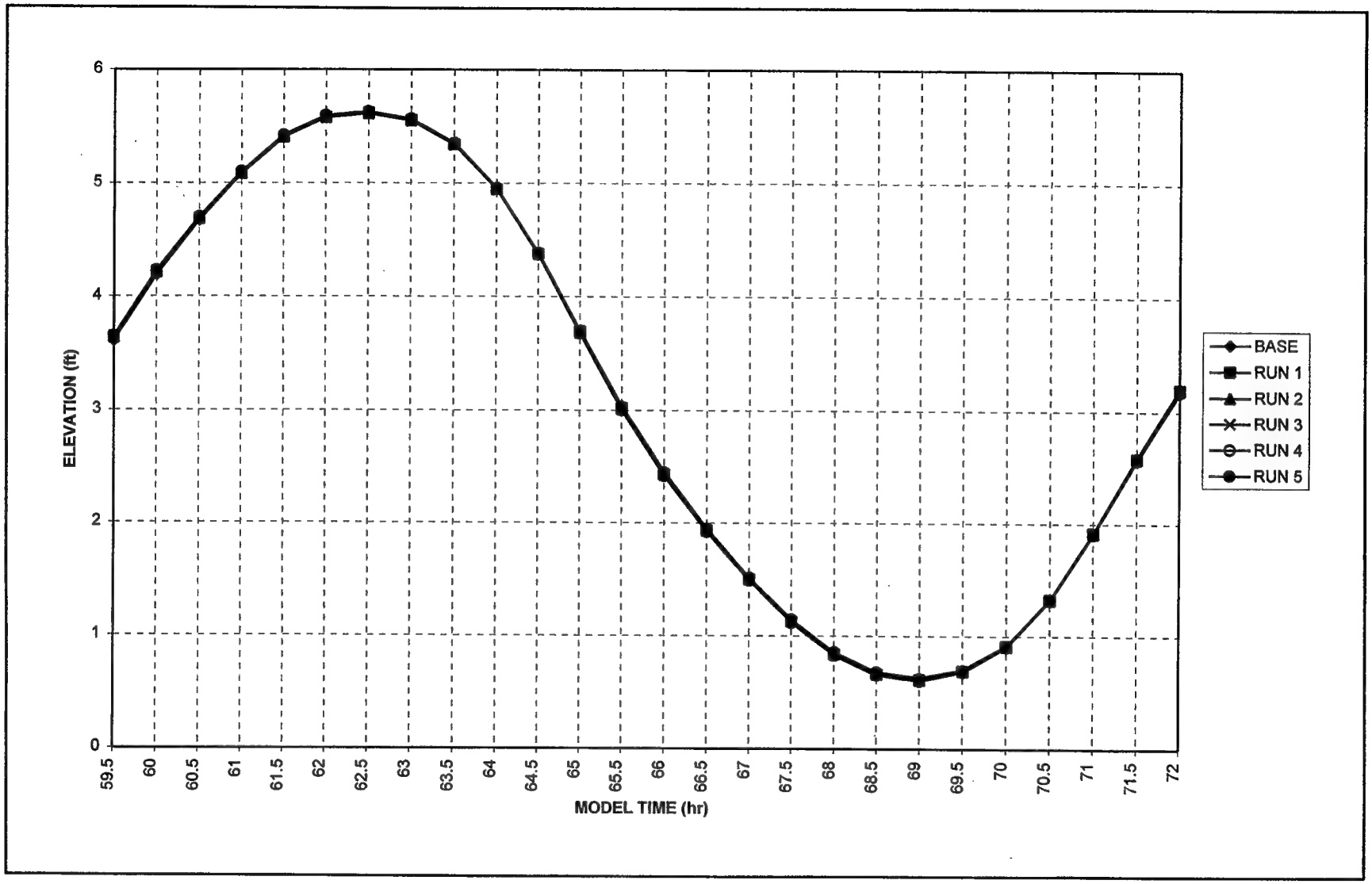

Figure 67. Water surface elevation at station 12

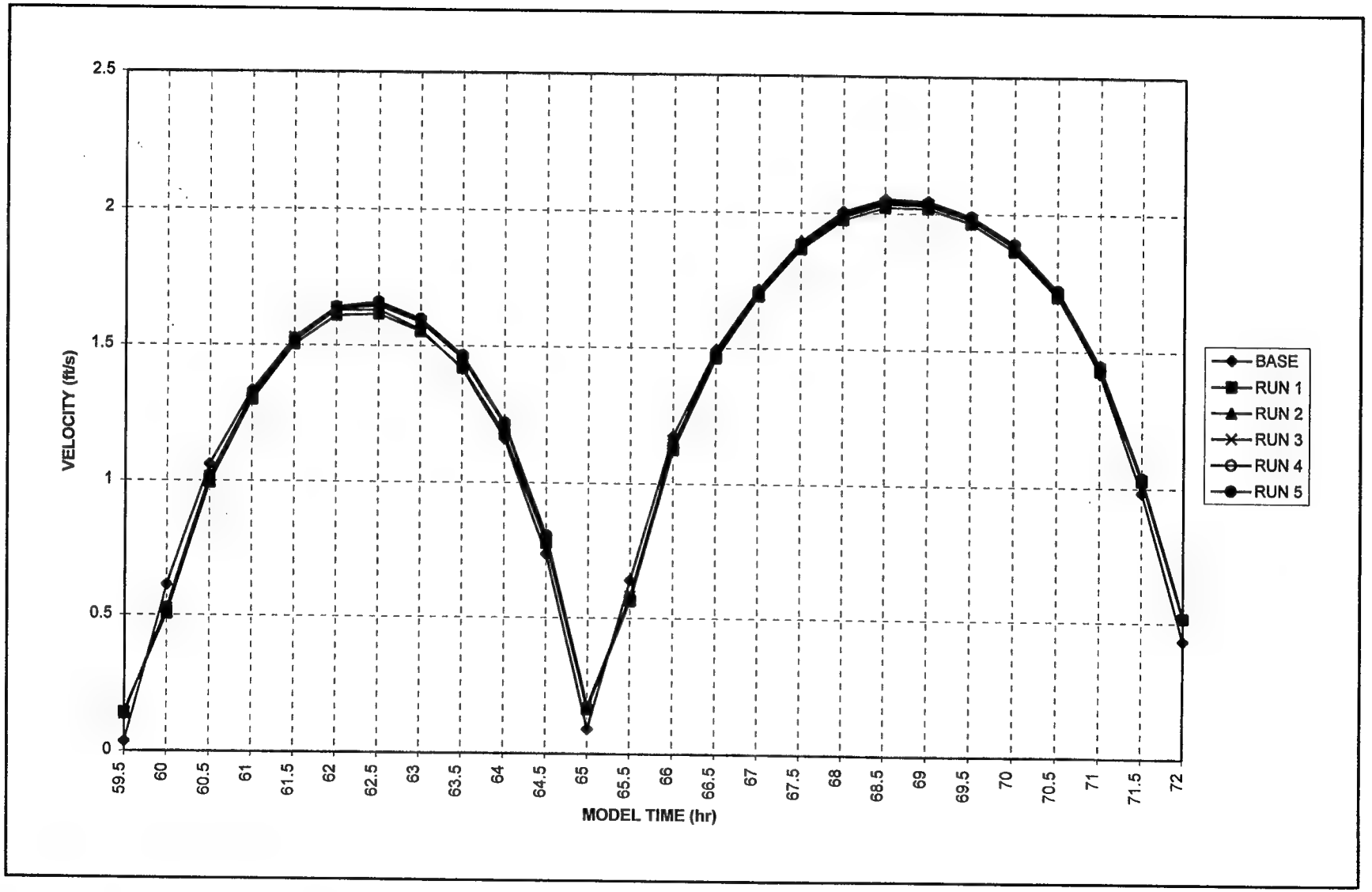

Figure 68. Velocity magnitude at station 13 (to convert velocities to meters per second, multiply by 0.3048)

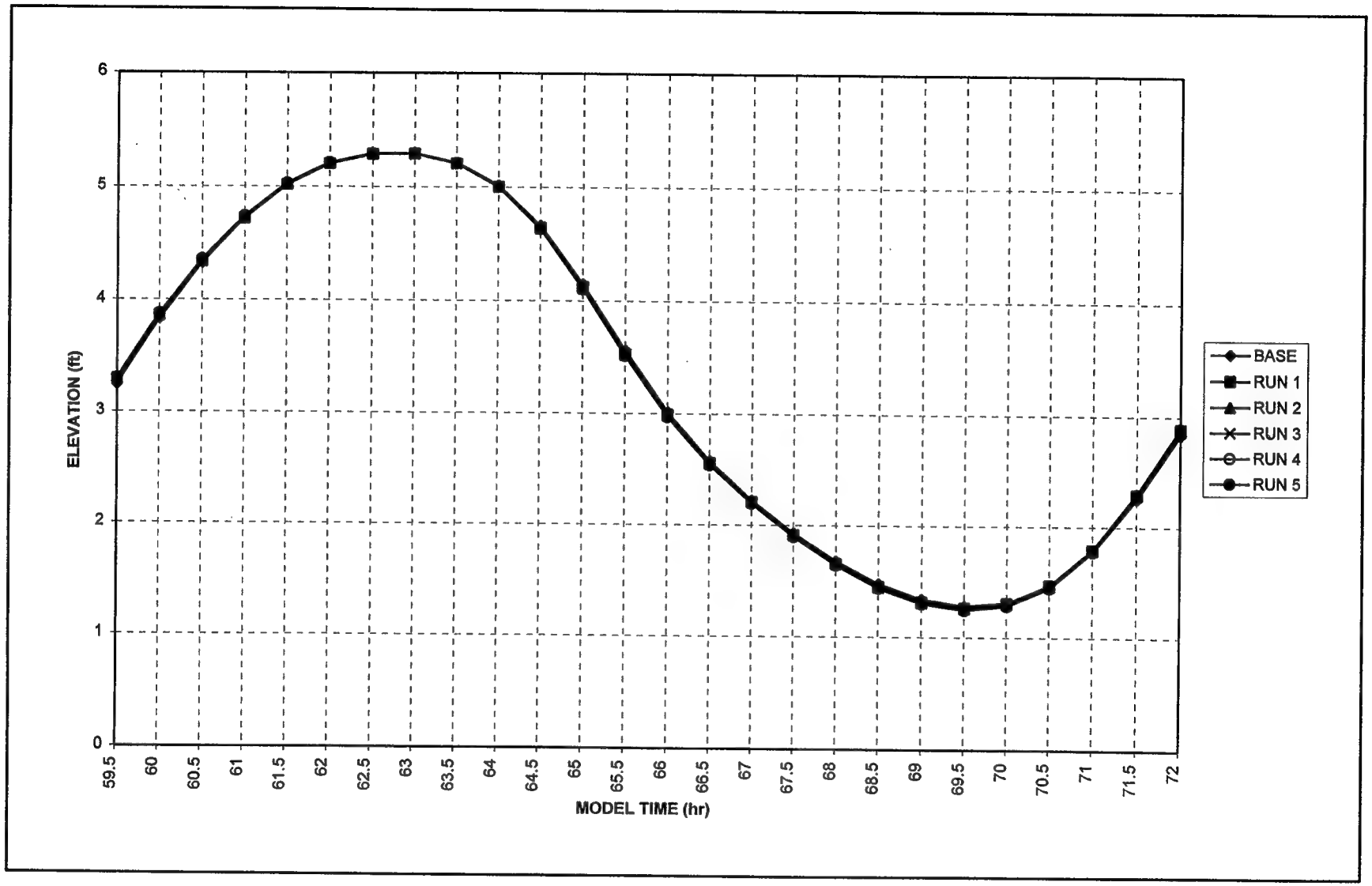

Figure 69. Water surface elevation at station 13

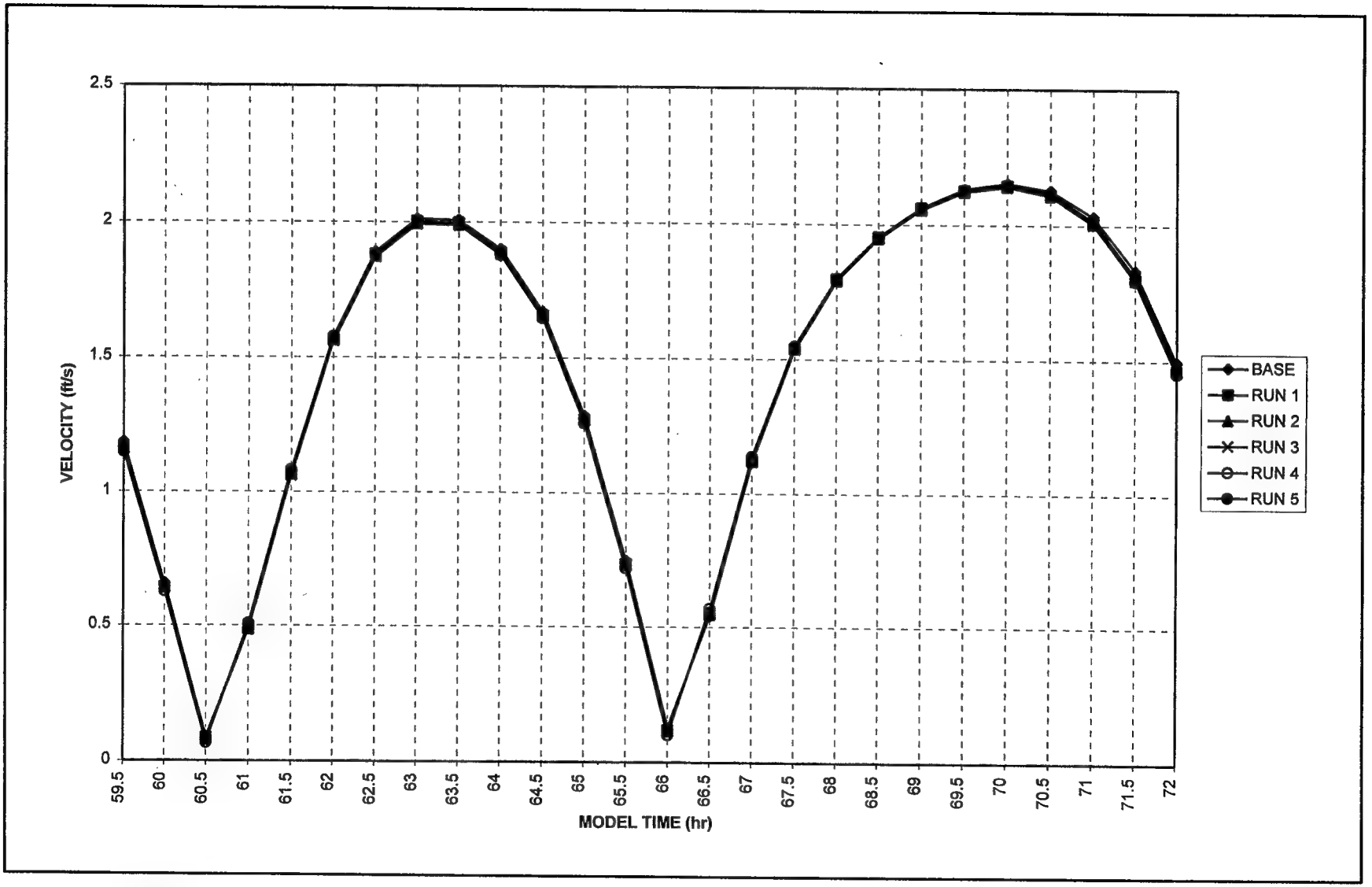

Figure 70. Velocity magnitude at station 14 (to convert velocities to meters per second, multiply by 0.3048)

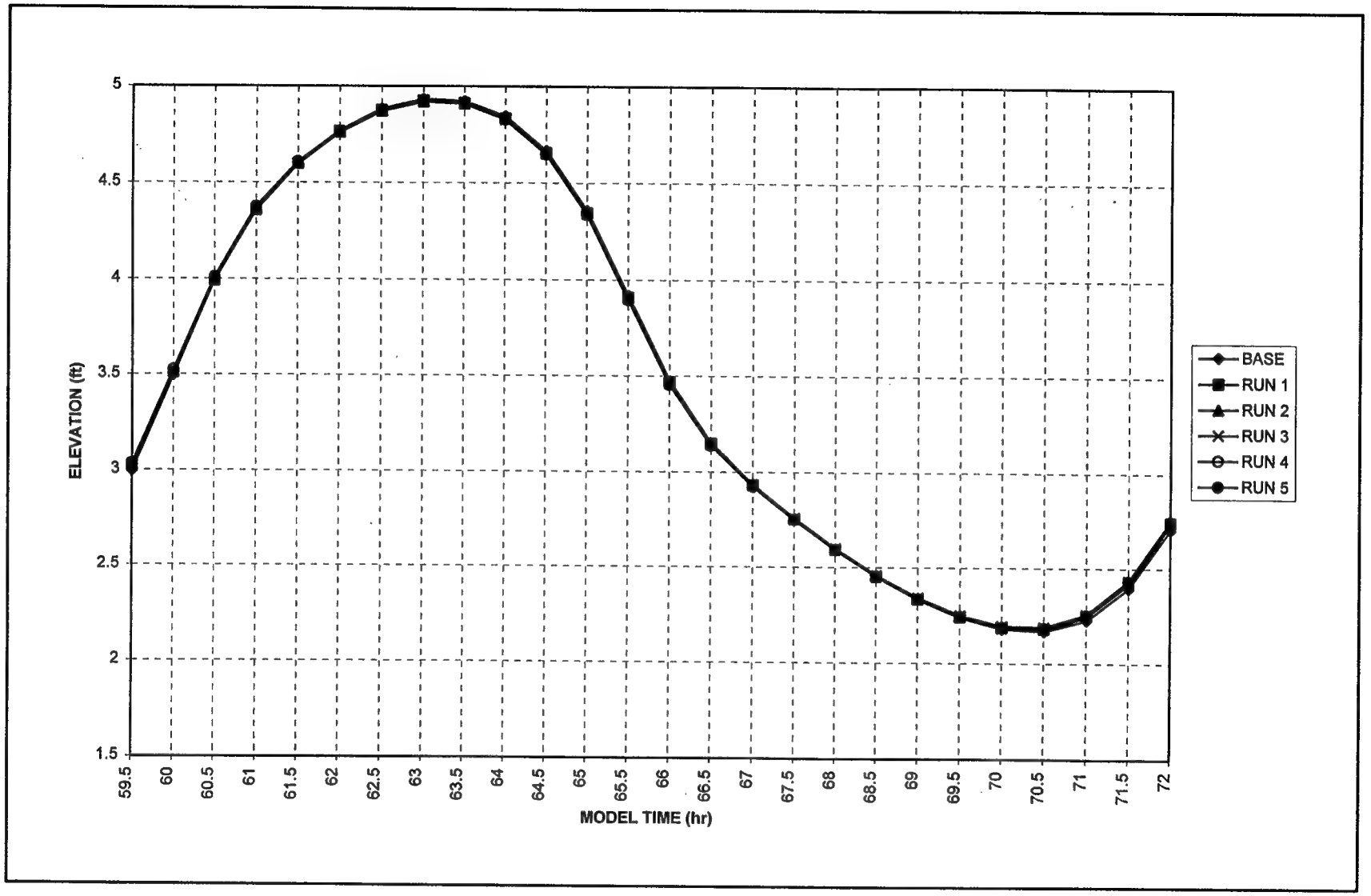

Figure 71. Water surface elevation at station 14

Figure 72. Erosion and deposition of fine sand, existing conditions (to convert scale to kilometers, multiply by 1.6)

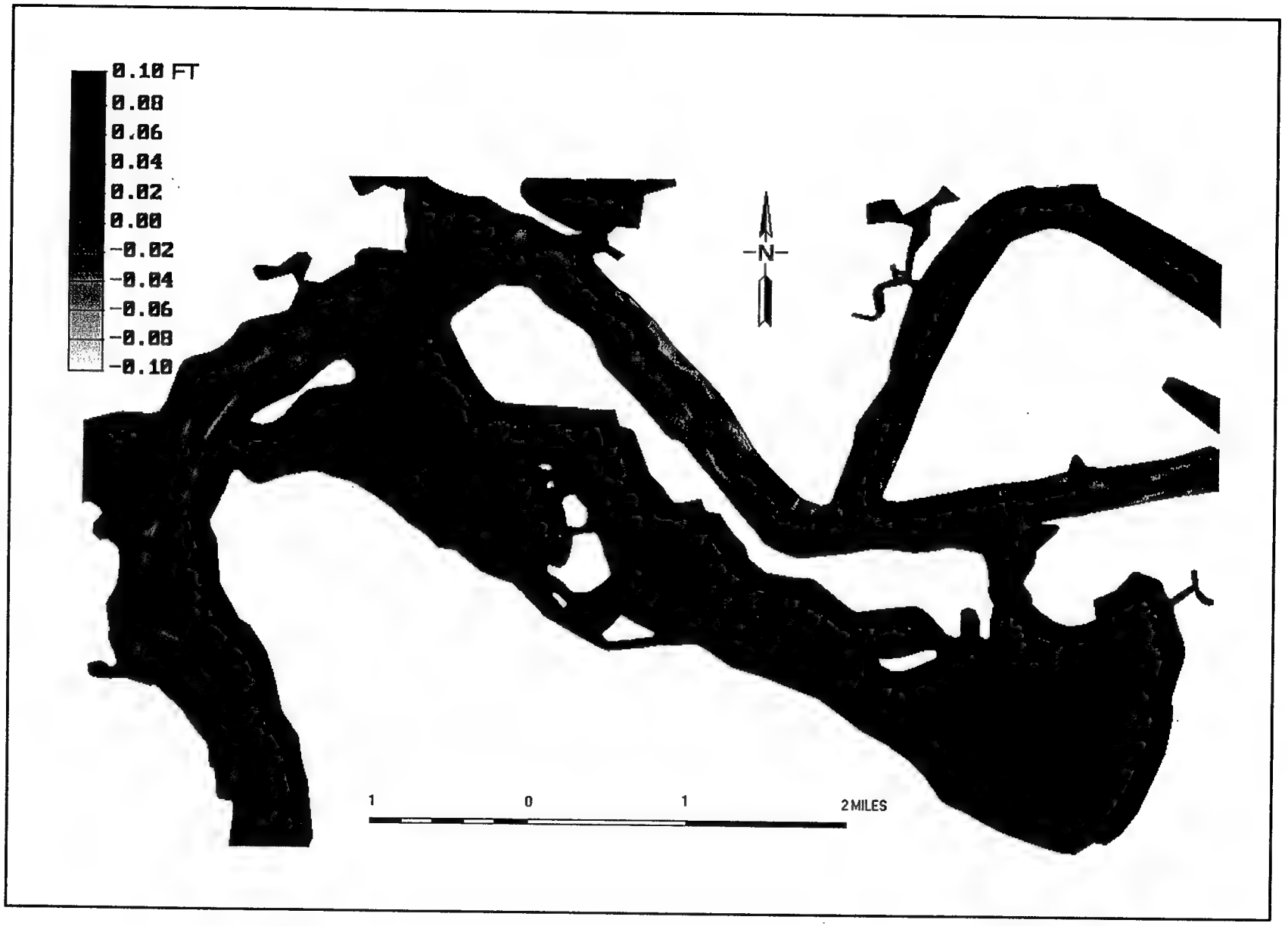

Figure 73. Erosion and deposition of medium size sand, existing conditions (to convert scale to kilometers, multiply by 1.6)

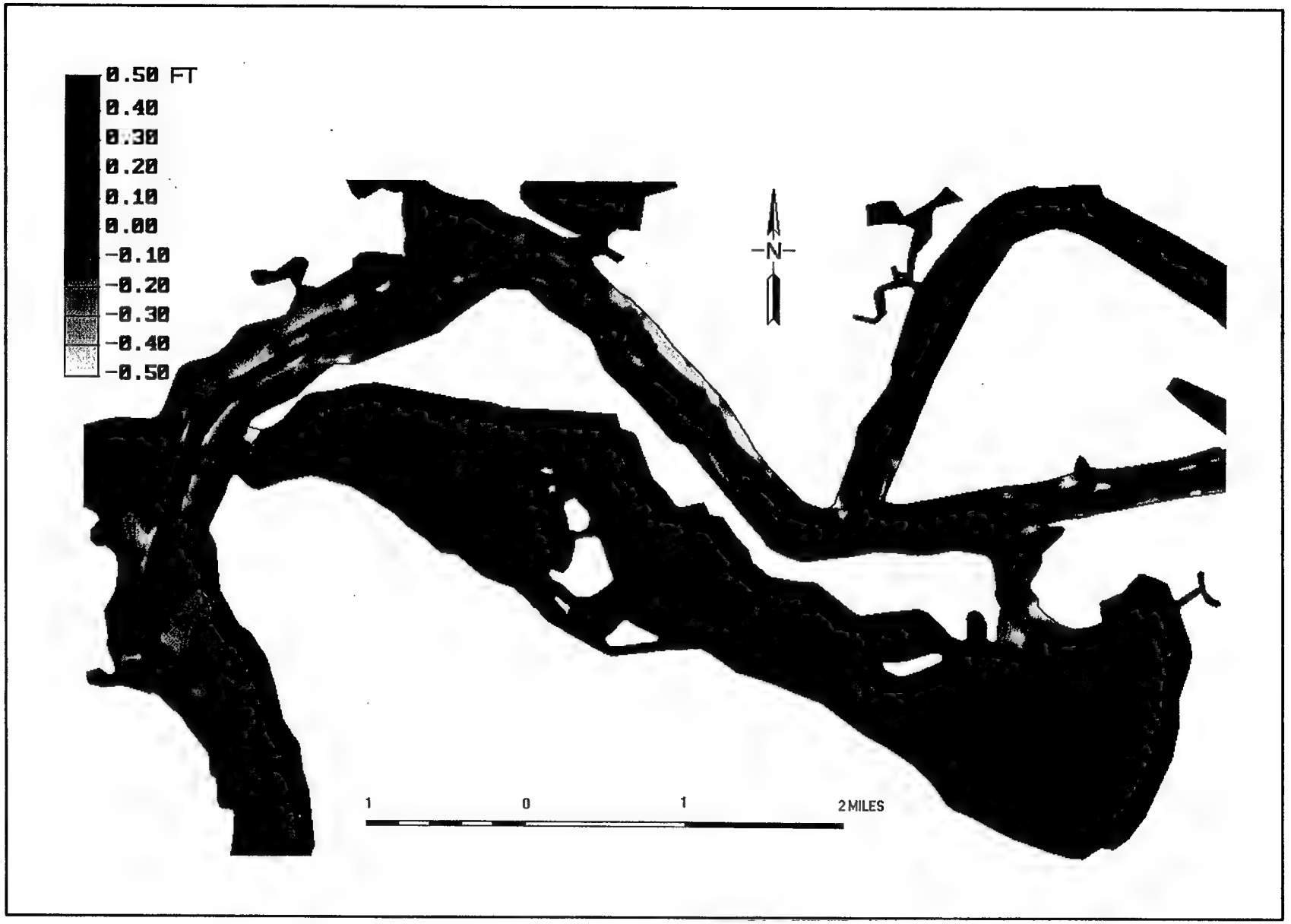

Figure 74. Erosion and deposition of fine sand, Plan 1 (to convert scale to kilometers, multiply by 1.6)

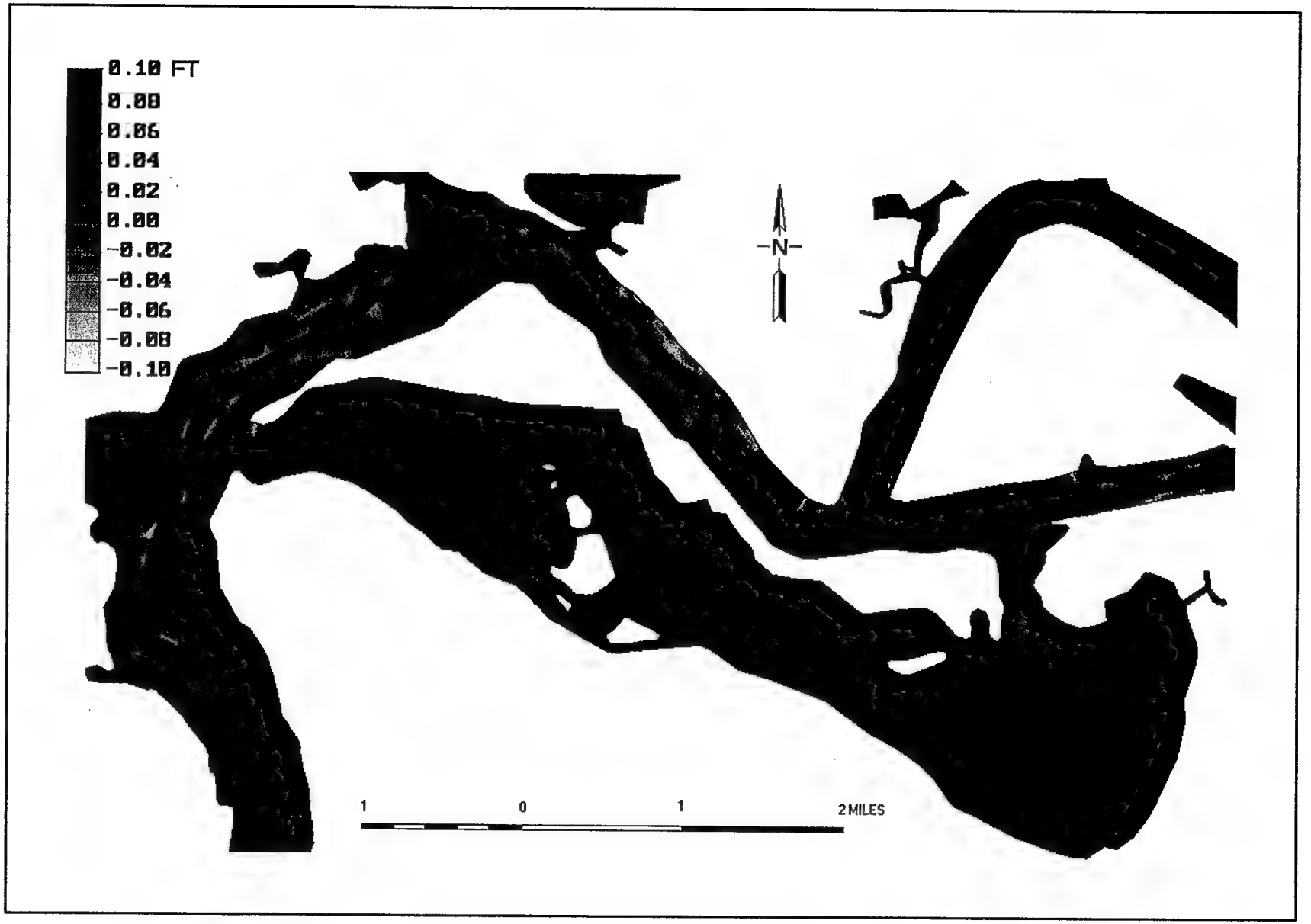

Figure 75. Erosion and deposition of medium size sand, Plan 1 (to convert scale to kilometers, multiply by 1.6)

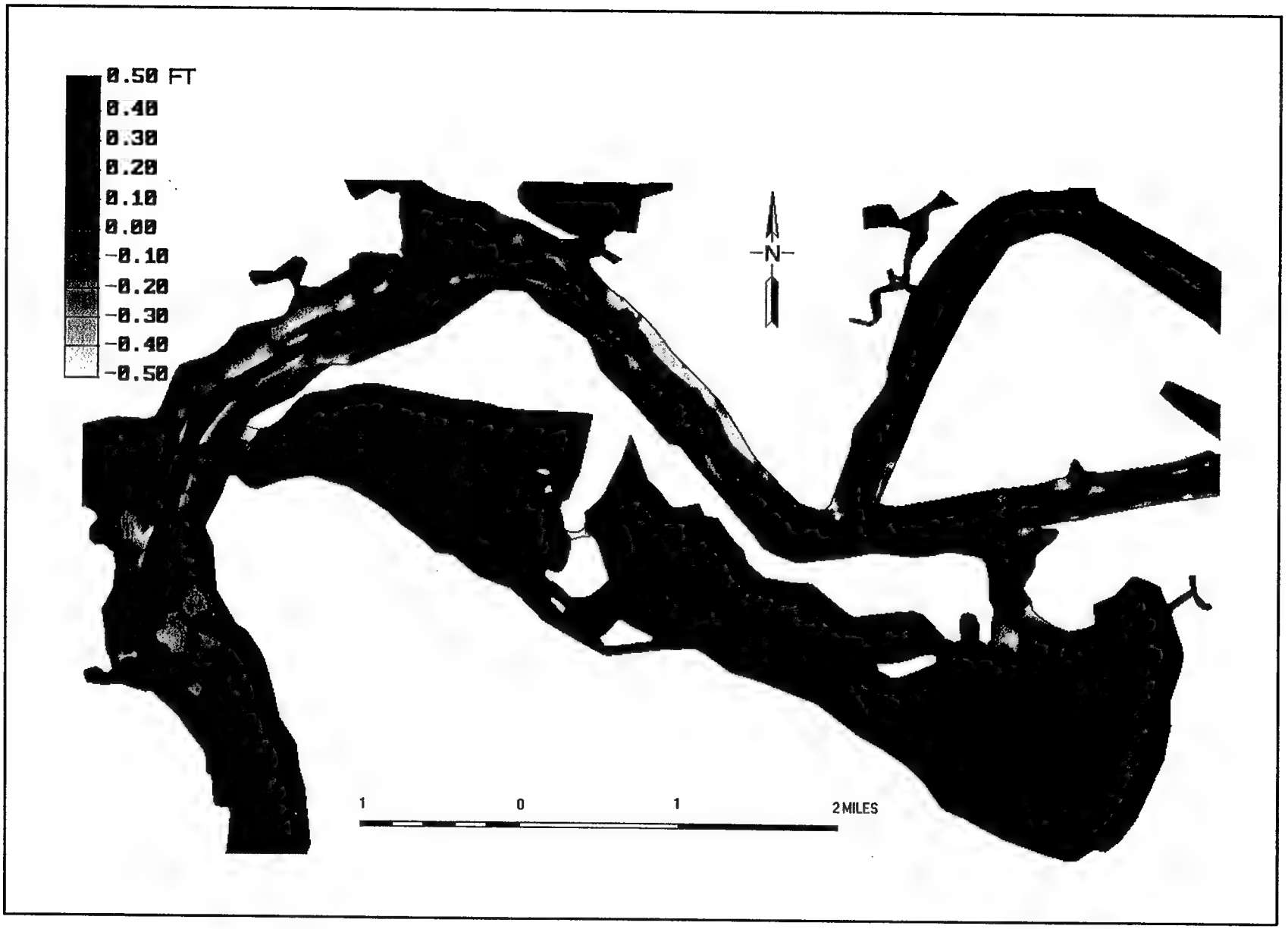

Figure 76. Erosion and deposition of fine sand, Plan 2 (to convert scale to kilometers, multiply by 1.6)

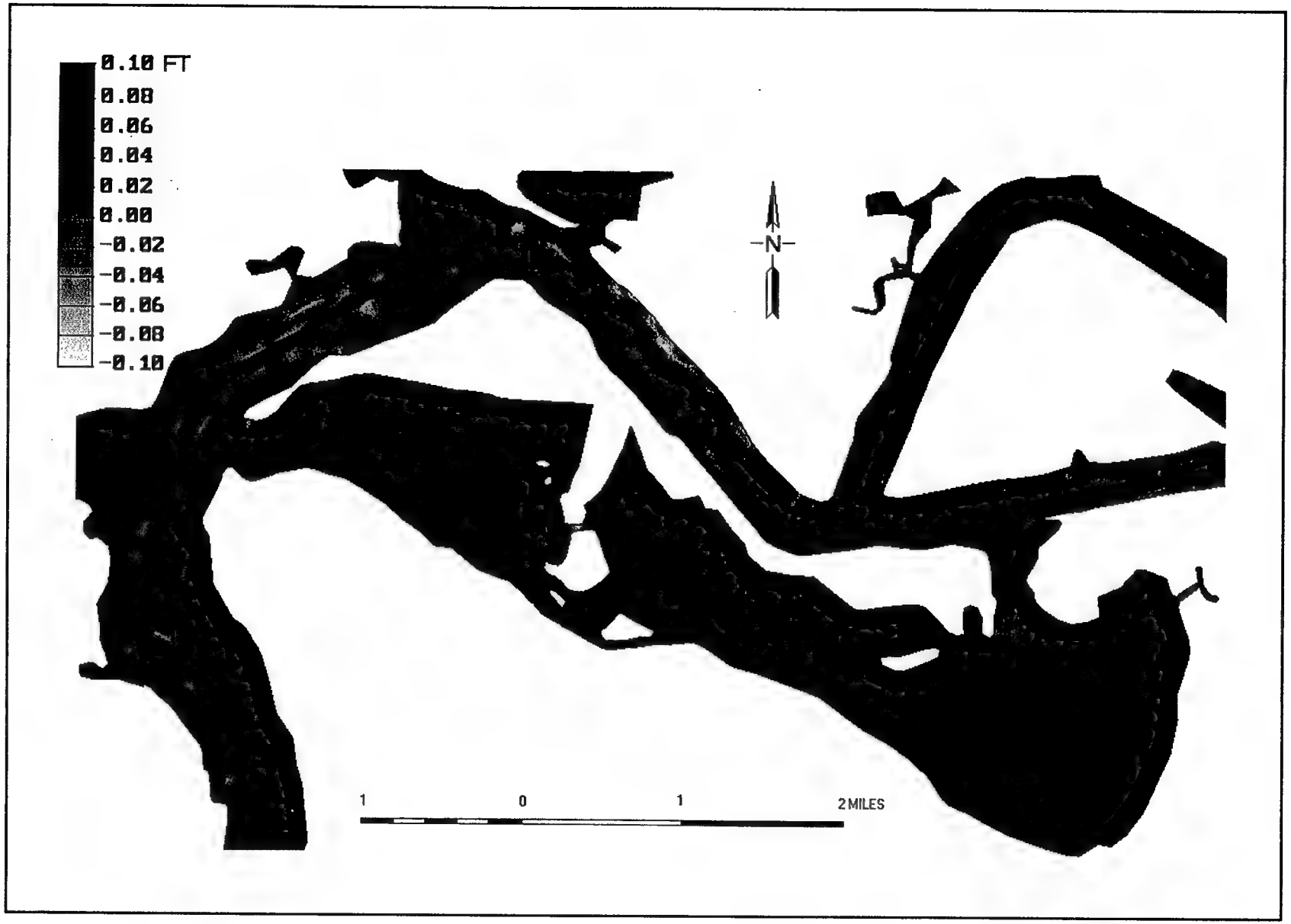

Figure 77. Erosion and deposition of medium size sand, Plan 2 (to convert scale to kilometers, multiply by 1.6)

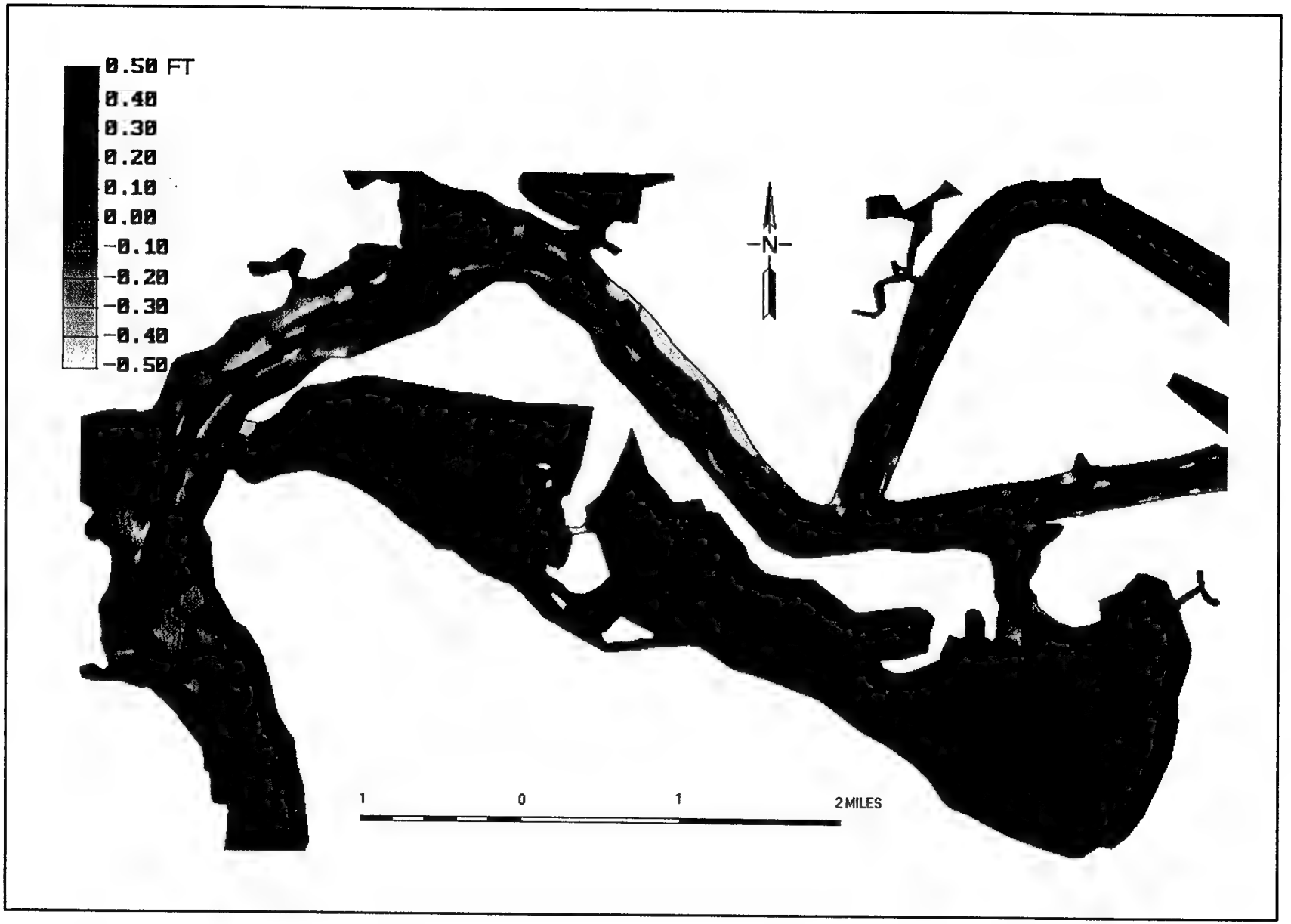

Figure 78. Erosion and deposition of fine sand, Plan 3 (to convert scale to kilometers, multiply by 1.6)

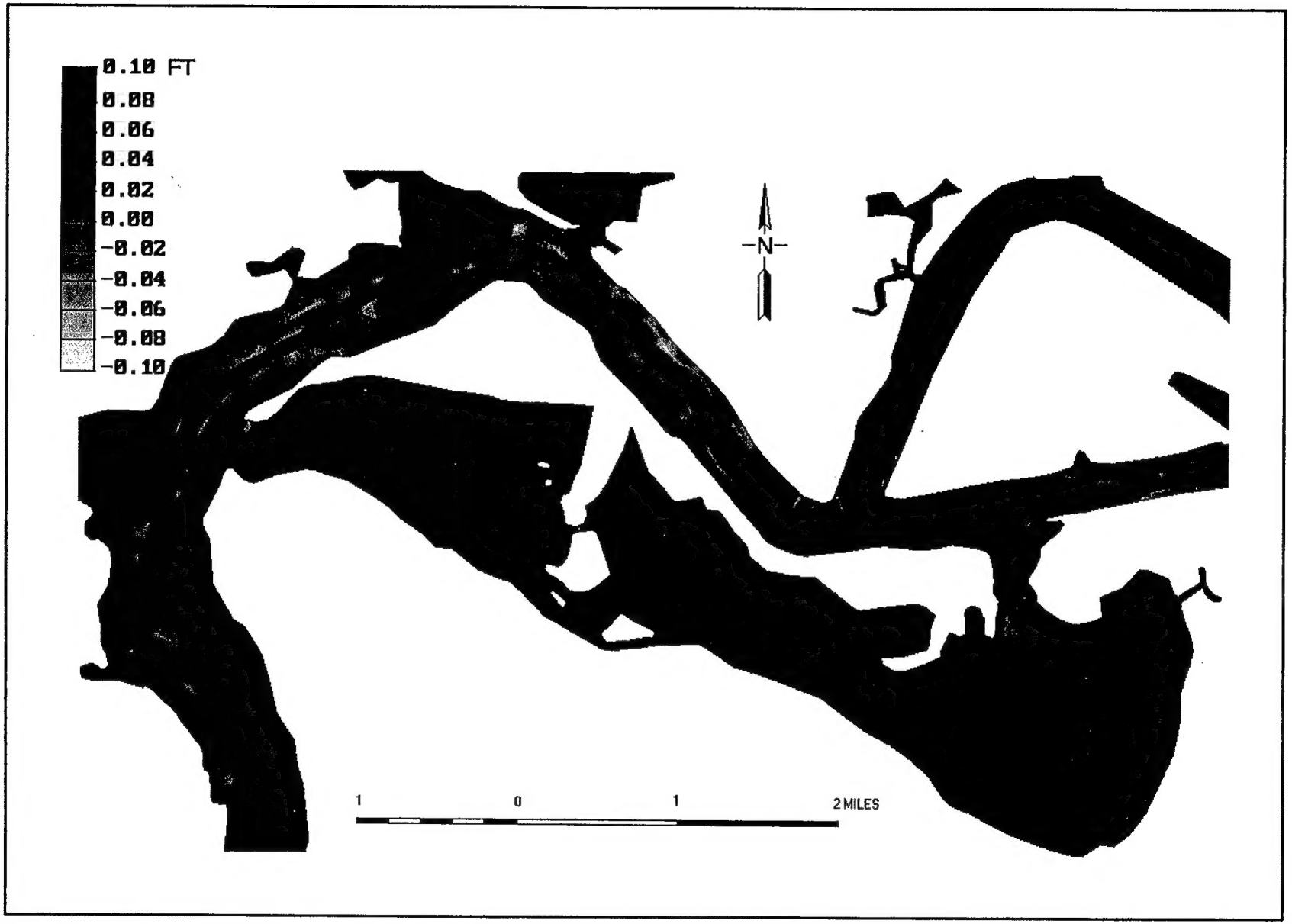

Figure 79. Erosion and deposition of medium size sand, Plan 3 (to convert scale to kilometers, multiply by 1.6)

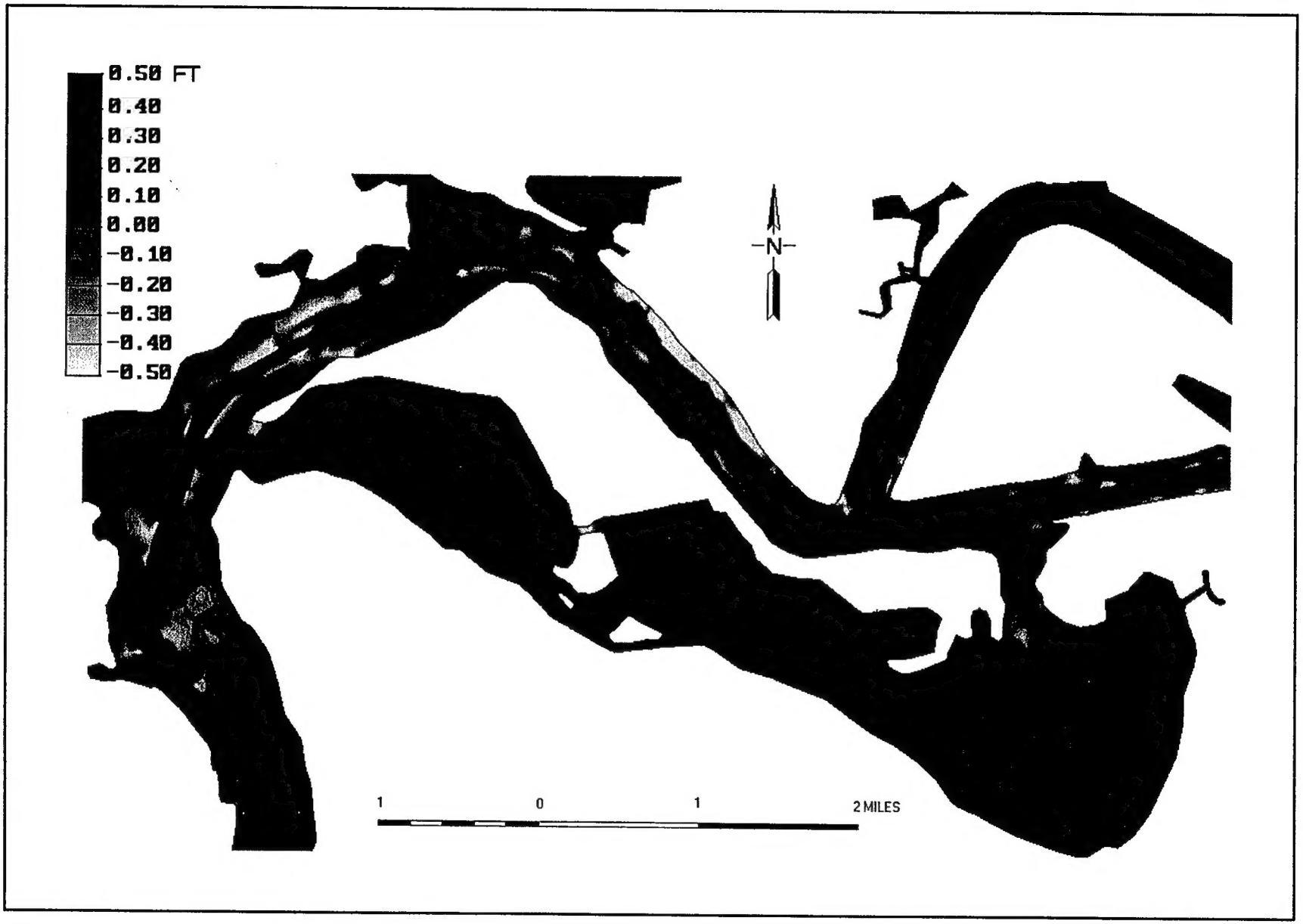

Figure 80. Erosion and deposition of fine sand, Plan 4 (to convert scale to kilometers, multiply by 1.6)

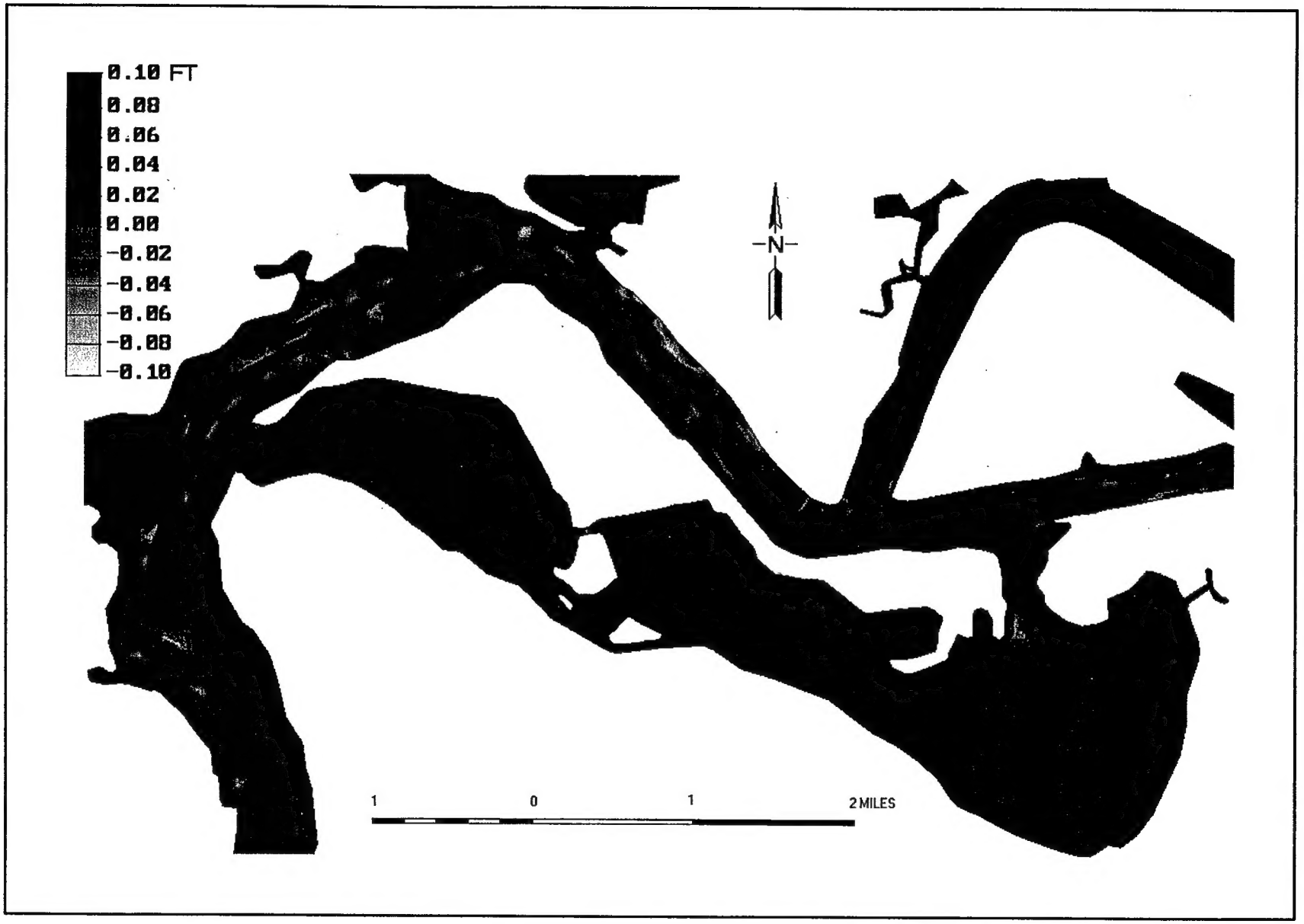

Figure 81. Erosion and deposition of medium size sand, Plan 4 (to convert scale to kilometers, multiply by 1.6)

REPORT DOCUMENTATION PAGE

Form Approved
OMB No. 0704-0188

1. AGENCY USE ONLY *(Leave blank)*	2. REPORT DATE	3. REPORT TYPE AND DATES COVERED
	May 1997	Final report

4. TITLE AND SUBTITLE
Hydrodynamic and Sediment Transport, Mill Cove, St. Johns River, Florida; Numerical Modeling Study

5. FUNDING NUMBERS

6. AUTHOR(S)
José A. Sánchez, Lisa C. Roig

7. PERFORMING ORGANIZATION NAME(S) AND ADDRESS(ES)
U.S. Army Engineer Waterways Experiment Station
3909 Halls Ferry Road, Vicksburg, MS 39180-6199

8. PERFORMING ORGANIZATION REPORT NUMBER
Technical Report CHL-97-8

9. SPONSORING/MONITORING AGENCY NAME(S) AND ADDRESS(ES)
U.S. Army Engineer District, Jacksonville
P.O. Box 4970
Jacksonville, FL 32232-0019

10. SPONSORING/MONITORING AGENCY REPORT NUMBER

11. SUPPLEMENTARY NOTES
Available from National Technical Information Service, 5285 Port Royal Road, Springfield, VA 22161.

12a. DISTRIBUTION/AVAILABILITY STATEMENT
Approved for public release; distribution is unlimited.

12b. DISTRIBUTION CODE

13. ABSTRACT ***(Maximum 200 words)***

The U.S. Army Engineer District, Jacksonville, is investigating how to improve tidal flushing in Mill Cove, lower St. Johns River, Florida, to maintain water quality and to prevent excessive sedimentation. Four plans have been proposed to reshape the shoreline within the cove. One additional proposed plan will also modify the bathymetry in the area. RMA2-WES, a two-dimensional, vertically averaged hydrodynamic model, was used to compare the circulation patterns that occur in the present-day Mill Cove against the circulation patterns that would result from the five plan configurations. Sediment transport was simulated using SED2D-WES, a two-dimensional, vertically averaged model of sediment advection and dispersion in the water column, with the channel bed acting as a source and/or sink for sediment as it deposits and erodes. Currents and tides were compared to prototype data to validate the numerical model. The study addressed changes within Mill Cove as well as any influence these changes had in the navigation channel.

14. SUBJECT TERMS

Hydrodynamic	Model	St. Johns River
Jacksonville, Florida	Numerical	SED2D
Mill Cove	RMA2	Sediment

15. NUMBER OF PAGES
114

16. PRICE CODE

17. SECURITY CLASSIFICATION OF REPORT	18. SECURITY CLASSIFICATION OF THIS PAGE	19. SECURITY CLASSIFICATION OF ABSTRACT	20. LIMITATION OF ABSTRACT
UNCLASSIFIED	UNCLASSIFIED		